SANDRA GUAUQUE-OLARTE

THE TRANSCRIPTOME OF HUMAN EPICARDIAL, MEDIASTINAL AND SUBCUTANEOUS ADIPOSE TISSUES IN MEN WITH CORONARY ARTERY DISEASE

Mémoire présenté
à la Faculté des études supérieures de l'Université Laval
dans le cadre du programme de maîtrise en biologie cellulaire et moléculaire
pour l'obtention du grade de maître ès sciences (M.Sc.)

DÉPARTEMENT DE MÉDECINE MOLÉCULAIRE
FACULTÉ DE MÉDECINE
UNIVERSITÉ LAVAL
QUÉBEC

2011

Résumé

Le tissu adipeux épicardique (TAE) est localisé à la surface du cœur en contact avec les artères coronaires, ce qui suggère un rôle dans la pathogénèse de la maladie coronarienne. Les objectifs de cette étude étaient d'identifier les gènes différentiellemment régulés entre les tissus graisseux épicardique, médiastinal et sous-cutané à l'aide des biopuces d'ADN et d'étudier leurs rôles dans le développement des maladies cardiovasculaires. Les résultats ont montré une grande similarité d'expression entre les tissus adipeux épicardique et médiastinal. Toutefois, certains gènes impliqués dans les maladies cardiovasculaires étaient régulés différemment entre ces deux tissus. L'expression des gènes codant pour le récepteur A1 de l'adénosine (ADORA1) et la prostaglandine D2 synthase (PTGDS), impliqué dans les ischémies myocardiques et la progression de l'athérosclérose, respectivement, était significativement élevée dans le TAE. Cette étude est une première étape pour comprendre le rôle biologique du TAE et ses implications dans les maladies cardiovasculaires.

Abstract

Increased visceral adipose tissue has been associated with the development of cardiovascular diseases (CVD). Epicardial adipose tissue (EAT) is the visceral fat depot located on the surface of the heart especially around the epica rdial coronary vessels with extension into the myocardium. The proximity of EAT to the coronary arteries suggests a role in the pathogenesis of coronary artery disease (CAD). EAT thickness was significantly correlated with the severity of CAD. However, the biological functions of EAT and its relationship with the development of CVD remain largely elusive. The objectives of this study were to identify genes that were up- or down-regulated among three distinct adipose tissues, namely EAT, mediastinal and subcutaneous using whole-genome gene expression microarrays and to study the possible relationships of these genes with the development of CVD.

Overall, the transcriptional profiles of EAT and mediastinal adipose tissue were similar compared to subcutaneous adipose tissue. Despite this similarity, a number of genes involved in cardiovascular diseases were up-regulated in EAT. The expression of the adenosine A1 receptor (ADORA1), involved in myocardial ischemia, was significantly up-regulated in EAT. Levels of the prostaglandin D2 synthase (PTGDS) gene, recently associated with the progression of atherosclerosis, were significantly different in the three pairwise comparisons (epicardial > mediastinal > subcutaneous). Overexpression of ADORA1 and PTGDS in EAT may confer cardioprotection against myocardial ischemia and CAD. This study is an important first step to understand the biological function of EAT and its potential implications in CVD.

Avant-Propos

The present “mémoire” shows the results of a microarray experiment comparing the gene expression of epicardial, mediastinal and subcutaneous adipose tissues of individuals with CAD. There are three sections in this “mémoire”. The first chapter provides an introduction to cardiovascular diseases and risk factors, obesity, and adipose tissues. This chapter also summarizes the current knowledge about epicardial adipose tissue and the experimental approaches that we used. The second chapter is a scientific manuscript presenting the results of this study. This manuscript was recently submitted to the journal PLoS ONE and is currently under review. In addition, the results of this project were presented in local scientific meetings and at the 60th Annual Meeting of the American Society of Human Genetics (ASHG) that was held in Washington, DC, November 2-6, 2010. Finally, chapter III presents a general conclusion of the study.

The manuscript was written by Sandra Guauque-Olarte and Dr. Yohan Bossé with the contributions of five co-authors. The experimental design was conceived by Dr. Bossé and Dr. Patrick Mathieu. The experiments were performed by Sandra Guauque-Olarte, Nathalie Gaudreault, and Dominique Fournier. Sandra Guauque-Olarte, Dr. Patrick Mathieu, Dr. Pascale Mauriège, and Dr. Yohan Bossé contributed to the biological interpretation of the data. All authors participated in data analysis and revision of the manuscript.

I would like to thank Dr. Yohan Bossé for giving me the opportunity of being part of his research group. His guidance and advices make me a better scientist. I also want to acknowledge Nathalie Gaudreault and Dominique Fournier for training me with the laboratory techniques. Their patience and moral support help me to achieve my objectives during this part of my life. I thank the bioinformatics support of Maxime Lamontagne and Justin Dang Uy Nguyen. During the last two years, I have improved

my critical thinking, writing skills, and technical abilities. Thanks to all my research colleagues.

I want to thank Dr. Patrick Mathieu and his research group, especially Diala el Husseini and Valérie Ducharme. Dr. Mathieu shared his clinical and biological knowledge with me, and helped me to better understand the clinical implications of my project. I also thank Dr. Pascale Mauriège for her time and important contributions to this project.

My sincere acknowledgment to Émilie Pelletier Beaumont, Mélanie Côté, and Benoit Arsenault for sharing with me their experiences with graduate studies.

I want to thank my two families, Guauque-Olarte and Lopez-Acevedo, my aunt Transito, my sister and best friend Luz Angela, and my friends around the world. They provide constant support and love even from the distance. Finally, my special thanks to Carlos for making my life easier every day far from my family with his love.

To my lovely nephew, Beto.

Table of Contents

Table list

Figure list

Abbreviations

AA	Arachidonic acid
ADORA1	Adenosine A1 receptor
ADRA2A	Alpha-2A-adrenergic receptor
Apo	Apolipoprotein
BMI	Body mass index
CAD	Coronary artery disease
CABG	Coronary artery bypass grafting
CCL2	CC-chemokine ligand 2
CRP	C-reactive protein
CVD	Cardiovascular disease
EAT	Epicardial adipose tissue
FFA	Free fatty acids
GAPDH	Glyceraldehyde-3-phosphate dehydrogenase
GWAS	Genome-wide association study
HDL	High-density lipoprotein
IMT	Intima-media thickness
IL-6	Interleukin-6
LDL	Low-density lipoprotein
LIPE	Hormone sensitive lipase
MRI	Magnetic resonance imaging
mRNA	Messenger RNA
PAI-1	Plasminogen activator inhibitor-1
PCR	Polymerase chain reaction
PTGDS	Prostaglandin D2 synthase
PVAT	Perivascular adipose tissue
RNA-Seq	RNA-sequencing
qPCR	Quantitative real-time PCR
SMCs	Smooth muscle cells
TNF-α	Tumor necrosis factor-α

Chapter I

Introduction

Cardiovascular disease (CVD) is the number one cause of death globally[1]. Obesity is a risk factor for developing CVD[2,3]. In obesity, the excess of adipose tissue can be preferentially accumulated in either the abdominal subcutaneous or visceral compartments. The latter is considered more atherogenic. Increase of visceral fat is closely related with the amount of ectopic fat in the liver, the muscles and the heart[4]. Epicardial adipose tissue (EAT) is the visceral adipose depot located on the surface of the myocardium and surrounding the coronary arteries[5]. EAT is increased in obesity. The thickness of EAT is associated with coronary artery disease (CAD) and is utilized as a new tool for cardiometabolic risk assessment[6]. We used gene expression microarrays, a tool to compare the gene expression profile, in order to identify genes differentially expressed between three adipose tissues compartments, namely epicardial, mediastinal and subcutaneous.

The chapter I of this "mémoire" comprises a literature review about obesity, adipose tissue and its consequences on the development of CVD. This chapter also provides a description of CAD and risk factors. Chapter I also contains a definition of EAT, its location, and a summary of studies associating this adipose tissue with the presence and severity of CAD. In addition, the techniques used to measure the volume and thickness of EAT are described. Finally, an explanation of the microarrays and quantitative real-time PCR (qPCR) technologies is presented, along with key terms that allow the interpretation of microarray results.

Section 1

1.1 Coronary artery disease

CVD is the principal cause of death globally[1,7]. Among the CVD, CAD causes the majority of deaths per year[7] and it is mostly mediated by atherosclerosis[8], which is a complex condition that results in reduced or absent blood flow in one or more of the arteries that encircle and supply the heart. Atherosclerosis is a progressive disease characterized by the accumulation of lipids and fibrous elements in the large arteries[8]. It is traditionally viewed as a disease of the vascular intima, following endothelial cell dysfunction, inflammatory cell recruitment[9], and foam cell formation. More recently, dysfunction of medial smooth muscle cells (SMCs) and adventitial cells has also been demonstrated to play a role in the pathogenesis of atherosclerosis.

Atherosclerosis begins with the formation of fatty streaks, which are small lesions consisting of subendothelial accumulations of cholesterol-engorged macrophages or foam cells. These lesions are the precursors of more advanced lesions characterized by the accumulation of lipid-rich necrotic debris and SMCs[9]. Lipoprotein particles accumulate in the intima at sites of lesion. Then monocytes and lymphocytes adhere to the surface of the endothelium and migrate across the endothelial monolayer into the intima. The monocytes differentiate into macrophages and form the foam cells[10]. When foam cells die, a lipid-rich necrotic core is formed. SMCs migrate to the intima from the medial layer and secrete collagen to form a plaque[8]. Atheromatous plaques can become increasingly complex with calcification, ulceration at the luminal surface, and hemorrhage from small vessels that grow into the lesions from the media of the blood vessel wall[8,11]. Advanced lesions can be sufficiently large to block blood flow causing episodes of angina due to ischemia of the heart muscle. Ruptures of the plaques can also cause the formation of thrombus that results in acute occlusion of the blood vessels[9], resulting in myocardial infarction or stroke[8,10,12].

1.2 Risk factors of CAD and their genetic component

Known risk factors for the development of CAD are gender, type 2 diabetes, hypertension, obesity, high levels of total and low-density lipoprotein (LDL) cholesterol, low levels of high-density lipoprotein (HDL) cholesterol, and elevated levels of triglycerides, lipopoprotein (a) [Lp(a)], homocysteine, fibrinogen and C-reactive protein (CRP)[13]. All these risk factors have a significant genetic component with heritability ranging from 20 to 80%[8]. Behavioral risk factors of CAD include smoking, diet, exercise, infection, fetal environment, and air pollution[8,13]. Many common genetic variants have been significantly associated or linked to CAD risk factors by using the candidate gene and genome-wide linkage approaches[14]. Polymorphisms in genes encoding the LDL receptor, apolipoproteins (apo) and Lp(a) were shown to explain part of the variations in plasma cholesterol levels[8]. Similarly, genetic variants in the hepatic lipase gene were shown to affect HDL-cholesterol levels[8]. Other genes were implicated in blood pressure as the angiotensinogen[15] and the β2-adrenergic receptor[16].

Recently, genome-wide association studies (GWAS) have led to the identification of novel susceptibility alleles for CAD risk factors such as body mass index (BMI)[17,18], plasma lipid levels[19], and circulating markers of inflammation[20]. This methodology uses the information of hundreds of thousands of single nucleotide polymorphisms (SNPs) in the human genome. SNPs in the fat mass and obesity associated gene were convincingly associated with BMI[17] and with obesity in adults and children[18,21]. Seven loci for CRP levels were also identified[21]. These loci harbor genes that were previously implicated in the metabolic syndrome (APOE), insulin resistance (LEPR), and atherosclerosis (IL6R, CRP)[21]. A meta-analysis involving more than 100 000 individuals gathered from 46 lipid GWASs[19] identified 95 significant loci for plasma concentrations of total cholesterol, LDL-cholesterol, HDL-cholesterol and triglycerides. Among them, well-known drug targets for the treatment of hyperlipidaemia, namely HMGCR (statins) and NPC1L1 (ezetimibe)[19]. It should be

noted that in all these GWASs, many SNPs identified were located in intergenic regions or in genes of unknown function and will require additional investigations.

Section 2

2.1 Obesity as a risk for cardiovascular diseases

Obesity has reached global epidemic proportions in both adults and children[22]. Obesity is known to cause adverse effects on people's health, such as insulin resistance, hypertension, dyslipidemia, systemic inflammation, prothrombotic state, and CAD[23,24]. Nowadays obesity is considered an independent risk factor of CVD[2,3]. Epidemiological data have established a close association between obesity and increased cardiovascular morbidity and mortality[25,26]. Many studies have tried to identify the molecular mechanism linking obesity and CVD. Inflammation is a common factor in both diseases[24]. Inflammation increases with obesity and particularly with the accumulation of visceral adipose tissue[4,27]. The consequences of obesity on CVD and type 2 diabetes are suspected to be mediated by dysfunctions of adipose tissue such as the increase lipid storage capacity of the adipose cells (adipocytes), enlargement of adipocytes, and insulin resistance[28]. Enlarged adipocytes have a reduced buffering capacity for lipid storage, exposing other tissues to an excessive influx of lipids, leading to ectopic fat deposition and insulin resistance in situations where energy intake exceeds energy expenditure[29]. Obesity contributes to CVD via other pathological mechanism like atherosclerosis, hypercoagulability, and platelet dysfunction[27].

Figure 1 describes the mechanisms linking obesity and CAD or CVD. The pathogenic pathways involve the production of inflammatory cytokines such as tumor necrosis factor-α (TNF-α) and interleukin-6 (IL-6) by adipose tissue, insulin resistance, endothelial dysfunction via plasminogen activator inhibitor-1 (PAI-1) and inter-cellular adhesion molecule 1 (ICAM-1)[30].

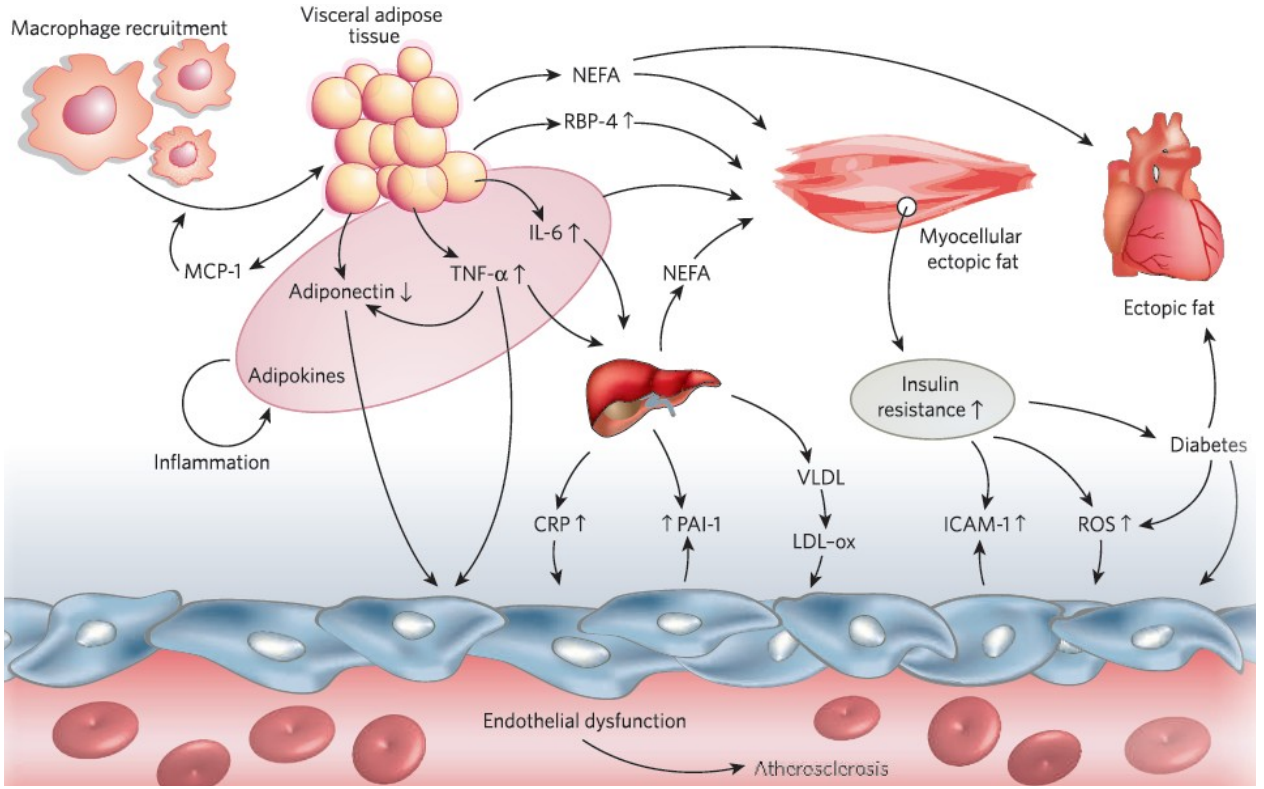

Figure 1. Both visceral fat and insulin resistance may contribute to cardiovascular disease in obesity. visceral fat contributes to endothelial dysfunction through the direct effect of adipokines, mainly adiponectin and tumor necrosis factor- α (TNF-α), which are secreted by fat tissue after macrophage recruitment (through monocyte chemoattractant protein-1, CCL2 or MCP-1). Indirect effects of TNF-α and interleukin-6 (IL-6) might influence inflammation (C-reactive protein, CRP) and endothelial dysfunction. Insulin resistance induced by IL-6, TNF-α and adiponectin, non-esterified fatty acids (NEFA) and retinolbinding protein 4 (RBP-4) may induce oxidative stress and subsequent endothelial dysfunction [Plasminogen activator inhibitor-1 (PAI-1) and inter-cellular adhesion molecule 1 (ICAM-1)]. Fat accumulation, insulin resistance, liver-induced inflammation and dyslipidemia may all lead to the premature atherosclerotic process[30]. Figure license number: 2571541128373.

2.2 Adipose tissue as an active organ

Adipose tissue is now considered a metabolically active organ that produces hormones and pro-inflammatory factors, contributing to the adverse cardiovascular consequences of obesity[31,32,33]. In addition to its energy storage role, the excess or deficiency (lipodystrophy) of adipose tissue might regulates many pathological conditions such as hyperglycemia, hypertension, and the metabolic syndrome in both humans and rodents[31,34]. In addition to adipocytes, which is the most abundant cell type,white adipose tissue also contains pre-adipocytes, endothelial cells, fibroblasts, leukocytes and macrophages[31,33,35] (Figure 2). Resident macrophages in adipose tissue could originate from either blood monocytes[36] or transdifferentiate from local pre-adipocytes[37]. Heterogeneity of cell types in adipose tissue is likely to ensure the different functions of this tissue in metabolism and the immune response[35,38].

Various adipose tissue-derived molecules have been characterized and are referred to as adipokines[39]. Adipokines are expressed by adipocytes and/or the non-adipocyte fraction of adipose tissue[40]. Adipokines are thought to provide an important link between obesity, insulin resistance and related inflammatory disorders. The most well-known adipokines are adiponectin, leptin, resistin and visfatin. Adiponectin inhibits monocyte adhesion, macrophage transformation, and proliferation and migration of SMCs in blood vessels[41]. Leptin mediates the suppression of the reproductive, thyroid and growth hormones, and modulates appetite, sympathetic nerve activity, thermogenesis, and immunity[42,43]. The levels of resistin in plasma correlates with markers of inflammation and is increased in patients with abdominal aortic aneurysm, CAD[44] and heart failure[45]. Visfatin is linked to several inflammatory conditions, β-cell function and CVD[46]. Other molecules produced by adipose tissue are the cytokines TNF-α, IL-6, IL-1 and CC-chemokine ligand 2 (CCL2 or MCP-1) as well as mediators of the clotting process such as PAI-1 and certain complement factors[31,35,47]. Most adipokines play important roles at the interface between the immune and metabolic systems[35,48].

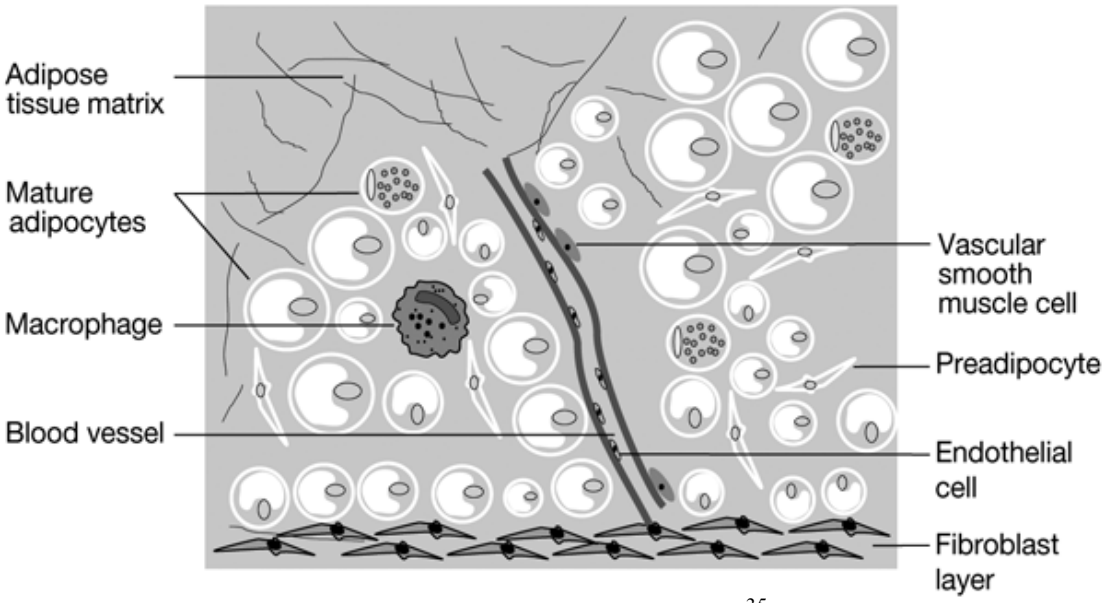

Figure 2. Different cell constituents of adipose tissue[35]. Figure license number: 2571541414527.

2.3 Adipose tissue distribution and risk for cardiovascular diseases

Many studies have demonstrated that it is not only the excess of adipose tissue that is relevant for the development of CVD, but also its distribution[4,49]. Individuals with increased intra-abdominal fat accumulation have atherogenic lipid profiles and have an increased CVD risk[50]. The mechanisms contributing to preferential accumulation of adipose tissue in certain anatomical regions are still elusive[51]. Different adipose depots have different characteristics[52] and functions[53] as supported by several studies performed mainly in abdominal visceral and subcutaneous adipose tissues. Visceral adipose tissue is considered to be more pathogenic than the subcutaneous adipose depot, which might be due to its proximity with the organs regulating metabolism[4,54]. Waist circumference, a measurement of visceral adiposity, is a significant predictor of morbidity and mortality independently of BMI[55]. Waist circumference was associated with increased risk of CAD in women[56] and myocardial infarction in men and women[57]. In addition, visceral fat measured by computed tomography is an independent predictor of mortality in men[55]. Although epidemiologic studies demonstrated that excess visceral fat is a factor that increases metabolic[55] and

cardiovascular disease risk[58,59,60], the mechanistic link remains not fully understood[58,59,60].

Under normal conditions, part of the increase energy surplus, frequently caused by a high fat and sugar diet and/or a sedentary lifestyle, is stored in the subcutaneous abdominal adipose tissue[61]. An absence, deficiency or dysfunction of this tissue, can cause a preferential storage of the energy excess in intra-abdominal fat[61], the accumulation of ectopic fat in the liver and muscles as well as an increase in perivascular fat (PVAT) and EAT[4]. Recent studies have linked ectopic fat accumulation, as cardiac (EAT or intra-myocardial fat) and/or visceral and/or hepatic fat, with the development of atherosclerosis, CAD and hypertension[2]. Ectopic fat is the accumulation of triglycerides within cells of non-adipose tissue that normally contain only small amounts of fat[2] and within and around other tissues/organs[62]. Fat in the liver, or liver steatosis, causes hepatic insulin resistance through hepatic overload of free fatty acids (FFA) and increased hepatic gluconeogenesis[52,63,64]. Subjects with non-alcoholic fatty liver disease present increased insulin resistance in liver, muscle and adipose tissue, and the phenomenon increases with the degree of obesity[63,65]. Fatty liver is recognized as a risk factor for CVD[66]. Triglycerides accumulating ectopically in muscles are also associated with lipotoxicity and impaired glucose metabolism[67,68].

As mentioned above, an increase in visceral adipose tissue has been associated with the development of CVD[4,54,64,69]. This association is believed to be the result of a greater release of FFA into the portal vein from lipolysis of visceral fat, leading to an increase of circulating FFA. Differences in adipose tissue metabolism have been found in different regions of the body[62]. The male upper body segment obesity is a risk factor for obesity-linked diseases whereas the female femoro-gluteal lower body segment obesity is less harmful[70]. New studies suggest that anatomically separated

adipose tissue depots are functionally diverse, originate from distinct precursor cells and exert both systemic and paracrine effects on tissue and organ function[71].

Visceral fat has a unique inflammatory profile. Compared to subcutaneous abdominal fat, intra-abdominal visceral fat expresses higher levels of inflammatory biomarkers such as chemokine receptor 2 (CCR2) and macrophage migration inhibitory factor (MIF)[72]. In addition, visceral fat expresses higher levels of IL-6 and TNF-α[27]. When compared with BMI-matched controls with increased subcutaneous fat, subjects with increased amounts of visceral fat presented increased circulating levels of CRP, TNF-α, IL-6, PAI-1[27], and are thus at increased risk of CVD[27,73]. ApoE−/− mice transplanted with visceral adipose tissue showed larger atherosclerotic lesions and a significant elevation in plasma CCL2 than sham-operated mice. Moreover, transplantation of subcutaneous adipose tissue does not increase atherosclerosis, suggesting that visceral and not subcutaneous fat contributes to atherosclerosis[74,75].

2.4 Perivascular adipose tissue

PVAT is the adipose tissue that surrounds most of the arteries[76]. Even though most of the systemic arteries (except the cerebral vasculature) are surrounded by PVAT, functional roles of this adipose tissue other than being a structural support of blood vessels has not been well studied[77]. EAT, located over the myocardium and the coronary arteries, and PVAT are known contributors to atherosclerosis and CAD development[78]. Reactive fibroblasts and inflammatory cells in the adventitia of the arteries have been the focus of extensive investigations, while perivascular adipocytes that reside at the adventitial border of atherosclerosis-prone blood vessels, remain poorly studied. Numerous factors secreted by adipocytes might potentially modulate the development of vascular disease, including pro-inflammatory cytokines and adipokines, angiogenic molecules, and stem cell homing factors[71]. PVAT secretes higher pro-inflammatory cytokines such as IL-6, IL-8, and CCL2 than subcutaneous adipose tissue[75,77]. PVAT surrounding atherosclerotic regions of the aorta contains dramatically more CD68+ macrophages and CD3+ T-lymphocytes than PVAT

covering normal arteries, suggesting greater inflammatory cell infiltration[79]. The absence of a barrier between PVAT and the adventitia suggests that factors secreted by PVAT might access the blood vessel wall, and may indicate a possible function of PVAT as a paracrine organ that transduces metabolic signals to blood vessels[32,77]. In addition, it is known that PVAT exerts paracrine influences on blood vessel contractility[71,80].

Section 3

3.1 Epicardial adipose tissue

3.1.1 Origin and distribution of epicardial adipose tissue

EAT originates from the splanchnopleuric mesoderm, the same origin of omental and mesenteric fat[78], and is considered to be the "real" visceral fat on the surface of the human heart[5]. PVAT around the coronary arteries is part of the EAT[76]. The amount and location of EAT have been assessed by autopsy and imaging studies in normal, hypertensive, and CAD patients, in both males and females. EAT is located on the atrioventricular and interventricular grooves, and around the epicardial coronary vessels. EAT is also found around the atria, over the free wall and the apex of the right ventricle, and it can extend into the myocardium. However, the major part of EAT is located on the lateral right ventricular wall[78,81,82,83,84] (Figure 3).

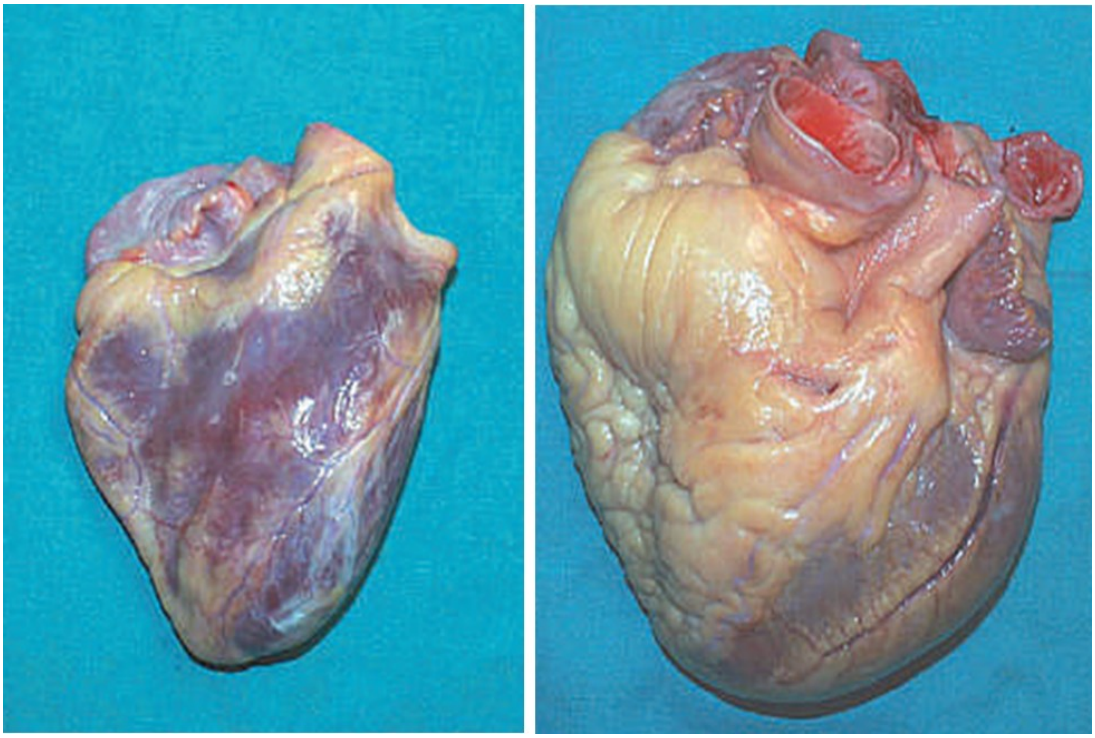

Figure 3. Macroscopic appearance of EAT in the anterior site of a normal (210 g) and a hypertrophic (900 g) heart, respectively. EAT correlates with the weight of the heart. Adapted from Iacobellis et al.[85]. Figure license number: 2571550248181.

EAT is present in wild and domesticated animals like monkeys, rabbits, and pigs but is almost absent in laboratory rodents. The presence of EAT is not a consequence of ageing, obesity or a sedentary lifestyle since it is present in lean wild mammals. Thus, it may have a physiological role[82].

3.1.2 Quantification of epicardial adipose tissue

The amount and thickness of EAT have been studied by autopsies and from different methods like multi-detector computer tomography, magnetic resonance imaging (MRI), and echocardiography. Autopsy studies have revealed that EAT accounts for approximately 20% (ranging from 15% to 25%) of the mass of the heart[5,78]. Shirani et al.[86] studied 30 male and female patients without clinical evidence of cardiac disease, and found that adipose tissue comprised 4% to 52% (mean 22 ± 11) of the total heart weight (mean weight of adipose tissue being 105 ± 83 g). Corradi et al.[84] studied 66 males and 51 females, divided in four groups of normal, ischemic, hypertrophic, and hypertrophic–ischemic hearts. They found that EAT accounts for 14.7% of the total heart weight and 20.7% of the total ventricular weight. In addition, they observed that the ratio of EAT and cardiac muscles did not change in the presence of myocardial ischemia or hypertrophy. In the presence of cardiac hypertrophy, there was a positive correlation between the amount of EAT and the underlying myocardium mass. In a study of 148 autopsies of subjects (55% males, age ranging from 6 months to 68 years) who died from non-cardiac consequences, the amount of EAT in the lateral right ventricle wall in both male and female subjects increased with age, with statistical analyses showing significant differences between subjects aged 0–19 years, 20–39 years and 40 years and over[87] (Figure 4).

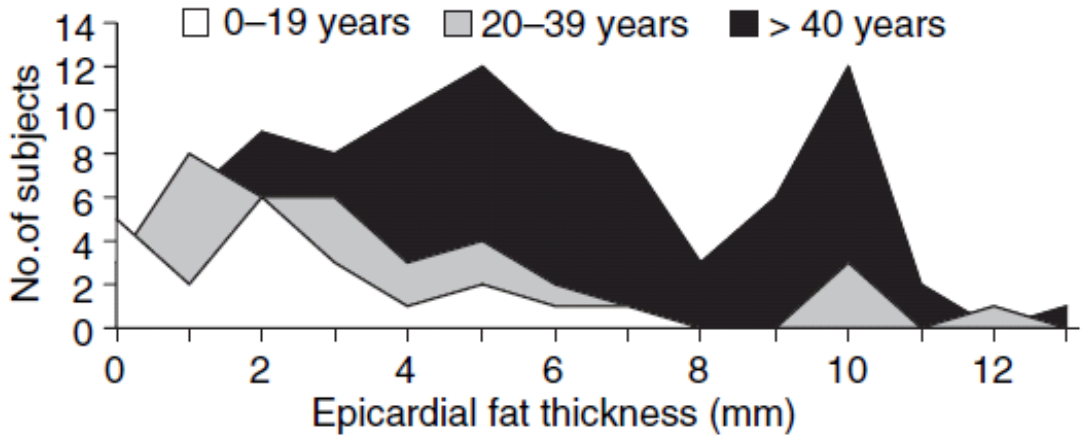

Figure 4. Thickness of EAT in lateral right ventricle wall by age. The amount of EAT in the right ventricle increases with age. The greatest amount of fat was seen in subjects over 40 years of age[87]. Figure license number: 2571561420805.

EAT thickness measured by echocardiography on the free wall of the right ventricle varies from 1.1 mm to 22.6 mm, with a mean of 7 mm in men and 6.5 mm in women[50,88]. Iacobellis et al.[88] analyzed 246 patients (48.8% males) with a median BMI of 32 kg/m^2. Natale et al.[50] studied 459 patients (58% males) with grade I and II essential hypertension and mean BMI of 28.0 ± 4.0 kg/m^2, and 50 normal volunteers. Another study[89] reported a mean EAT of 6.38 mm (ranging from 1.10 mm to 16.55 mm) among 203 patients who underwent echocardiography and diagnostic coronary angiography with a mean BMI of 24 kg/m^2. In all cases, EAT was identified as an echo-free space in the pericardial layers on the two-dimensional echocardiography, and its thickness was measured perpendicularly on the free wall of the right ventricle at end-diastole for three cardiac cycles, with a modification made by Iacobellis et al.[88] who measured the thickness at end-systole. Furthermore, EAT can appear as a hyperechoic space if it is massive[88].

Abbara et al.[83] measured the thickness of EAT by 16 slice multi-detector computed tomography in 59 patients (69% males) and found a mean EAT thickness of 5.3 ± 1.6 mm. Patients over 65 years had 22% greater amount of EAT than patients younger than 65. Although MRI is the gold standard to assess visceral fat, it is costly[90], and

has significant limitation in terms of its lower spatial resolution[83]. Iacobellis et al.[90] compared EAT thickness by MRI and echocardiography and found a high correlation between the measurements obtained by the two methods ($r = 0.91$, $p = 0.001$). Abbara et al.[83] suggested that echocardiography cannot provide an adequate window of all cardiac segments and is highly dependent on acoustic windows, which are inadequate for assessment in obese patients. Despite this fact, echocardiography is currently used to measure EAT thickness and amount. It is a non-invasive method routinely performed in high-risk cardiac patients and less expensive than MRI. Additionally, echocardiography provides data on traditional cardiac parameters, as well as left ventricular mass, diastolic and systolic functions[88].

3.1.3 Functions of epicardial adipose tissue

In the 18th and 19th centuries, physicians attributed cases of sudden death to the fatty heart. Although they noticed the importance of the fat covering the heart[78,91], only a small number of studies have been made to understand the physiology of EAT, which may be due to the absence of EAT in experimental animals like mice and rats[82]. It is only in recent years that the interest for EAT has relived. Accordingly, the function of EAT is not completely understood, but some putative physiological role has been assigned to this tissue from observational data and by comparing EAT with other adipose tissue such as abdominal subcutaneous and omental. Some function ascribe to EAT are: a lipid-storing depot[78,81,85], an endocrine organ, and an inflammatory tissue secreting cytokines and chemokines[92,93]. Furthermore, its proximity to the adventitia of the coronary arteries and the underlying myocardium suggests a role in the pathogenesis of CAD[5,78].

EAT might maintain fatty acid and energy homeostasis in the coronary microcirculation. EAT is also known to collect the excess of circulating fatty acids, which is the principal source of energy of the heart[78]. Excess of fatty acids in the heart can induce cardiotoxicity and interfere with the generation and propagation of the contractile cycle of the heart that in turn can cause ventricular arrhythmias and

alterations in repolarization[85,94]. It was shown that enhanced incorporation and oxidation of fatty acids by the myocardium in obesity, diabetes, and ischemia cardiomyopathy contributes to the development of cardiac lipotoxicity[95]. The mechanisms for this lipotoxicity is not fully elucidated but the accumulation of toxic intermediates of fatty acid metabolism, suppression of glucose utilization, and uncoupling of oxidative metabolism from electron transfer were suggested[96]. Due to its high rate of lipolysis, EAT might serve as a source of FFA to supply myocardial energy when demand increases such as during exercise or under ischemic conditions[78,85]. EAT secretes adiponectin, adrenomedulin, and omentin, which might have a role in regulating energy substrate and Ca^{2+} metabolism[91].

The EAT of 44 patients who underwent coronary artery bypass grafting (CABG) surgery and six who underwent heart valve replacement were recently studied[97]. Briefly it was found that EAT expresses markers of non-shivering thermogenesis that are observed in brown adipose tissue such as uncoupling protein-1, and the brown adipocytes differentiation transcription factors PR-domain-missing 16 and peroxisome-proliferator-activated receptor γ co-activator-1α. In fact, the expression levels of these markers were higher in EAT compared to substernal and subcutaneous thoracic, omental, and leg adipose tissues. This study suggests a possible role of EAT to act as brown fat to protect the myocardium and coronary vessels against hypothermia.

EAT surrounds the coronary arteries. It was proposed that EAT might serve as structural support of the blood vessels preventing the torsion induced by arterial blood wave and cardiac contraction[78]. EAT might also have vasoactive properties. It is known that PVAT have anticontractile effects as seen in studies using medium and large arteries[80,98]. PVAT in patients with obesity and metabolic syndrome completely lost this property. In vitro experiments in animal and human small arteries suggested that hypoxia and inflammation attenuated the local vasoactive properties of PVAT by oxidative stress[98]. In addition, the loss of function of perivascular adipose tissue have

been related with increased blood pressure[98], a strong risk factor for coronary and non-coronary cardiovascular events and mortality[99]. EAT surrounding the coronary arteries may also exert positive arterial remodelling[100], which is the mechanism that maintains the luminal size despite the development of an atherosclerotic plaque allowing the asymmetrical expansion of the vessel wall and accommodation of atherosclerotic plaques[101]. If a coronary vessel was constrained by the myocardium, the ability to expand and accommodate atherosclerotic plaques would be restricted[100]. Indeed, previous studies in humans and rabbits demonstrated that segments of an artery surrounded by EAT developed atherosclerosis at a faster rate compared to the intra-myocardial segments of the same artery[102]. Taken together, EAT may exert both beneficial and damaging effects on cardiac physiology. It is extremely important to clarify the functions of EAT and its contribution in the development and/or progression of heart diseases.

3.1.4 Epicardial adipose tissue and inflammation

EAT produces pro-inflammatory cytokines and chemokines[103]. In a study comparing EAT with leg subcutaneous fat in 42 patients who underwent CABG (86% males, mean BMI = 31 ± 1 kg/m^2), Mazurek et al.[92] found that EAT exhibited significantly higher mRNA and protein levels of CCL2, and inflammatory cytokines such as IL-1β, IL-6, IL-6 receptor, and TNF-α. Cytokine levels expressed in EAT did not correlate with their plasma levels. In addition, they performed a microarray experiment in a subgroup of patients (n = 11) and found high expression of genes involved in immune response like the immunoglobulin-κ 1-39. The results were independent of obesity, diabetes, or therapies with statin or ACE inhibitors. Another study[104] have correlated the thickness of EAT with the plasma levels of CCL2 and soluble IL-6 receptor/IL-6 measured by ELISA in 42 subjects, fifteen normal weight patients and 27 severely obese women (BMI 43.5 ± 4.8 kg/m^2). Vohl et al.[105] showed high expression levels of IL-6 and other cytokines in omental compared to abdominal subcutaneous. Inflammatory mediators in EAT also differ between patients with or without CAD. Comparing 46 patients with CAD (80.4% males, BMI = 24.9 ± 3.8 kg/m^2) and 12

with non-CAD (75% males, BMI = 24.9 ± 3.7 kg/m^2), protein levels of TNF-α, IL-6, leptin and vistatin measured by ELISA were found to be higher in omental fat and EAT of patients with CAD[106]. In EAT the levels of the pro-inflammatory chemokine (C-C motif) ligand 5 were increased in patients with CAD[25]. In contrast, the protein levels of the anti-inflammatory adipokine adiponectin was significantly lower in EAT from CAD compared to non-CAD patients[25,107].

A recent study by Company et al.[58,59] concluded that EAT is not homogeneous in its inflammatory response to aerobic exercise training in a pig model of familial hypercholesterolemia with CAD. EAT surrounding the coronary arteries remained pro-inflammatory after chronic exercise. In contrast, the training regimen reduced the inflammatory response of peri-myocardial EAT. Although EAT covering the myocardium and omental fat shared similar inflammatory profiles, their metabolic mRNA responses to exercise was different. IL1-Ra, IL-6, IL-8 mRNA levels were measured in this study. The pro-inflammatory properties of EAT are now being more studied as they are increasingly recognized as possible therapeutic targets in the prevention and/or treatment of CAD.

3.1.5 Consequences of weight loss on epicardial adipose tissue

Few studies have analyzed the effect of weight loss on EAT volume. In a study conducted by Kim et al.[108], 27 moderately obese men (age 45.8 ± 1.7 years; BMI 30.5 ± 0.7 kg/m^2) followed a daily low-calorie diet as part of a clinical 12-week weight loss interventional study. EAT thickness, evaluated by transthoracic echocardiography, diminished by 17%, which is less than other adipose tissue depots such as the omental compartment that decreased by 33%. In this study, EAT and omental fat reduction positively correlated ($r = 0.802$, $P < 0.001$). In 20 severely obese subjects (40% males, age 35 ± 10 years, BMI 45 ± 5 kg/m^2) who underwent 6-month very low calorie diet weight loss program, echocardiography EAT thickness diminished 30% and faster than overall body weight loss[109]. In this study the authors did not mention the percentage of reduction of other adipose tissue compartments.

Similar results were observed by Willens et al.[110], who analyzed EAT changes in an echocardiography retrospective study of 23 severely obese patients (35% males, BMI = 54 ± 12 kg/m^2) after 8.3 ± 3.7 months of a bariatric surgery. In general, the magnitude of the decrease in EAT was related to initial EAT thickness. In this context, diet-induced weight loss, bariatric surgery, and very low-calorie diets allow non-pharmacological reduction of EAT.

3.1.6 Differences with other adipose tissue compartments

The comparison of different adipose depots has provided clues about the function of EAT. In addition to the high expression of inflammatory mediators, a number of properties differentiate EAT from other fat depots. Adipocyte size was smaller in EAT compared to omental or perirenal fat in sheeps[111]. In a study involving 11 CAD patients and 10 men undergoing valve replacement (BMI = 27.3 ± 4.41 kg/m^2), the size of adipocytes was smaller in EAT compared to subcutaneous and peritoneal fat. In the whole cohort, adipocytes sizes were 92.19 ± 7.97 μm, 82.50 ± 10.69 μm, and 73.65 ± 8.25 μm in subcutaneous (at the sterni level), peritoneal and EAT, respectively. EAT adipocyte size correlated positively with insulin resistance and serum leptin, and negatively with serum and mRNA expression of adiponectin. In CAD patients, EAT adipocytes were bigger compared to subjects who underwent valve replacement (79.49 ± 7.73 vs. 68.62 ± 6.13 μm, respectively; $P < 0.01$)[112]. The pro-inflammatory profile of large adipocytes is greater compared to smaller adipocytes[112].

Low mRNA expression for several key enzymes implicated in lipogenesis (lipoprotein lipase, stearoyl-CoA desaturase and acetyl-CoA carboxylase-α) was found in EAT compared to 6 other adipose depots[111]. Furthermore, the expression of lipoprotein lipase and acetyl-CoA carboxylase-α positively correlated with the size of adipocytes[111]. The fatty acid profile of EAT also differed compared to other fat depots. The distribution of fatty acids – palmitic (C16:0), palmitoleic (C16:1), stearic (C18:0) and oleic (C18:1) in EAT was similar to omental and perirenal fat but

different from sternal and popliteal fat in sheeps[111]. Fatty acids could modulate metabolic processes like glucose metabolism and lipid storage. In young adult guinea pigs, the rate of FFA release by EAT was twice that of perirenal fat, indicating increased lipolytic activity in EAT[82]. In humans, Pezeshkian et al.[113] studied fatty acid composition of EAT and leg subcutaneous adipose tissue collected from 42 patients with CAD (81% males, BMI = 27.6 ± 4.5 kg/m^2). EAT contained more proportions of saturated fatty acids, including myristic (C14:0), palmitic (C16:0), and stearic (18:0) acids and lower proportions of the unsaturated fatty acids, including palmitoleic (16:1n-7), oleic (18:1n-9), linoleic (18:2n-6), and linolenic (18:3n-3) acids and monounsaturated fatty acids. These differences in fatty acid composition suggest a depot-specific impact of stored fatty acids on adipocyte function and metabolism, such as the rate of deposition and mobilization, and perhaps the rate of endogenous synthesis of fatty acids. A high rate of incorporation of fatty acids was also seen in EAT compared to other fat depots[78]. Finally, compared to intra-abdominal fat (perirenal and omental) glucose utilization was lower in EAT[82].

3.1.7 Microarray experiments in epicardial adipose tissue

The metabolic differences observed in EAT suggest specific gene regulation patterns in this adipose depot. Only two studies have compared genome-wide transcriptional profiles of EAT with subcutaneous adipose tissue from the same individuals[92,114]. The study of Mazurek et al.[92] compared EAT with leg subcutaneous fat in a subset of 11 out of 42 patients with CAD (86% males, mean BMI = 31.0 ± 1.0 kg/m^2). Microarrays were performed with the Affymerix human U133A chips that evaluated 14 585 genes. A total of 1003 genes were differentially expressed between EAT and the leg subcutaneous adipose tissue. 805 of those genes were upregulated and 198 were downregulated in EAT. Up-regulated genes included inflammatory and immune response genes like CCL2, 3, 11, and 21, IL6, IL7, and the immunoglobulin-κ 1 to 39.

Dutour et al.[114] showed overexpression of the secretory type II phospholipase A2 (sPLA2-IIA) in EAT compared to chest subcutaneous fat using pangenomic cDNA

microarrays. sPLA2-IIA is the enzyme which catalyzes the rate limiting step in the formation of pro-inflammatory lipid mediators. The study cohort consisted in two groups of 30 subjects who underwent cardiac surgery for CAD, valve replacement or myxoma resection. The microarray experiment identified 1751 genes overexpressed in EAT compared with subcutaneous fat in CAD subjects and 263 genes overexpressed in EAT compared with subcutaneous fat in non-CAD subjects. So far, no study has compared the genome-wide mRNA profile of EAT with mediastinal and subcutaneous adipose tissue from the same individuals.

The two microarray studies described above[92,114] compared gene expression of EAT to subcutaneous adipose tissue and suffer from a number of limitations. The study of Mazurek et al.[92] focused on the inflammatory mediators present in EAT and was limited to 14 585 genes. They did not compare CAD with non-CAD patients and the study population was composed of men and women. Men and women are characterized by important differences in adipose tissue distribution, hormones, and production of inflammatory mediators[115], which might all influence the levels of gene expression in the adipose tissues. In both studies the authors did not mention the fold change threshold that was used to consider a gene as significantly differentially expressed. The study of Dutour et al.[114] focused on the expression of the secretory type II phospholipase A2 gene among thousands that were significantly altered between the two adipose tissues compartments. They compared patients with or without CAD, but did not specify sex of the patients.

Section 4

4.1 Epicardial adipose tissue as a marker of cardiometabolic risk and CAD

As mentioned in the previous sections, EAT correlates with the presence of CAD, and is likely to be implicated in the pathogenesis of CAD and cardiomyopathy due to its proximity to the adventitia of the coronary arteries and the underlying myocardium. As described by Iacobellis et al.[90] echocardiographic EAT is a marker of omental fat measured by magnetic resonance imaging. In the latter study, EAT thickness was also correlated to waist circumference ($r^2 = 0.428$, $P = 0.01$), fasting insulin ($r^2 = 0.387$, $P = 0.03$), and arterial blood pressure ($r^2 = 0.387$, $P = 0.02$). EAT thickness correlated with all the features of the metabolic syndrome and was related to inflammation and adverse lipid profile[116]. These correlations suggest that EAT measurement can be used as a marker for cardiometabolic risk stratification[6]. A reduction in EAT also correlated with weight loss–related improvement in both left ventricular mass and diastolic function to a greater extent than with BMI and waist circumference changes[109]. In the study of Pezeshkian et al.[113] which involved 42 patients with CAD, EAT rather than leg subcutaneous fatty acid composition was related to blood pressure.

EAT thickness was significantly correlated with the severity of CAD and is a marker of carotid artery stiffness, an early manifestation of atherosclerosis[50]. In this study EAT thickness higher than 7 mm was more frequent in patients who had higher systolic, diastolic and pulse pressure, and increased left ventricular mass index, carotid intima-media thickness (IMT), diastolic and stiffness parameters compared with those with EAT < 7 mm ($P < 0.001$). EAT thickness positively correlated with age, pulse pressure, stiffness parameters, carotid IMT, systolic blood pressure, and duration of hypertension. In addition, age, carotid IMT, and stiffness parameters were independently related to EAT thickness.

Mean EAT thickness of 9.5 mm in men and 7.5 mm in women should be considered the threshold values for high-risk echocardiographic EAT thickness as suggested by Iacobellis et al.[88]. In this study, 246 patients participated, 58% of which had the metabolic syndrome. Echocardiographic EAT thickness was also correlated with the severity of coronary artery stenosis in patients with known CAD[89,117,118], independently of obesity as defined by BMI ($r = 0.68$, $P < 0.01$)[119]. Significant correlations were found between EAT thickness and age ($r = 0.332$, $P < 0.001$), CRP ($r = 0.182$, $P = 0.009$), BMI ($r = 0.142$, $P = 0.044$) and waist circumference ($r = 0.229$, $P = 0.001$). Patients with higher EAT thickness were associated with a high Gensini's score ($P = 0.014$), a scoring system estimating the severity of CAD[89]. In addition, EAT and peri-coronary EAT thickness correlated with coronary artery calcification, a marker of CAD[120,121]. Table 1 summarizes several studies associating the thickness or volume of EAT with the presence of CAD or the risk of CVD. Mahabadi et al.[122] in a study involving 1267 patients (46.2% males, BMI 28.2 ± 5.1) of the Framingham Heart Study, found an association of both EAT and omental fat volume with CVD including CAD, congestive heart failure, stroke, and myocardial infarction. These associations were statistically significant after adjustment for BMI and waist circumference. Moreover, the amount of EAT measured by computed tomography was associated with obesity and the metabolic syndrome in 60 patients (73% males, 27.0 ± 4.0 kg) with clinically suspected CAD[123].

Table 1. Studies associating the volume or thickness of EAT with CAD and CVD risk.

N (% male)*	Mean BMI ± SD (kg/m^2)	Characteristics of the patients	Method	EAT thickness or volume threshold associated with CAD	EAT thickness or volume threshold associated with CVD	Ref.
72 (50)	33.8 ± 13.7 (males) 34.3 ± 15.4 (females)	MS	Echocardiography		Mean 9.87 ± 2.55 (males) Mean 7.58 ± 3.02 (females)	6
459 (59)	28.0 ± 4.0	Essential hypertension grade I and II	Echocardiography	7 mm		50
246 (48.8)	32.0	MS (58%)	Echocardiography		Mean 9.5 mm (males) Mean 7.5 mm (females)	88
203 (53.2)	24.0	CAD	Echocardiography	7.6 mm		89
20 (100)	29.0 ± 4.0	CAD	Echocardiography	Mean 12.9 ± 2.7 mm		119
527 (51) Asian	24.7 ± 3.2 (EAT < 3mm) 25.7 ± 2.9 (EAT > 3mm)	MS (62%) CAD (49%) Diabetes (24%) Unstable angina (40%)	Echocardiography	Mean 4 mm	Mean 3.5 mm	117
50	33.5 ± 5.1	MS	Echocardiography		Mean 6.16 ± 1.47 mm	116
190 (55)	27.0 ± 4.0	CAD	Multislice computed tomography	Mean 99 ± 40 ml		121
573 (0)	Quartiles of mean EAT thickness (I) 25.1 ± 4.3 (II) 26.1 ± 4.0 (III) 27.2 ± 3.8 (IV) 28.5 ± 4.9	Healthy post-menopausal women	Multidetector-row computed tomography		Mean 11.2 + 2.2 mm	120

N (% male)*	Mean BMI ± SD (kg/m^2)	Characteristics of the patients	Method	EAT thickness or volume threshold associated with CAD	EAT thickness or volume threshold associated with CVD	Ref.
224 (80) Asian	26.1 ± 3.3	CAD	Multidetector Computed tomography	12.2 mm (left atrioventricular groove)		[124]
128 (70)	< 27 (51%) > 27 (49%)	Clinically suspected CAD	Computed tomography		Mean EAT volume 100 ml Mean peri-coronary fat 9 ml (BMI < 27)	[125]
151 (55)	32.0 ± 7.0	Clinically suspected CAD	Multislice computed tomography	100 ml		[126]
200 (46.5)	24.5 ± 2.5	CAD (50%)	64 multidetector-row computed tomography	Mean 18.7 cm^2 (pericardial fat)		[127]
71 (78)	-	Stable effort angina	64 multidetector computed tomography	50 ml/m^2		[128]

*When not specified the study population is Caucasian. MS: Metabolic syndrome.

4.2 Mechanisms associating epicardial adipose tissue with CAD

Although the amount and thickness of EAT correlates with the presence of CAD, the role of EAT and PVAT in CAD is a subject of debate. There is no molecular evidence explaining the relation found between EAT and PVAT with both CAD and CVD risk. However, hypothetical mechanisms have been proposed, relating systemic and local (paracrine) effects of adipose tissue[71,78,81]. Pro-inflammatory products of adipose tissue are able to diffuse to the surrounding tissues and structures. Cytokines and adipokines secreted by adipose tissue may interact with endothelial cells and cause endothelial dysfunction, hypercoagulability, increased chemotaxis by CCL2, and adhesion of monocytes to the endothelium by increasing the expression of adhesion molecules[76] (Figure 5).

Paracrine effects may be exerted directly on the adjacent tissues leading to influx of tissue macrophages into the artery wall from 'outside to inside' and to proliferation of SMCs[76] (Figure 6). EAT and the myocardium share the same microcirculation, and EAT is in contact with the myocardium and the adventitia of the coronary arteries[119]. Inflammatory cell infiltration as well as inflammatory and immune response mediators, such as TNF-α and CCL2, are increased in EAT and perivascular EAT surrounding the aorta of patients with CAD compared to patients without CAD[106]. Of the adipokines identified in human EAT, adiponectin and leptin are produced exclusively by adipocytes[81]. The other adipokines are expressed in varying amounts by adipocytes and stromal preadipocytes, macrophages, lymphocytes, fibroblasts, and endothelium[40]. Adipokines secreted from adipocytes and the non-adipocyte fraction of EAT overlay the lipid core of atherosclerotic plaques and can diffuse in the interstitial fluid across the adventitia, media, and intima and interact respectively with the vascular SMCs, endothelium, and cellular components of the plaque[76]. Adipokines and FFA can also diffuse from EAT into the underlying myocardium.

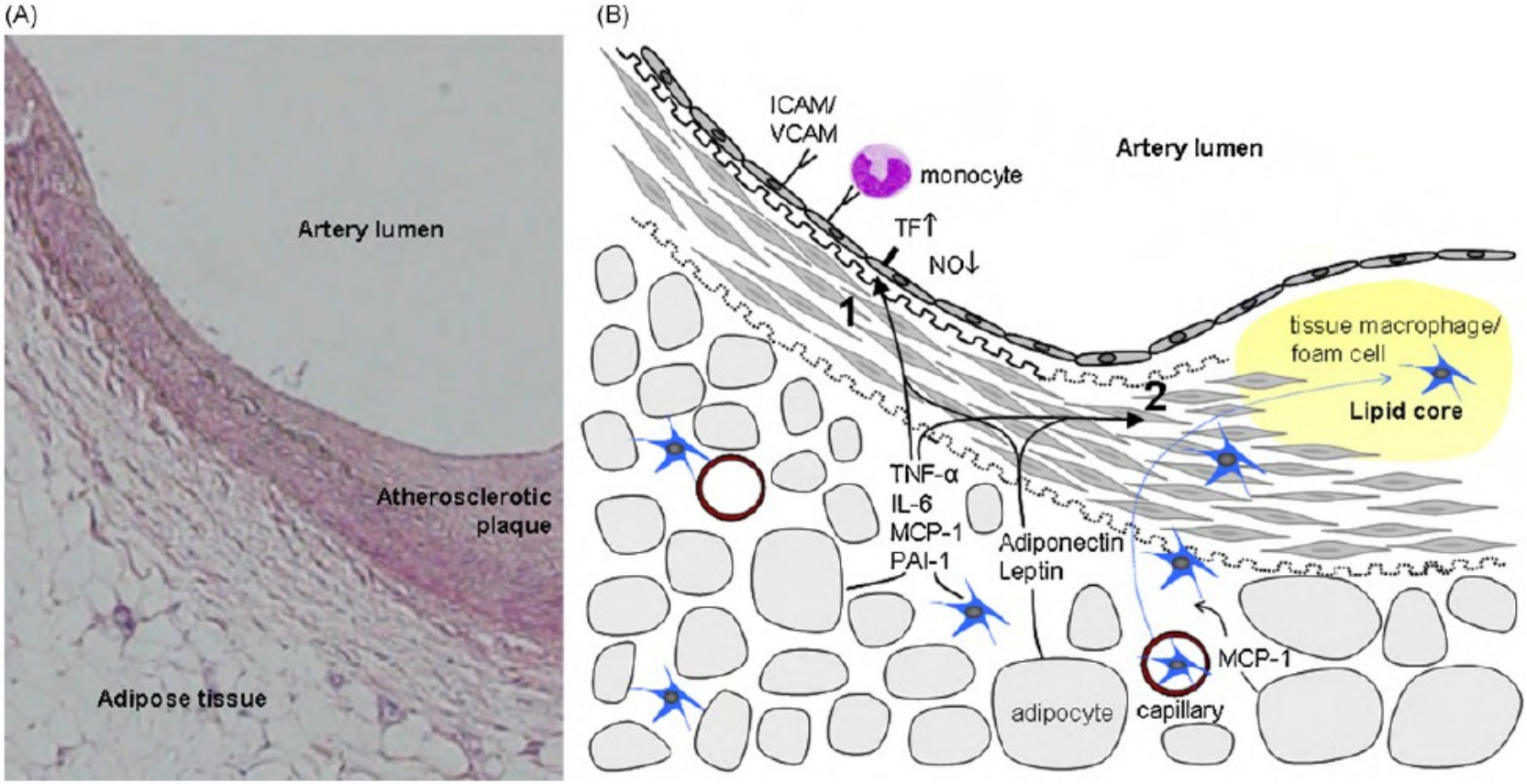

Figure 5. Perivascular adipose tissue and its possible involvement in atherogenesis. (A) Histologic reproduction of the coronary artery and surrounding tissue. PVAT is in close proximity with the artery wall which enables diffusion of adipokines and cytokines produced by the PVAT. (B) Model of the artery wall and PVAT (see text). Tumor necrosis factor alpha (TNF-α); interleukin (IL)-6; plasminogen activator inhibitor (PAI)-1); monocyte chemoattractant protein (MCP)-1 (CCL2)[76]. Figure license number: 2571560007220.

Another mechanism involves the vasa vasora. Adipokines secreted by EAT over the vasa vasora cross the vessel into its lumen and are transported downstream to react with cells in the media and the intima around the plaques[81] (Figure 6).

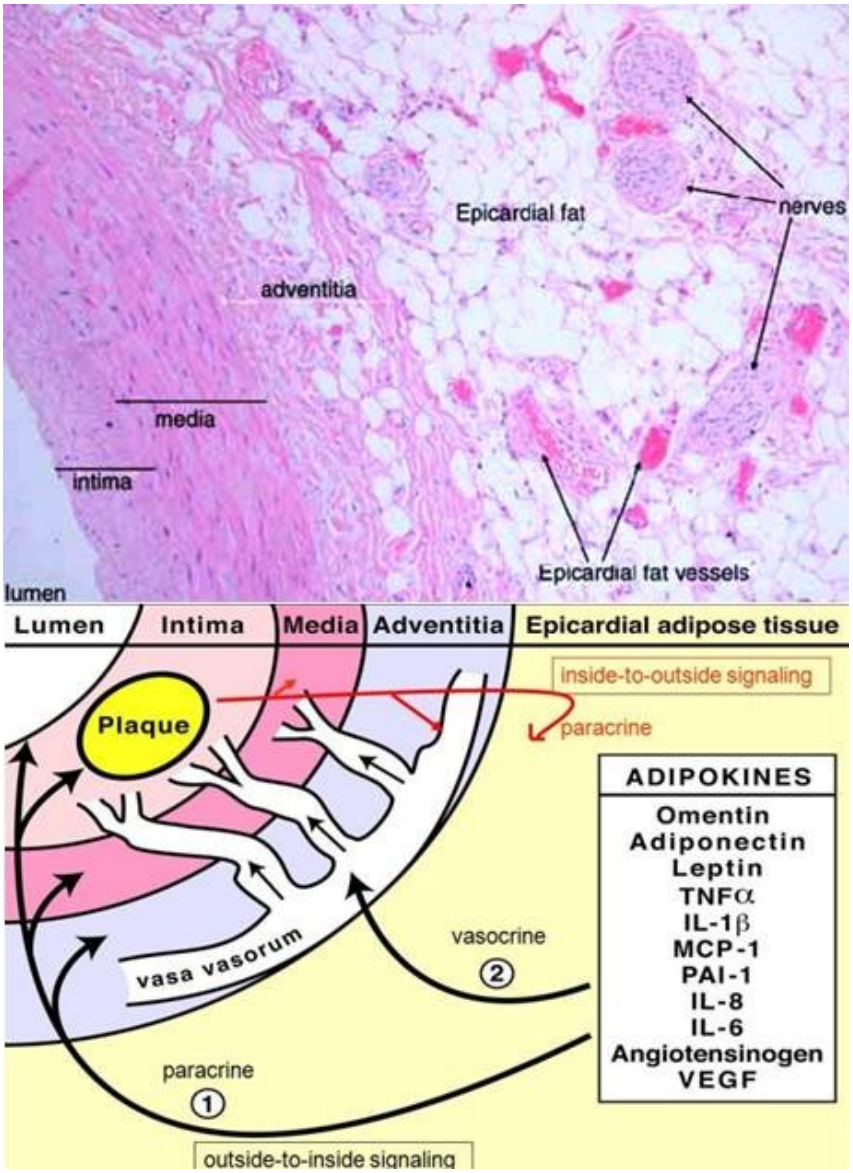

Figure 6. Mechanisms involving the vasa vasora and the paracrine effects of adipokines release by EAT in CAD[81]. Figure license number: 2571560469311.

Section 5

5.1 Characteristics of the study subjects

A total of 31 overweight white men who underwent CABG at the Institut universitaire de cardiologie et de pneumologie de Québec participated in the study. The subjects had 1 to 3 coronary vessels affected. Adipose tissues of 6 subjects were chosen for whole-genome gene expression analysis. The average age of subjects in the microarray experiment was 66 years (ranging from 48 to 76 years).

The inclusion criteria of the study were:

- Male aged 40 years to 80 years.
- BMI < 40 kg/m^2.
- Non-smoker or has stopped smoking for at least 6 months.
- Subject living in the Québec region.

The exclusion criteria included:

- Systolic dysfunction (left ventricular ejection fraction < 40%).
- Impaired renal function (creatinine > 150 μmol/L).
- Chronic inflammatory or auto-immune disease.
- Valvular disease grade 3 or 4 (or pending surgical repair).
- Taking medication for weight loss.
- Uncontrolled high blood pressure (≥ 160/90 mmHg).
- Moderate to severe stroke or transient ischemic attack.
- Cancer not in remission.
- Chronic obstructive pulmonary disease (emphysema, chronic bronchitis, asthma) or taking Ventolin.
- Orthopedic or peripheral vascular impediment to exercise.
- Retinopathy.
- Diabetes (insulin).

5.2 Location of the three adipose tissue depots compared in this study

Adipose tissues from 3 compartments, namely epicardial, mediastinal, and subcutaneous, were taken from the chest of each individual. EAT corresponds to the adipose depot in direct contact with the heart located between the myocardium and the visceral pericardium. Mediastinal fat was defined as the fat within the mediastinum, outside the pericardial sac (Figure 7).

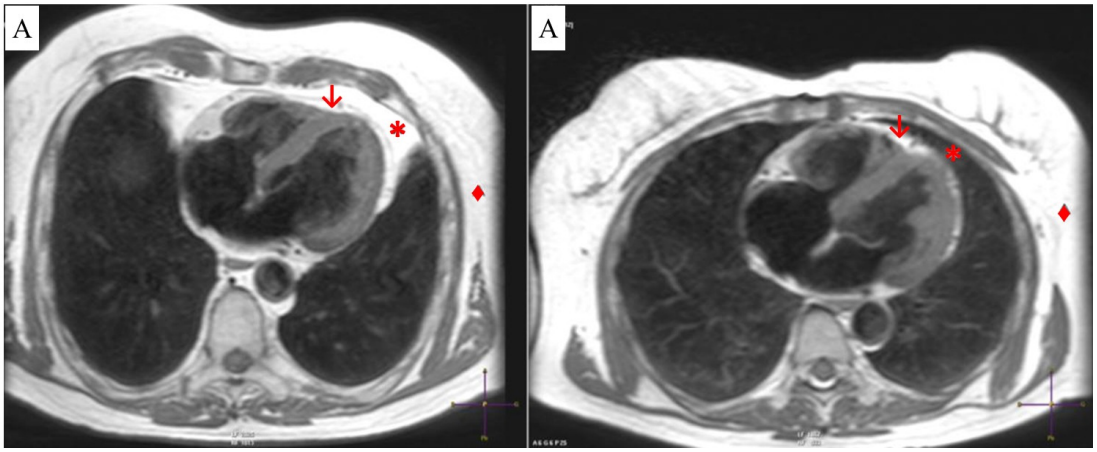

Figure 7. Cross-sections of the chest showing epicardial (↓), mediastinal (*) and subcutaneous (♦) adipose tissues by magnetic resonance imaging. Fat is distinguished by its bright white appearance. A) & B) Subjects with high and low amount of epicardial and mediastinal fat, respectively[54]. Figure license number: 2571560886714.

5.3 Experimental techniques

5.3.1 Whole-genome gene expression microarrays

In the present study, a whole-genome gene expression microarray experiment was performed to compare the expression of all known genes in the human genome across the three adipose tissue compartments. Microarrays provide a comprehensive picture of genes expressed in specific cell types or tissues. The comparison of the gene expression profiles from distinct tissues allows the identification of genes or set of genes that are differentially expressed among groups[129]. These genes can then provide great insights about the biological processes that are activated or shut down in a specific tissue and subsequently elucidated new disease mechanisms or potential therapeutic targets[129,130,131]. Genes that are up- or down-regulated in one tissue

compared to another may encode proteins that are part of the same multiprotein machine implicated in a complex coordinated activity, such as DNA replication or RNA splicing[130].

DNA microarrays consist of a glass microscope slide or silicon substrate (chip) studded with a large number of DNA fragments, each containing a nucleotide sequence that serves as a probe for a specific mRNA. The probes can be synthesized from large DNA fragments generated by polymerase chain reaction (PCR) and then spotted onto the chips by a robot. The probes can also be oligonucleotides that are synthesized directly onto the chips[132]. The probes are hybridized with mRNAs that are converted into cDNA and labeled with a fluorescent dye. The position of the probes in the chip as well as the mRNA that hybridize with each probe is predetermined[132]. The microarrays let for thousands of hybridization reactions in parallel. The level of gene expression is estimated from the raw intensities of the fluorescence emitted by the labeled sequence bound to the probes[129,130]. Some microarray platforms are single-channel arrays wherein 1 sample is hybridized on each array. While in 2-channel arrays, 2 samples are hybridized simultaneously on a single array with 2 different fluorescent dyes. Some arrays interrogate the expression levels of all known genes, while others are custom arrays that measure the expression levels of genes known to be associated with a particular disease or genes of interest to an individual researcher[129].

5.3.1.1 Illumina microarrays technology

Table 2 shows the probe content of the Illumina HumanWG-6 v3.0 BeadChip, the microarray platform used in this study. The experiment was performed at the McGill University and Génome Québec Innovation Centre (http://www.gqinnovation center.com). The Human WG-6 v3.0 BeadChip platform interrogates more than 48,000 probes derived from human genes in the NCBI RefSeq and UniGene databases. This chip provides genome-wide transcriptional coverage of well-characterized genes, candidate genes, and splice variants, with a significant portion

targeting well-established sequences supported by peer-reviewed literature. BeadChips are constructed by introducing oligonucleotide-bearing, 3-micron beads into microwells fixed into the surface of a slide-sized silicon substrate. Each bead contains hundreds of thousands of copies of covalently attached, full-length oligonucleotide probes and is represented with an average 30-fold redundancy on every BeadChip. After random bead assembly, 29-mer address sequences present on each bead are used for a hybridization-based procedure to map the array, identifying the location of each bead. The HumanWG-6 BeadChip permits processing of 6 samples on the same chip. In this experiment, 3 chips were used (for a total of 18 samples). All steps downstream of hybridization are performed in parallel for each chip, significantly reducing experimental variation and handling (Whole-Genome Expression Analysis Using the Sentrix® Human-6 and HumanRef-8 Expression BeadChips, http://www.illumina.com/Documents/products/techbulletins/techbulletin_whole_genome_expression.pdf).

Table 2. Probes content on the Illumina HumanWG-6 v3.0 BeadChip.

Probes	**Description**	**Human WG-6v3.0**
RefSeq content (Build 36.2, Release 22)		
NM	Coding transcript, well-established annotation	27,455
XM	Coding transcript, provisional annotation	7,870
NR	Non-coding transcript, well-established annotation	446
XR	Non-coding transcript, provisional annotation	196
Supplementary Content		
UniGene (Build 199)	Experimentally confirmed mRNA sequences that align to EST clusters	12,837
TOTAL		48,804

Taking from: Whole-Genome Expression Analysis Using the Sentrix® Human-6 and HumanRef-8 Expression BeadChips, http://www.illumina.com/Documents/products/techbulletins/techbulletin_whole_genome_expression.pdf.

The procedure to label and hybridize mRNA is rigorously standardized. Briefly, RNA extracted from samples must be converted to single-stranded cDNA and subsequently to cRNA. In the process the target material is amplified and labeled with biotin. The labeled cRNA is hybridized to the chip at 58°C overnight, and washed the following day. Signal is developed using streptavidin-Cy3 and the chip is scanned by the Illumina BeadArray Reader. The GenomeStudio™ software is used to generate raw data resulting in standard file formats containing the signal values per probe. The complete dataset of our experiment has been deposited in the National Center for Biotechnology Information's Gene Expression Omnibus repository[133] and are accessible through GEO Series accession number GSE24425 (http://www.ncbi.nlm.nih.gov/geo/query/acc.cgi?acc=GSE24425).

5.3.1.2 Concepts about microarrays

It is necessary to explain key concepts in order to understand the dataset generated by a microarray experiment. The raw data that is obtained by the GenomeStudio™ software needs to be log2-transformed and quantile normalized. In our study we used the lumi package in R to perform these steps. Log2 normalization allows a more comprehensive interpretation of results by treating down- and up-regulated genes on the same scale. The quantile normalization minimizes the sources of variation of non-biological origin between the arrays[134,135]. Following proper quality controls, gene expression can then be compared across experimental groups. In our study we used the Significant Analysis of Microarrays (SAM) method[136] to identify genes differentially expressed (up- and down-regulated) between the three adipose tissue compartments. The entire process of the microarray experiment is summarized in Figure 8.

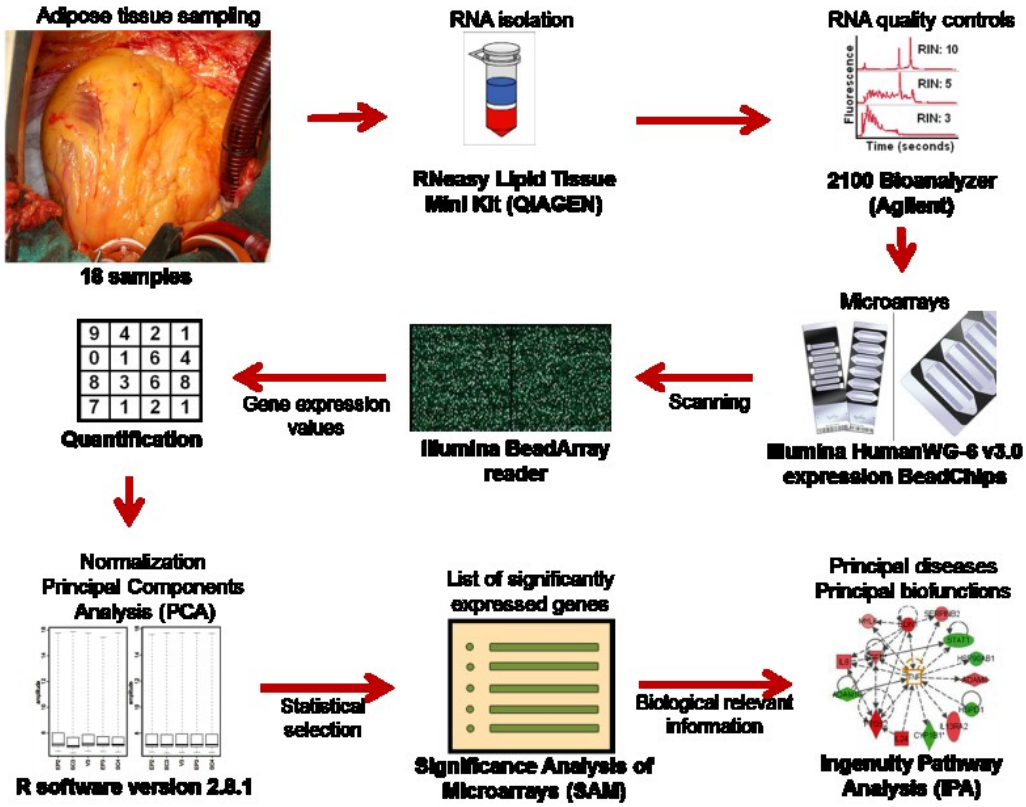

Figure 8. Flow chart showing the microarray experiment and analysis. The RNA of 18 samples (6 samples per adipose tissue) was isolated. The quality of RNA was then verified using the Agilent 2100 bioanalyzer. The complementary RNA was hybridized onto the Illumina HumanWG-6 v3.0 BeadChip. The chips were scan by the Illumina BeadArray reader. The GenomeStudio™ software generated a dataset containing the signal values per probe, which were then log2 transformed and quantile-normalized using the R software. The Significant analysis of microarrays (SAM) method was used to determine the significantly up- and down-regulated genes in three pairwise comparisons in order to generate lists of genes differentially expressed across tissues. Finally, the Ingenuity Pathways Analysis (IPA) system was used to facilitate the biological interpretation of the dataset.

5.3.2 Quantitative real-time PCR

The fluorescence-based qPCR enables the detection and measurements of minute amounts of nucleic acids in a wide range of samples from numerous sources. qPCR is widely used in molecular diagnostics (eg. microbial quantification, gene dosage determination), life sciences, agriculture, and medicine due to its speed, sensitivity, and specificity[137]. For investigators studying gene expression, qPCR is the gold

standard for validation of microarrays in a large number of samples, a limitation of the microarrays due to the high cost of this technology[138]. qPCR includes the reverse transcription of RNA to cDNA, the amplification of cDNA by PCR, and the detection and quantification of the PCR products in real time[139]. Normalization of qPCR results is needed to assess the amount of nucleic acids. In addition, normalization controls are performed for monitoring variations in extraction yield, reverse-transcription yield, and efficiency of amplification, thus enabling comparisons of mRNA concentrations across different experimental conditions or tissues. Generally, reference genes are used for normalization. They consist of endogenous genes having similar expression between all samples in a given study. Those genes may undergo all steps of the qPCR with the same kinetics as the target gene[137,138]. Such genes include β-actin, glyceraldehyde-3-phosphate dehydrogenase (GAPDH), cyclophilin, tubulin, or 18S RNA, since they are ubiquitously expressed in cells and tissues[138]. In the present study, we quantified four genes by qPCR that were significantly deregulated across tissues in the microarrays experiment. qPCR was performed on technical replicates, that is the same RNA samples used in the microarray experiment, and on biological replicates, consisting of RNA derived from 25 different patients with similar clinical characteristics. GAPDH was used as a reference gene.

The two most frequent methods to quantify the amount of mRNA in a qPCR experiment are the standard curve and the C_T (threshold cycle) methods. The standard curve method is an absolute quantification in which the copy number or amount (nanograms) of cDNA is extrapolated from a standard curve obtained from a serial dilution of cDNA of known concentration generally reverse transcripted from the same experimental mRNA[140]. The C_T is the PCR cycle at which the fluorescent signal of the dye crosses an arbitrary set threshold in the exponential phase of amplification. The C_T method use arithmetic formulas to calculate the number of cDNA copies and eliminates the need for standard curves, but it is necessary to ensure that the qPCR efficiency is close to 1 and the qPCR efficiencies of the target and the reference genes are extremely similar[140]. In our study we used the standard curve method due to the

low expression of some of our target genes and the difficulty to obtain highly similar target and reference genes qPCR efficiencies. Nevertheless our target and reference genes qPCR efficiencies are higher than 0.9. The qPCR fold changes were obtained by dividing normalized nanograms of cDNA between two groups of tissues (e.g. EAT vs subcutaneous fat).

Section 6

6.1 Hypotheses

EAT correlates with the presence of CAD and is likely to be implicated in the pathogenesis of the disease owing to its proximity to the adventitia of the coronary arteries. EAT also presents specific characteristics compared to other adipose tissue compartments. Accordingly, we hypothesize that a large number of genes are up- or down-regulated in EAT compared to other adipose tissue compartments and that the differentially expressed genes may provide insights about the distinct biology of EAT. We also suspect that the gene expression profiles of EAT and the mediastinal adipose tissue are more similar compared to the subcutaneous adipose tissue.

6.2 Objectives

The first objective is to identify genes that are up- or down-regulated in human EAT compared with mediastinal and subcutaneous adipose tissues and study their possible relationships with the development of cardiovascular diseases. The second objective is to converge to a few genes differentially expressed in EAT that are biologically relevant for CVD that will provide new therapeutic and biomarker targets for future experimental studies in CVD.

Chapter II

Le transcriptome de tissus graisseux épicardique, médiastinal et sous-cutané chez des hommes avec maladie coronarienne

Les fonctions biologiques du tissu adipeux épicardique (TAE) sont peu connues. Toutefois, sa proximité avec l'adventice des artères coronaires suggère un rôle dans la pathogénèse de la maladie coronarienne. Les objectifs de cette étude étaient d'identifier les gènes différentiellemment régulés entre les tissus graisseux épicardique, médiastinal et sous-cutané chez les mêmes individus et de vérifier leurs rôles dans le développement des maladies cardiovasculaires. L'ARN des tissus adipeux provenait de patients ayant subi une chirurgie cardiaque à l'Institut universitaire de cardiologie et de pneumologie de Québec. L'expression des gènes des tissus de six patients a été mesurée à l'aide de la biopuce Illumina HumanWG-6 v3. Le logiciel R version 2.8.1 fut utilisé pour normaliser et transformer les données brutes en valeurs d'expression. La méthode « Significance Analysis of Microarrays » a été utilisée afin d'identifier les gènes différentiellemment exprimés entre les trois compartiments adipeux. Le taux de faux positif et la différence d'expression ont été fixés à moins de 10% et à plus de 2 fois, respectivement. L'outil bioinformatique « Ingenuity Pathway Analysis » a permis d'identifier les principales fonctions biologiques des gènes différentiellemment régulés. L'expression de quatre gènes d'intérêts fut confirmée par PCR quantitative chez 31 individus. Dans le TAE, 22 et 73 gènes étaient régulés à la hausse comparativement aux tissus adipeux médiastinal et sous-cutané, respectivement. Comparativement au TAE, 94 gènes étaient régulés à

la baisse dans le tissu sous-cutané et aucun gène dans le tissu médiastinal. L'expression du gène du récepteur A1 de l'adénosine (ADORA1), impliqué dans les ischémies myocardiques, était significativement plus élevée dans le TAE. Les niveaux d'expression d'ADORA1 et de la prostaglandine D2 synthase (PTGDS), associé à la progression de l'athérosclérose, furent confirmés par PCR quantitative chez les 31 patients. En conclusion, les résultats montrent une grande similarité d'expression entre les tissus adipeux épicardique et médiastinal. Toutefois, certains gènes impliqués dans les maladies cardiovasculaires étaient régulés différentiellemment entre le TAE et le tissu médiastinal.

The Transcriptome of Human Epicardial, Mediastinal and Subcutaneous Adipose Tissues in Men with Coronary Artery Disease

Sandra Guauque-Olarte, BSc[1], Nathalie Gaudreault, BSc[1], Marie-Ève Piché, MD, PhD[1], Dominique Fournier, MSc[1], Pascale Mauriège, PhD[1,2], Patrick Mathieu, MD[1], Yohan Bossé, PhD[1,3]

1) Centre de recherche Institut universitaire de cardiologie et de pneumologie de Québec, Laval University, Quebec, Canada;
2) Division of kinesiology, Department of social and preventive medicine, Faculty of medicine, Laval University, Quebec, Canada;
3) Department of Molecular Medicine, Laval University, Quebec, Canada.

Short title: The Transcriptome of Epicardial Adipose Tissue

Address all correspondence to:
Yohan Bossé, Ph.D.
Assistant Professor, Laval University
Institut universitaire de cardiologie et de pneumologie de Québec
Pavillon Marguerite-d'Youville, Y4190
2725, chemin Sainte-Foy
Québec (Québec)
Canada, G1V 4G5
Tel: 418-656-8711 ext. 3725
Fax: 418-656-4602
email: yohan.bosse@crhl.ulaval.ca

Abstract

Background— The biological functions of epicardial adipose tissue (EAT) remain largely unknown. However, the proximity of EAT to the coronary arteries suggests a role in the pathogenesis of coronary artery disease (CAD). The objectives of this study were to identify genes differentially regulated among three adipose tissues, namely EAT, mediastinal (MAT) and subcutaneous (SAT) and to study their possible relationships with the development of cardiovascular diseases.

Methods and Results— Samples were collected from subjects undergoing coronary artery bypass grafting surgeries. Gene expression was evaluated in the three adipose depots of six men using the Illumina® HumanWG-6 v3.0 expression BeadChips. Twenty-two and 73 genes were up-regulated in EAT compared to MAT and SAT, respectively. Ninety-four genes were down-regulated in EAT compared to SAT. However, none were significantly down-regulated in EAT compared to MAT. More specifically, the expression of the adenosine A1 receptor (ADORA1), implicated in myocardial ischemia, was significantly up-regulated in EAT. Levels of the prostaglandin D2 synthase (PTGDS) gene, recently associated with the progression of atherosclerosis, were significantly different in the three pairwise comparisons (EAT > MAT > SAT). The results of ADORA1 and PTGDS were confirmed by quantitative real-time PCR in 25 biological replicates.

Conclusions— Overall, the transcriptional profiles of EAT and MAT were similar compared to the SAT. Despite this similarity, two genes involved in cardiovascular diseases, ADORA1 and PTGDS, were up-regulated in EAT. These results provide insights about the biology of EAT and its potential implication in CAD.

Key words: Epicardial adipose tissue; gene expression; microarrays; cardiovascular diseases

Introduction

Increased visceral adipose tissue has been associated with the development of cardiovascular diseases [1,2,3]. EAT is the visceral fat depot located on the surface of the heart [4] especially around the epicardial coronary vessels with extension into the myocardium [5,6,7]. As shown by clinical imaging and histological studies, EAT increases with obesity [5,8] and correlates with intra-abdominal fat mass [9]. Adipose tissue is now considered as a metabolically active organ which produces hormones and pro-inflammatory factors, contributing to the adverse cardiovascular consequences of obesity [1,5].

The function of EAT is not completely understood [7], possible roles have been suggested such as lipid storage and endocrine secretion [4,5]. It is also an active inflammatory tissue known to secret cytokines and chemokines [10,11], which are key factors involved in atherosclerosis [12]. EAT correlates with the presence of CAD [5] and is likely to be implicated in its pathogenesis. Previous studies in humans and rabbits demonstrated that segments of an artery surrounded by EAT develop atherosclerosis at a faster rate compared to the intra-myocardial segments of the same artery [1,13]. Therefore, EAT may play a role especially in the severity of the pathology [14]. EAT has the potential to be both beneficial and damaging for the heart function. It is known to collect the excess of circulating fatty acids, which induce cardiotoxicity [5], and interfere with the generation and propagation of the contractile cycle of the heart, causing ventricular arrhythmias and alterations in repolarization [14]. In addition, due to its high rate of lipolysis, EAT may serve as a source of free fatty acids (FFA) to supply myocardial energy demand in times of need, especially under ischemic conditions [5,14]. In contrast, EAT thickness was significantly correlated with the severity of CAD [7] and reflects carotid artery stiffness, an early manifestation of atherosclerosis [15]. Iacobellis et al. [9] have recently proposed that echocardiographic EAT thickness measurement might be useful for cardiometabolic risk stratification.

A number of properties differentiate EAT from other fat depots, specifically its smaller adipocyte size, low mRNA expression for several key enzymes implicated in lipogenesis (lipoprotein lipase, stearoyl-CoA desaturase and acetyl-CoA carboxylase-α) [5,14], slow regression during weight loss [16], and different fatty acid composition [17], among others [5]. These differences suggest that EAT presents specific gene regulation patterns. Only two studies have compared genome-wide transcriptional profiles of EAT with SAT from the same individuals [10,18]. Moreover, no studies have compared the genome-wide mRNA profile of EAT with MAT and SAT from the same individuals.

In the present study, we compared the transcriptional profile of EAT with that of MAT and SAT from the same individuals by using whole-genome gene expression microarrays. We found that EAT and MAT share highly similar mRNA profiles. However, few genes related with cardiovascular diseases were up-regulated in EAT compared to MAT. The expression of the genes ADORA1, involved in myocardial ischemia and dilated cardiomyopathy [19], and PTGDS, recently associated with the progression of atherosclerosis [20,21] were significantly up-regulated in EAT.

Methods

Ethics Statement

A written informed consent was obtained from all participants. The study was approved by the ethics committee of the Institut universitaire de cardiologie et de pneumologie de Québec.

Study population

A total of 31 overweight men who underwent coronary artery bypass grafting (CABG) at the Institut universitaire de cardiologie et de pneumologie de Québec participated in the study. The subjects presented 1 to 3 affected vessels. The clinical characteristics of the subjects are summarized in Table 1. To reduce heterogeneity, only adipose tissues from white male subjects were selected. The average age of subjects in the microarray experiment was 66 years (range 48 to 76 years). All subjects had a body mass index (BMI) < 40 kg/m2, were non-smokers or had stopped smoking for at least 6 months. The exclusion criteria were impaired renal function, chronic inflammatory or auto-immune diseases, aortic or mitral valve replacement, cancer, insulin treatment, and/or chronic obstructive pulmonary disease.

BMI was calculated as weight in kilograms divided by height in meters squared [22]. Obesity, overweight, and normal weight were defined as BMI ≥ 30 kg/m2, 25 to 29.9 kg/m2, and 20 to 24.9 kg/m2, respectively. Waist circumference was obtained using a measuring tape directly on the skin with the subject standing. Measurements were taken at the end of expiration at the level midway between the lower rib margin and the iliac crest. The diagnosis of hypertension was based on a resting systolic or diastolic blood pressure > 140 or > 90 mmHg, respectively, or an actual hypertensive treatment. Dyslipidemia was defined as low-density lipoprotein cholesterol ≥ 3 mmol/L or the utilization of hypolipidemic agents. Nine out of 31 subjects had a clinical diagnosis of type 2 diabetes.

Adipose tissue collection

Adipose tissues from 3 compartments, namely epicardial, mediastinal, and subcutaneous, were taken from the chest of each individual. EAT correspond to the adipose depot in direct contact with the heart located between the myocardium and the visceral pericardium. MAT was defined as the fat within the mediastinum, outside the pericardial sac. The samples were collected from surgeries performed between October 2007 and August 2009. Immediately after resection, the tissues were snap-frozen in liquid nitrogen and stored in a local biobank at -80°C until RNA isolation.

RNA extraction

RNA was isolated from 100 mg of tissue using the RNeasy Lipid Tissue Mini Kit (QIAGEN, Mississauga, Ontario) according to manufacturer's instructions. Before proceeding with microarrays experiments, the integrity of the RNA was assessed using the Agilent 2100 Bioanalyzer (Agilent technologies, Santa Clara, California) (Table S1). RNA concentration and purity for the quantitative real-time PCR (qPCR) validation was measured by the GeneQuant pro UV/Vis Spectrophotometer (Biochrom, Cambridge, UK).

Microarrays

Adipose tissues of 6 subjects were chosen for whole-genome gene expression analysis. For each subject, gene expression was evaluated in the 3 adipose tissue compartments using the HumanWG-6 v3.0 expression BeadChips (Illumina, San Diego, California). The latter interrogated more than 48,000 probes derived from human genes in the NCBI RefSeq and UniGene databases. The RNA was labeled and hybridized using a standard Illumina protocol performed at the McGill University and Génome Québec Innovation Centre (http://www.gqinnovationcenter.com). Briefly, RNA extracted from the adipose tissue was converted to single-stranded cDNA using an oligo (dT) tagged with a phage T7 enabling the amplification and labeling of the cDNA by an in vitro transcription reaction which incorporates biotin UTP. The labeled cRNA was then hybridized to the chip at 58°C overnight, and washed the

following day. Signal was developed using streptavidin-Cy3 and the chip was scanned by the Illumina BeadArray Reader. The GenomeStudio™ software was used to generate raw data resulting in standard file formats containing the signal values per probe. The complete data set has been deposited in the National Center for Biotechnology Information's Gene Expression Omnibus repository [23] and are accessible through GEO Series accession number GSE24425 (http://www.ncbi.nlm.nih.gov/geo/query/acc.cgi?acc=GSE24425).

Microarray analysis

The raw data was log2-transformed and quantile normalized using the lumi package in R [24,25]. The Significant Analysis of Microarrays (SAM) method [26] was utilized to identify genes differentially expressed among three pairwise comparisons (EAT vs MAT, EAT vs SAT, and MAT vs SAT). The false discovery rate (FDR) and the fold change threshold were set at 5% and 2.0, respectively. A false discovery rate of 10% was also explored for the comparison between EAT vs MAT. Fold changes were obtained by 1) calculating the log2 scale mean expression values of each transcript within each adipose tissue compartment, 2) subtracting transcript's averages between any two compartments, and 3) power transforming the differences at base 2 (antilog).

qPCR

qPCR was used to validate the expression of four significant genes in EAT, SAT and MAT of 25 subjects (biological replicates) as well as the 6 subjects used in the microarray experiment (technical replicates). The QuantiTect Reverse Transcription Kit (QIAGEN) was used to synthesize cDNA from 2 μg of RNA of each sample as described by the manufacturer. GAPDH was utilized as a reference gene [27]. The latter gene was interrogated by three probes in the microarray experiment and similar signal intensities were observed in the three adipose tissues. The primers were designed using the software Primer3 v.0.4.0 (http://frodo.wi.mit.edu/primer3) and synthesized by Integrated DNA Technologies (Toronto, Ontario). The genes, forward

(F) and reverse (R) primer sequences used for qPCR were GAPDH (F: 5'-ATGTTCGTCATGGGTGTGAA and R: 5'-GGTGCTAAGCAGTTGGTGGT), ADORA1 (F: 5'-GCGAGTTCGAGAAGGTCATC and R: 5'-GCTGCTTGCGGATTAGGTAG), ADRA2A (F: 5'-CGACCAGAAGTGGTACGTCA and R: 5'-GTAGATGCGCACGTAGACCA), LIPE (F: 5'-GAGTTAAGTGGGCGCAAGTC and R: 5'-AAGTCCCTCAGGGTCAGGTT), and PTGDS (F: 5'-AACCAGTGTGAGACCCGAAC and R: 5'-AGCGCGTACTGGTCGTAGTC).

The lengths of the amplicons were between 88 and 131 bp. The same cDNA sample was used to prepare the standard curves for each gene and was made from a pool of 36 SAT samples. For each gene, the experimental samples were tested in triplicate using the Rotor-Gene 6000 (Corbett Life Science, Concorde, Australia) in a final reaction volume of 20 µl containing 5 µl of 50X diluted cDNA, 10µl of 2X QuantiTect SYBR Green PCR Kit (QIAGEN), and primers (0.3 µM for ADORA1, GAPDH, LIPE, and PTGDS; and 0.5 µM for ADRA2A). The final concentration of MgCl2 was 3 mM for ADORA1 and 2.5 mM for the other genes. The qPCR conditions were the same for all genes, 95°C for 15 min, and then 50 cycles at 94°C for 10 sec, 59°C for 30 sec, and 72°C for 30 sec. A melting curve analysis was performed at the end of each run and all showed a single peak, indicating specificity of the amplified products. According to the Rotor-gene 6000 series software v1.7 (Corbett Life Science), all standard curves had a correlation coefficient and efficiency higher than 0.98 and 0.9, respectively. For each gene, the nanograms of cDNA of each sample were calculated according to the standard curve method and normalized to GAPDH. The fold changes were obtained by dividing nanograms of cDNA between two groups of tissues (e.g. EAT vs SAT). Paired t-tests were used to assess significance differences in gene expression between any pairwise comparisons.

Biological pathways

The Ingenuity Pathway Analysis system (IPA) (Ingenuity Systems, www.ingenuity.com) was used to identify the principal biofunctions and diseases

among the differentially expressed genes. The results of each pairwise comparison, containing fold changes and q-values from SAM, were uploaded in IPA. Core analyses were then performed to overlay the results of each comparison into the Ingenuity Knowledge Base in order to identify particular diseases, molecular or cellular functions, metabolic and cell signaling pathways that were particularly enriched for genes claimed significant in our microarray experiment.

Results

Table 1 shows the clinical characteristics of the subjects. BMI ranged between 24.6 and 30.5 kg/m2 for subjects used in the microarray experiment (n = 6) and between 22.8 and 35.6 kg/m2 for those used as biological replicates (n = 25). No significant differences were observed for age, BMI and waist circumference between both groups.

Microarrays

The intrapair correlation coefficients for each tissue were obtained from normalized expression data and ranged from 0.96 and 0.99 for EAT and SAT; and from 0.94 and 0.98 for MAT (Figures S1, S2, and S3).

A total of 28 probes were significantly up or down-regulated between EAT and MAT, 199 between EAT and SAT, and 237 between MAT and SAT. The Tables S2, S3, and S4 list all the significant up- and down-regulated probes for the comparisons EAT vs MAT, EAT vs SAT, and MAT vs SAT, respectively. These probes correspond to 305 unique genes among the three pairwise comparisons. Table 2 shows the number of genes that were up- and down-regulated in each pairwise comparison. Briefly, 22 and 73 were up-regulated in EAT compared with MAT and SAT, respectively. Compared to EAT, 94 were down-regulated in SAT and none in MAT. Compared to SAT, 116 were up-regulated and 74 down-regulated in MAT. PTGDS was the only gene significantly different in the three comparisons with the highest expression in EAT followed by MAT and SAT. The overlap among the 305 unique genes among the 3 comparisons is shown in a Venn diagram (Figure S4).

Figure 1 shows the top 10 genes significantly up- and down-regulated for the three comparisons. Full annotations and main biological processes related with these genes can be found in Tables S5, S6, and S7. Briefly, 5 and 9 genes in the top ten genes were involved in inflammatory and immune response when comparing EAT and MAT with SAT, respectively. Furthermore, among the 116 genes up-regulated in

MAT vs SAT, 38 genes (33%) are involved in inflammatory response, such as chemokines and immunoglobulines. Compared to SAT, 23% (17 of 73) of the significantly up-regulated genes in EAT are implicated in inflammatory response.

Biological pathways

Transcripts deemed significant were analyzed using IPA in order to identify molecular pathways and functional assignments that differ between adipose tissue compartments. In the comparison EAT vs MAT, three groups of Toxicity functions were significant, namely cardiotoxicity, hepatotoxicity, and nephrotocicity. Five genes significantly up-regulated were realted in cardiotoxicity: acyl-CoA synthetase long-chain family member 1 (ACSL1), adenosine A1 receptor (ADORA1), collagen type VI alpha 6 (COL6A6), cysteine-rich secretory protein LCCL domain containing 2 (CRISPLD2), and SRY (sex determining region Y)-box 9 (SOX9). Furthermore, ACSL1 was also associated in hepatotoxicity and PTGDS in nephrotocixity.

The 22 significant genes in the comparison EAT and MAT were analyzed using the Function and disease tool in IPA. As a result, 8 genes significantly up-regulated in EAT vs MAT were related to cardiovascular functions (Figure 2). Interestingly, among those genes, three (ACSL1, neuromedin B (NMB), and PTGDS) were involved in the metabolism, internalization, and secretion of arachidonic acid. The same analysis was performed for the significantly up-regulated genes in the comparison EAT vs SAT. In addition to ADORA1 and PTGDS, 11 genes were related to CAD functions. Similarly, 11 significant down-regulated genes were related with cardiovascular functions in the same comparison (Figure 3).

qPCR

Validation by qPCR was performed in 25 independent subjects. Four genes were selected for this validation including ADORA1, the most significantly gene in the comparison EAT vs MAT (q-value 0.0); ADRA2A, significantly down-regulated in EAT vs SAT; LIPE, significantly down-regulated in MAT vs SAT; and PTGDS, the

only gene significantly up-regulated in both EAT and MAT compared to SAT which is also associated with several cardiovascular functions. The differential regulations observed in the microarray experiment were confirmed for ADORA1 (EAT vs MAT), ADRA2A, LIPE and PTGDS (Figure 4). Although the comparison of ADORA1 between EAT and SAT was not significant by qPCR, the fold changes obtained by microarrays and qPCR followed the same trend (up-regulated). Using the 6 microarray subjects (technical replicates), only the LIPE gene was significantly differentially regulated comparing MAT with SAT. However, except for ADRA2A in the comparison MAT vs SAT, all the genes followed the same direction (up- or down-regulated). It should be noted that ADRA2A was not significant for this comparison in the microarray experiment. The microarray and qPCR results demonstrated that ADORA1 and PTGDS were up-regulated in EAT compared to MAT, ADRA2A was down-regulated in EAT vs SAT, and LIPE was down-regulated in MAT compared to SAT.

Discussion

Cardiovascular disease (CVD) is a leading global cause of death. Previous studies found a significant relation between EAT volume and the presence of CAD [28], but the role of EAT in CAD and other CVDs is still unclear. To expand our knowledge about the function of EAT and its relation with CVDs, we performed a microarray experiment to compare the gene expression profile of EAT, MAT, and SAT from subjects with CAD.

A total of 305 genes were significantly differentially regulated among three adipose tissues comparisons. Several genes involved in inflammatory and immune responses were identified among the top up-regulated genes comparing EAT and MAT with SAT. Likewise, Mazurek et al. [10] found that EAT exhibited significantly higher expression levels of chemokines, inflammatory cytokines, and immune response genes compared to SAT, independently of obesity and diabetes. In addition, other studies [10,29] showed that when compared to SAT the omental fat, incidentally a visceral fat with similar embryologic origin to EAT, express higher level of IL-6 and other cytokines. Another study [30] has correlated the thickness of EAT with the plasma levels of chemokine (C-C motif) ligand 2 (CCL2) and soluble IL-6 receptor/IL-6 in obese subjects. Together, these studies suggest a more atherogenic profile of visceral fat.

We observed highly similar mRNA expression patterns between EAT and MAT. Only 22 genes were differentially expressed between these tissues. Mahabadi et al. [31] showed that the amount of pericardial and intra-abdominal fat, but not MAT, were significantly associated with CVD. Hence, the location of EAT over the myocardium and its direct contact with the coronary arteries is supporting the idea that local and paracrine effects of secreted molecules by EAT have the potential to influence the development of CAD and/or myocardial dysfunction.

We validated four genes by qPCR. These genes were selected because they were among the top regulated genes, but also based on their importance in CAD and the biology of the adipose tissue. ADORA1 was the most significant up-regulated gene in the microarrays experiment comparing EAT with MAT. It is a G protein coupled-receptor (GPCR), which couples to Gi to decrease the secondary messenger cAMP. ADORA1 agonists have potential therapeutic uses to treat CVD [32]. The activation of ADORA1 has an important role in protecting the myocardium from ischemic damage. Under ischemic conditions, the concentration of extracellular endogenous adenosine increases as a protective mediator. Overexpression of ADORA1 in the heart of transgenic mice provides additional cardioprotection to that offered by adenosine [33,34]. In these mice there was a decrease in cell necrosis, improvement of myocardial energy, and recovery after ischemia [33,34]. Exogenous ADORA1 and ADORA3 agonists reduced cardiac infarct size and improved functional recovery in isolated heart models [35]. Myocardial injuries after ischemia-reperfusion induce apoptosis, and ADORA1 overexpression attenuated this apoptotic response [33]. Taken together, these studies confirm the importance of ADORA1 in the pathobiology of heart diseases, but do not explain how the up-regulation of this receptor in adjacent adipose tissues may affect myocardial or vascular function. In this regard, binding of adenosine to ADORA1 is well recognized to inhibit lipolysis, and omental fat cells are less responsive to this nucleoside than subcutaneous ones [36] because of a lower ADORA1 density in the former adipocytes [37]. Accordingly it is tempting to speculate that up-regulation of ADORA1 is a negative feedback mechanism to attenuate the higher FFA release observed in EAT [5].

ADRA2A belongs to the adrenergic receptors family of GPCRs which mediates the effect of the endogenous catecholamines. It plays a central role in the regulation of systemic sympathetic activity and hence cardiovascular responses such as heart rate and blood pressure [38]. ADRA2A is important in the regulation of both cardiovascular and endocrine systems [39]. Targeted disruption of this gene causes hypertension, tachycardia and impaired baroreceptor reflexes in mice [40,41]; and its

overexpression in pancreatic islets contributes to type 2 diabetes [42]. The DraI allele was previously associated with increased sympathetic activity, thereby predisposing to hypertension [40]. In our study, ADRA2A was significantly down-regulated in EAT and MAT compared to SAT. Similarly, Vohl et al. [29] observed that ADRA2A is down-regulated in omental compared to SAT. Thus, the lower expression of ADRA2A in EAT and omental adipose tissues may suggest a lower sensitivity to antilipolytic signals as already confirmed by Mauriège et al. [43,44] and Vikman et al. [45]. It is known that the rate of lipolysis in EAT is increased compared to other fat depots such as popliteal or perirenal [5], which might be in part mediated by a low expression of ADRA2A.

LIPE is an enzyme with lipolytic properties and catalyzes the rate-limiting step of lipolysis by hydrolyzing the stored triacylglycerols and diacylglycerols into fatty acids and glycerol [46]. In our study, LIPE was significantly down-regulated in EAT and MAT compared to SAT. This finding is concordant with the higher maximum lipolytic capacity, LIPE activity and mRNA expression in subcutaneous abdominal compared to omental fat cells [47]. Yet, visceral fat cells are known to have higher lipolytic activity compared to subcutaneous adipocytes. This situation may be partly explained by increased insulin action and alpha 2-adrenergic receptor mediated antilipolysis observed in subcutaneous fat depots [43,45,48]. In contrast, Fain et al. [49] found that EAT expressed higher levels of LIPE compared to SAT in a mixed population of men and women. However, our findings also support those of Vohl et al. [29] who found that LIPE was down-regulated in visceral fat compared to SAT in men. Other studies have found no difference in the expression of LIPE between visceral and subcutaneous fat [50,51]. Differences in adipose tissue gene expression between men and women may account for such disparities [52,53]. Cellular heterogeneity may also be considered as Montague et al. [50] studied isolated adipocytes (being separated from the stromal-vascular cells of the adipose tissue), while the whole adipose tissue was homogenized before RNA extraction in our study and the one of Vohl et al. [29]. Since LIPE is well known to be up-regulated in

adipocytes compared to preadipocytes [54], and as it is also expressed in macrophages [55], cell heterogeneity in whole adipose tissue biopsies might explain the differences between studies.

PTGDS is an enzyme involved in the synthesis of prostaglandin D2 (PGD2) [56]. PGD2 is a potent anticoagulant and vasodilatator [20]. PTGDS overexpression is thought to be an adaptative mechanism to prevent cardiovascular injuries because of its anti-inflammatory properties [56]. The PTGDS bioproducts PGD2 and 15d-PGJ2 lead to a reversion of the inflammatory state and plaque stabilization in human atherosclerosis [57]. PTGDS knockout mice developed atherosclerosis when compared with controls [58]. It may be up-regulated to protect against platelet aggregation in atherosclerotic blood vessels [59] and to inhibit the growth phenotype of vascular smooth muscle cells [59]. Moreover, PTGDS is considered a suitable biomarker of CAD as its levels in serum increase in subjects with stable CAD and with the severity of the disease [20]. In the present study, PTGDS was significantly up-regulated in EAT compared to MAT and SAT. This finding corroborates the study by Fain et al. [49], which showed higher levels of this transcript in EAT compared to substernal and subcutaneous fat in a group of men and women undergoing CABG [49]. The fact that the coronary arteries and their main epicardial branches are embedded in EAT [5] suggests that part of the higher PTGDS levels observed in atherosclerotic plaques of coronary arteries, compared to the internal mammary or the carotid arteries [20], may come from EAT. In our study, two other genes implicated in the arachidonic acid metabolism were also up-regulated in EAT, including ACSL1, the first enzyme in the incorporation of arachidonic acid into phospholipids, and NMB, that stimulates arachidonic acid release. This suggests the utilization of arachidonic acid and the production of pro-inflammatory mediators by EAT. Whether this up-regulation of genes involved in the arachidonic metabolism is a cause or a consequence of CAD remains to be elucidated.

This study has some limitations. First, it was limited to subjects with CAD, thus results cannot be extrapolated to non-CAD subjects. Measuring the levels of ADORA1, ADRA2A and PTGDS in CAD and non-CAD subjects would be of great interest to confirm their possible role in the particular characteristics of EAT and to improve our knowledge about the functions of this adipose tissue. Second, as we measured mRNA expression only, quantification of protein levels may reinforce or weaken the results observed, since protein levels can vary according to post-transcriptional and post-translational processes. Third, the sample size used in the microarray experiment is small. Four genes were robustly confirmed by qPCR in a larger sample size and similar experiments will be required to confirm all other genes claimed significant in the microarray data set. Finally, we did not take into account the various cell types which composed the different fat depots. Indeed, as adipose tissue contains adipocytes, preadipocytes, fibroblasts, vascular cells, and macrophages, this heterogeneity may modify gene expression levels depending on the proportion of each cell type. Nonetheless, this study identified several genes with potential implications in the pathogenesis of heart disorders that are differentially regulated in EAT.

Conclusion

The gene expression profiles of EAT and MAT are more alike compared to SAT. An important proportion of genes involved in inflammation are up-regulated in EAT and MAT compared to SAT, confirming that visceral adipose tissue may participate to heart diseases, including CAD. Our study also confirms the up-regulation of PTGDS in EAT compared to MAT and SAT. To the best of our knowledge, it is the first time that the overexpression of ADORA1 and the down-regulation of ADRA2A in EAT compared to SAT is documented, suggesting that the balance between these two genes may account for some of the regional differences observed in lipolysis. The up-regulation of PTGDS and ADORA1 suggests a possible cardioprotective role of EAT toward CAD, hypertension, and other cardiovascular dysfunctions. Moreover, the overexpression of genes implicated in the arachidonic acid pathway in EAT may influence the pro/anti-inflammatory properties of this tissue and will require additional investigations. Overall, our results provide insights about the biology of EAT and its potential implication in CAD.

Acknowledgments

The authors would like to thank the research team at the cardiovascular biobank of the Institut universitaire de cardiologie et de pneumologie de Québec for their valuable assistance. We also want to express our gratitude to M. Lacaille for his technical assistance.

References

1. Mathieu P, Pibarot P, Larose E, Poirier P, Marette A, et al. (2008) Visceral obesity and the heart. Int J Biochem Cell Biol 40: 821-836.

2. Mathieu P, Lemieux I, Despres JP (2010) Obesity, inflammation, and cardiovascular risk. Clin Pharmacol Ther 87: 407-416.

3. Despres JP, Lemieux I (2006) Abdominal obesity and metabolic syndrome. Nature 444: 881-887.

4. Sacks HS, Fain JN (2007) Human epicardial adipose tissue: a review. Am Heart J 153: 907-917.

5. Rabkin SW (2007) Epicardial fat: properties, function and relationship to obesity. Obes Rev 8: 253-261.

6. Iacobellis G, Willens HJ (2009) Echocardiographic epicardial fat: a review of research and clinical applications. J Am Soc Echocardiogr 22: 1311-1319; quiz 1417-1318.

7. Jeong JW, Jeong MH, Yun KH, Oh SK, Park EM, et al. (2007) Echocardiographic epicardial fat thickness and coronary artery disease. Circ J 71: 536-539.

8. Iacobellis G, Ribaudo MC, Assael F, Vecci E, Tiberti C, et al. (2003) Echocardiographic epicardial adipose tissue is related to anthropometric and clinical parameters of metabolic syndrome: a new indicator of cardiovascular risk. J Clin Endocrinol Metab 88: 5163-5168.

9. Iacobellis G, Willens HJ, Barbaro G, Sharma AM (2008) Threshold values of high-risk echocardiographic epicardial fat thickness. Obesity (Silver Spring) 16: 887-892.

10. Mazurek T, Zhang L, Zalewski A, Mannion JD, Diehl JT, et al. (2003) Human epicardial adipose tissue is a source of inflammatory mediators. Circulation 108: 2460-2466.

11. Baker AR, Harte AL, Howell N, Pritlove DC, Ranasinghe AM, et al. (2009) Epicardial adipose tissue as a source of nuclear factor-kappaB and c-Jun N-terminal kinase mediated inflammation in patients with coronary artery disease. J Clin Endocrinol Metab 94: 261-267.

12. Ait-Oufella H, Taleb S, Mallat Z, Tedgui A (2009) Cytokine network and T cell immunity in atherosclerosis. Semin Immunopathol 31: 23-33.
13. Ishii T, Asuwa N, Masuda S, Ishikawa Y (1998) The effects of a myocardial bridge on coronary atherosclerosis and ischaemia. J Pathol 185: 4-9.
14. Iacobellis G, Corradi D, Sharma AM (2005) Epicardial adipose tissue: anatomic, biomolecular and clinical relationships with the heart. Nat Clin Pract Cardiovasc Med 2: 536-543.
15. Natale F, Tedesco MA, Mocerino R, de Simone V, Di Marco GM, et al. (2009) Visceral adiposity and arterial stiffness: echocardiographic epicardial fat thickness reflects, better than waist circumference, carotid arterial stiffness in a large population of hypertensives. Eur J Echocardiogr 10: 549-555.
16. Kim MK, Tanaka K, Kim MJ, Matuso T, Endo T, et al. (2009) Comparison of epicardial, abdominal and regional fat compartments in response to weight loss. Nutr Metab Cardiovasc Dis 19: 760-766.
17. Pezeshkian M, Noori M, Najjarpour-Jabbari H, Abolfathi A, Darabi M, et al. (2009) Fatty acid composition of epicardial and subcutaneous human adipose tissue. Metab Syndr Relat Disord 7: 125-131.
18. Dutour A, Achard V, Sell H, Naour N, Collart F, et al. (2010) Secretory type II phospholipase A2 is produced and secreted by epicardial adipose tissue and overexpressed in patients with coronary artery disease. J Clin Endocrinol Metab 95: 963-967.
19. Funakoshi H, Chan TO, Good JC, Libonati JR, Piuhola J, et al. (2006) Regulated overexpression of the A1-adenosine receptor in mice results in adverse but reversible changes in cardiac morphology and function. Circulation 114: 2240-2250.
20. Inoue T, Eguchi Y, Matsumoto T, Kijima Y, Kato Y, et al. (2008) Lipocalin-type prostaglandin D synthase is a powerful biomarker for severity of stable coronary artery disease. Atherosclerosis 201: 385-391.
21. Miwa Y, Oda H, Shiina Y, Shikata K, Tsushima M, et al. (2008) Association of serum lipocalin-type prostaglandin D synthase levels with subclinical atherosclerosis in untreated asymptomatic subjects. Hypertens Res 31: 1931-1939.

22. Canoy D (2010) Coronary heart disease and body fat distribution. Curr Atheroscler Rep 12: 125-133.

23. Edgar R, Domrachev M, Lash AE (2002) Gene Expression Omnibus: NCBI gene expression and hybridization array data repository. Nucleic Acids Res 30: 207-210.

24. Bolstad BM, Irizarry RA, Astrand M, Speed TP (2003) A comparison of normalization methods for high density oligonucleotide array data based on variance and bias. Bioinformatics 19: 185-193.

25. Schmid R, Baum P, Ittrich C, Fundel-Clemens K, Huber W, et al. (2010) Comparison of normalization methods for Illumina BeadChip HumanHT-12 v3. BMC Genomics 11: 349.

26. Tusher VG, Tibshirani R, Chu G (2001) Significance analysis of microarrays applied to the ionizing radiation response. Proc Natl Acad Sci U S A 98: 5116-5121.

27. Gorzelniak K, Janke J, Engeli S, Sharma AM (2001) Validation of endogenous controls for gene expression studies in human adipocytes and preadipocytes. Horm Metab Res 33: 625-627.

28. Djaberi R, Schuijf JD, van Werkhoven JM, Nucifora G, Jukema JW, et al. (2008) Relation of epicardial adipose tissue to coronary atherosclerosis. Am J Cardiol 102: 1602-1607.

29. Vohl MC, Sladek R, Robitaille J, Gurd S, Marceau P, et al. (2004) A survey of genes differentially expressed in subcutaneous and visceral adipose tissue in men. Obes Res 12: 1217-1222.

30. Malavazos AE, Ermetici F, Coman C, Corsi MM, Morricone L, et al. (2007) Influence of epicardial adipose tissue and adipocytokine levels on cardiac abnormalities in visceral obesity. Int J Cardiol 121: 132-134.

31. Mahabadi AA, Massaro JM, Rosito GA, Levy D, Murabito JM, et al. (2009) Association of pericardial fat, intrathoracic fat, and visceral abdominal fat with cardiovascular disease burden: the Framingham Heart Study. Eur Heart J 30: 850-856.

32. Elzein E, Zablocki J (2008) A1 adenosine receptor agonists and their potential therapeutic applications. Expert Opin Investig Drugs 17: 1901-1910.

33. Regan SE, Broad M, Byford AM, Lankford AR, Cerniway RJ, et al. (2003) A1 adenosine receptor overexpression attenuates ischemia-reperfusion-induced apoptosis and caspase 3 activity. Am J Physiol Heart Circ Physiol 284: H859-866.

34. Matherne GP, Linden J, Byford AM, Gauthier NS, Headrick JP (1997) Transgenic A1 adenosine receptor overexpression increases myocardial resistance to ischemia. Proc Natl Acad Sci U S A 94: 6541-6546.

35. Urmaliya VB, Church JE, Coupar IM, Rose'Meyer RB, Pouton CW, et al. (2009) Cardioprotection induced by adenosine A1 receptor agonists in a cardiac cell ischemia model involves cooperative activation of adenosine A2A and A2B receptors by endogenous adenosine. J Cardiovasc Pharmacol 53: 424-433.

36. Vikman HL, Ranta S, Kiviluoto T, Ohisalo JJ (1991) Different metabolic regulation by adenosine in omental and subcutaneous adipose tissue. Acta Physiol Scand 142: 405-410.

37. Vikman HL, Ohisalo JJ (1993) Regulation of adenylate cyclase in plasma membranes of human intraabdominal and abdominal subcutaneous adipocytes. Metabolism 42: 739-742.

38. Kurnik D, Muszkat M, Li C, Sofowora GG, Solus J, et al. (2006) Variations in the alpha2A-adrenergic receptor gene and their functional effects. Clin Pharmacol Ther 79: 173-185.

39. Brede M, Philipp M, Knaus A, Muthig V, Hein L (2004) alpha2-adrenergic receptor subtypes - novel functions uncovered in gene-targeted mouse models. Biol Cell 96: 343-348.

40. Li JL, Canham RM, Vongpatanasin W, Leonard D, Auchus RJ, et al. (2006) Do allelic variants in alpha2A and alpha2C adrenergic receptors predispose to hypertension in blacks? Hypertension 47: 1140-1146.

41. Niederhoffer N, Hein L, Starke K (2004) Modulation of the baroreceptor reflex by alpha 2A-adrenoceptors: a study in alpha 2A knockout mice. Br J Pharmacol 141: 851-859.

42. Rosengren AH, Jokubka R, Tojjar D, Granhall C, Hansson O, et al. (2010) Overexpression of alpha2A-adrenergic receptors contributes to type 2 diabetes. Science 327: 217-220.

43. Mauriege P, Galitzky J, Berlan M, Lafontan M (1987) Heterogeneous distribution of beta and alpha-2 adrenoceptor binding sites in human fat cells from various fat deposits: functional consequences. Eur J Clin Invest 17: 156-165.

44. Mauriege P, Marette A, Atgie C, Bouchard C, Theriault G, et al. (1995) Regional variation in adipose tissue metabolism of severely obese premenopausal women. J Lipid Res 36: 672-684.

45. Vikman HL, Savola JM, Raasmaja A, Ohisalo JJ (1996) Alpha 2A-adrenergic regulation of cyclic AMP accumulation and lipolysis in human omental and subcutaneous adipocytes. Int J Obes Relat Metab Disord 20: 185-189.

46. Barakat H, Davis J, Lang D, Mustafa SJ, McConnaughey MM (2006) Differences in the expression of the adenosine A1 receptor in adipose tissue of obese black and white women. J Clin Endocrinol Metab 91: 1882-1886.

47. Reynisdottir S, Dauzats M, Thorne A, Langin D (1997) Comparison of hormone-sensitive lipase activity in visceral and subcutaneous human adipose tissue. J Clin Endocrinol Metab 82: 4162-4166.

48. Richelsen B, Pedersen SB, Moller-Pedersen T, Bak JF (1991) Regional differences in triglyceride breakdown in human adipose tissue: effects of catecholamines, insulin, and prostaglandin E2. Metabolism 40: 990-996.

49. Fain JN, Sacks HS, Bahouth SW, Tichansky DS, Madan AK, et al. (2010) Human epicardial adipokine messenger RNAs: comparisons of their expression in substernal, subcutaneous, and omental fat. Metabolism 59: 1379-1386.

50. Montague CT, Prins JB, Sanders L, Zhang J, Sewter CP, et al. (1998) Depot-related gene expression in human subcutaneous and omental adipocytes. Diabetes 47: 1384-1391.

51. Lefebvre AM, Laville M, Vega N, Riou JP, van Gaal L, et al. (1998) Depot-specific differences in adipose tissue gene expression in lean and obese subjects. Diabetes 47: 98-103.

52. Iglesias MJ, Eiras S, Pineiro R, Lopez-Otero D, Gallego R, et al. (2006) [Gender differences in adiponectin and leptin expression in epicardial and subcutaneous adipose tissue. Findings in patients undergoing cardiac surgery]. Rev Esp Cardiol 59: 1252-1260.

53. Linder K, Arner P, Flores-Morales A, Tollet-Egnell P, Norstedt G (2004) Differentially expressed genes in visceral or subcutaneous adipose tissue of obese men and women. J Lipid Res 45: 148-154.

54. Urs S, Smith C, Campbell B, Saxton AM, Taylor J, et al. (2004) Gene expression profiling in human preadipocytes and adipocytes by microarray analysis. J Nutr 134: 762-770.

55. Escary JL, Choy HA, Reue K, Wang XP, Castellani LW, et al. (1999) Paradoxical effect on atherosclerosis of hormone-sensitive lipase overexpression in macrophages. J Lipid Res 40: 397-404.

56. Hirawa N, Uehara Y, Yamakado M, Toya Y, Gomi T, et al. (2002) Lipocalin-type prostaglandin d synthase in essential hypertension. Hypertension 39: 449-454.

57. Cipollone F, Fazia M, Iezzi A, Ciabattoni G, Pini B, et al. (2004) Balance between PGD synthase and PGE synthase is a major determinant of atherosclerotic plaque instability in humans. Arterioscler Thromb Vasc Biol 24: 1259-1265.

58. Ragolia L, Palaia T, Hall CE, Maesaka JK, Eguchi N, et al. (2005) Accelerated glucose intolerance, nephropathy, and atherosclerosis in prostaglandin D2 synthase knock-out mice. J Biol Chem 280: 29946-29955.

59. Ragolia L, Palaia T, Paric E, Maesaka JK (2003) Prostaglandin D2 synthase inhibits the exaggerated growth phenotype of spontaneously hypertensive rat vascular smooth muscle cells. J Biol Chem 278: 22175-22181.

Figure Legends

Figure 1. The top 10 genes up- and down-regulated for the three pairwise comparisons. Comparisons between EAT vs MAT , EAT vs SAT, and MAT vs SAT, are in the upper, middle, and lower panels, respectively. Error bars correspond to standard errors. The full names and biological processes related with these genes are provided in the Tables S5, S6, and S7.

Figure 2. Cardiovascular functions linked to up-regulated genes in EAT compared to MAT. ACSL1, Acyl-CoA synthetase long-chain family member 1; ADORA1, adenosine A1 receptor; HSD17B1, hydroxysteroid (17-beta) dehydrogenase 1; MGP, matrix Gla protein; NMB, neuromedin B; PTGDS, prostaglandin D2 synthase; SERPINA5, serpin peptidase inhibitor -clade A (alpha-1 antiproteinase, antitrypsin)-member 5; and SOX9, SRY (sex determining region Y)-box 9. *Interaction with itself. →Acts on.

Figure 3. Cardiovascular functions linked to up- (red) and down-regulated (green) genes in EAT compared to SAT. ACTG2, actin, gamma 2, smooth muscle, enteric; ADRA2A, adrenergic, alpha-2A-, receptor; AMPH amphiphysin; BCHE, butyrylcholinesterase; C6, complement component 6; CBS, cystathionine-beta-synthase; CNTNAP2, contactin associated protein-like 2; COL3A1, collagen, type III, alpha 1; COL12A1, collagen, type XII, alpha 1; CTSG, cathepsin G; CXCR4, chemokine (C-X-C motif) receptor 4; FRAS1, Fraser syndrome 1; MAOB, monoamine oxidase B; MARCKSL1, MARCKS-like 1; MYH11, myosin, heavy chain 11, smooth muscle; NOX4, NADPH oxidase 4; NTRK2, neurotrophic tyrosine kinase, receptor, type 2; PAMR1, peptidase domain containing associated with muscle regeneration 1; PDE1A, phosphodiesterase 1A calmodulin-dependent; RARB, retinoic acid receptor beta; SEMA3C, sema domain, immunoglobulin domain (Ig), short basic domain, secreted, (semaphorin) 3C; and SERPINE2, serpin peptidase inhibitor clade E (nexin, plasminogen activator inhibitor type 1), member 2. *Interaction with itself.

Figure 4. Comparison of fold changes for ADORA1, ADRA2A, LIPE, and PTGDS. EAT vs MAT (A), EAT vs SAT (B) and MAT vs SAT (C). The red bars represent the fold changes obtained by microarrays. The green and violet bars represent the fold changes obtained by qPCR for technical and biological replicates, respectively. †Significant in the microarray experiment. *P <0.05, **P <0.001, and ***P <0.0001.

Figure 1.

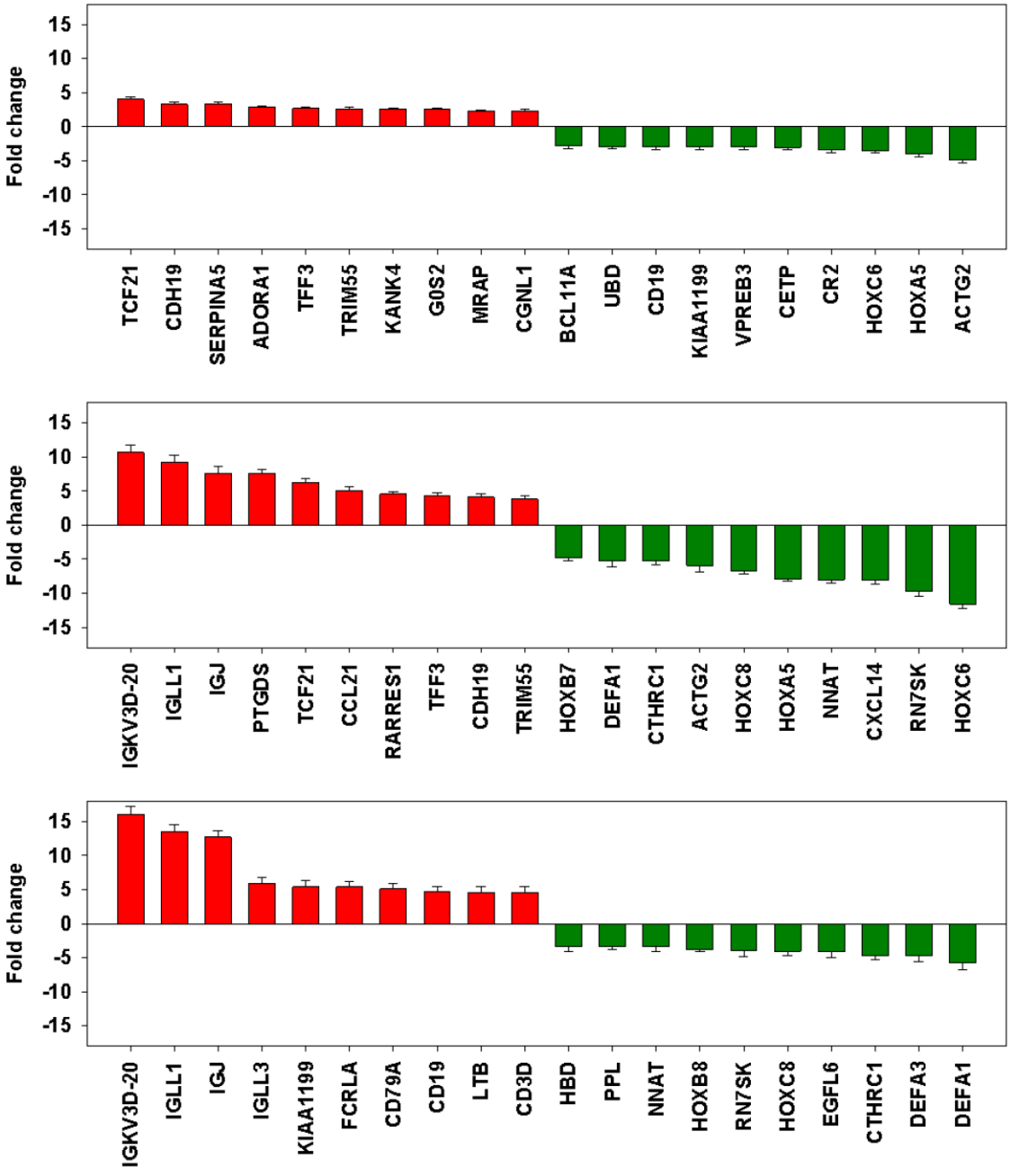
Fold change
15
10
5
0
-5
-10
-15
TCF21
CDH19
SERPINA5
ADORA1
TFF3
TRIM55
KANK4
G0S2
MRAP
CGNL1
BCL11A
UBD
CD19
KIAA1199
VPREB3
CETP
CR2
HOXC6
HOXA5
ACTG2
Fold change
IGKV3D-20
IGLL1
IGJ
PTGDS
TCF21
CCL21
RARRES1
TFF3
CDH19
TRIM55
HOXB7
DEFA1
CTHRC1
ACTG2
HOXC8
HOXA5
NNAT
CXCL14
RN7SK
HOXC6
Fold change
IGKV3D-20
IGLL1
IGJ
IGLL3
KIAA1199
FCRLA
CD79A
CD19
LTB
CD3D
HBD
PPL
NNAT
HOXB8
RN7SK
HOXC8
EGFL6
CTHRC1
DEFA3
DEFA1

Figure 2.

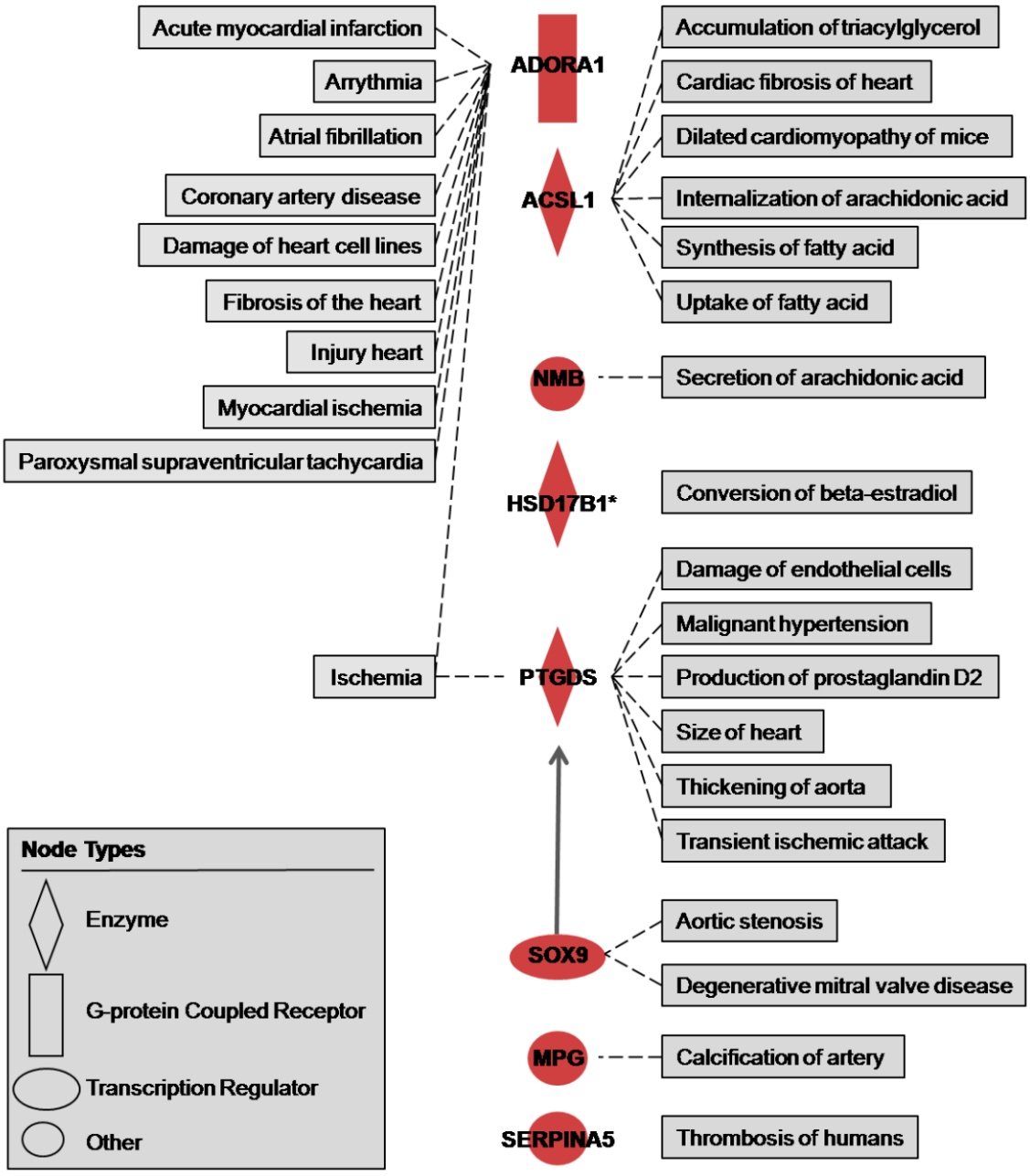
Acute myocardial infarction
Arrythmia
Atrial fibrillation
Coronary artery disease
Damage of heart cell lines
Fibrosis of the heart
Injury heart
Myocardial ischemia
Paroxysmal supraventricular tachycardia
Ischemia
ADORA1
ACSL1
NMB
HSD17B1*
PTGDS
SOX9
MPG
SERPINA5
Accumulation of triacylglycerol
Cardiac fibrosis of heart
Dilated cardiomyopathy of mice
Internalization of arachidonic acid
Synthesis of fatty acid
Uptake of fatty acid
Secretion of arachidonic acid
Conversion of beta-estradiol
Damage of endothelial cells
Malignant hypertension
Production of prostaglandin D2
Size of heart
Thickening of aorta
Transient ischemic attack
Aortic stenosis
Degenerative mitral valve disease
Calcification of artery
Thrombosis of humans
Node Types
Enzyme
G-protein Coupled Receptor
Transcription Regulator
Other

Figure 3.

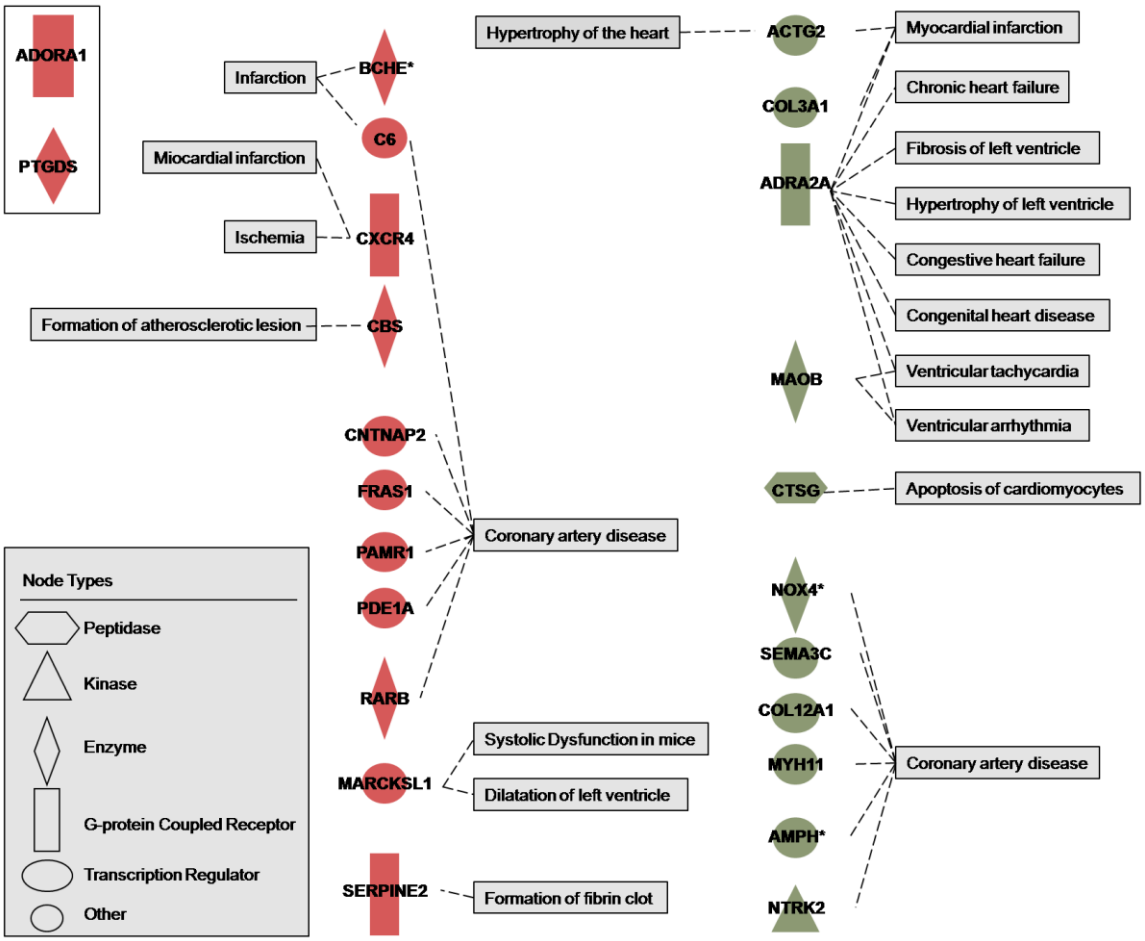
ADORA1
PTGDS
Infarction
BCHE*
C6
Miocardial infarction
Ischemia
CXCR4
Formation of atherosclerotic lesion
CBS
CNTNAP2
FRAS1
PAMR1
PDE1A
RARB
MARCKSL1
SERPINE2
Systolic Dysfunction in mice
Dilatation of left ventricle
Formation of fibrin clot
Coronary artery disease
Hypertrophy of the heart
ACTG2
COL3A1
ADRA2A
MAOB
CTSG
Myocardial infarction
Chronic heart failure
Fibrosis of left ventricle
Hypertrophy of left ventricle
Congestive heart failure
Congenital heart disease
Ventricular tachycardia
Ventricular arrhythmia
Apoptosis of cardiomyocytes
NOX4*
SEMA3C
COL12A1
MYH11
AMPH*
NTRK2
Coronary artery disease
Node Types
Peptidase
Kinase
Enzyme
G-protein Coupled Receptor
Transcription Regulator
Other

Figure 4.

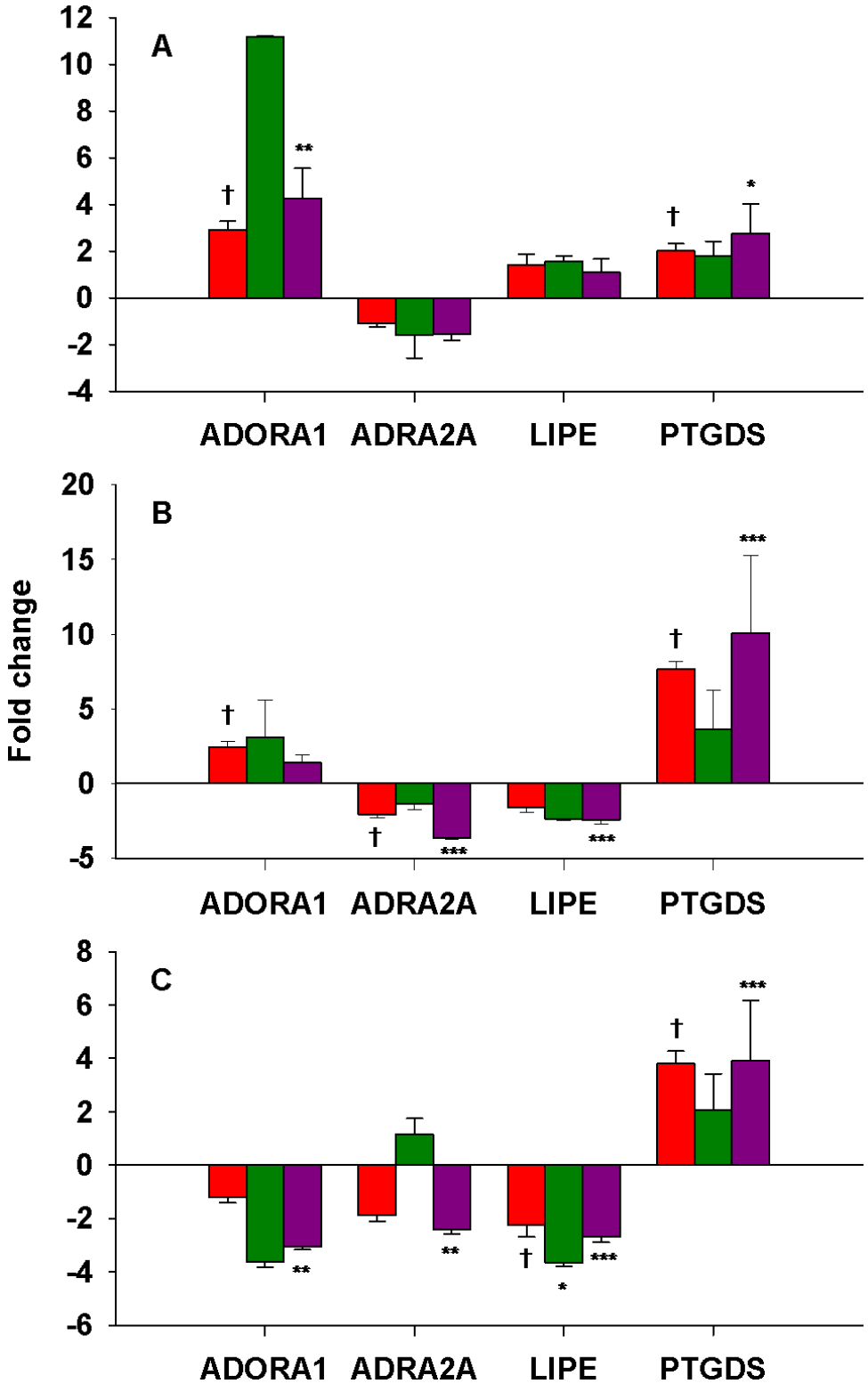

Table 1. Clinical characteristics of the study participants.

	Microarrays subjects	**Biological replicates**
	n = 6	**n = 25**
Age (years)	65.5 ± 12.6	60.2 ± 9.0
BMI (kg/m^2)	26.2 ± 2.2	27.9 ± 3.4
Waist circumference (cm)	104.1 ± 10.2	101.4 ± 9.2
Hypertension	83.3% (5)	56% (14)
Dyslipidemias	100% (6)	100% (25)
Type 2 Diabetes	16.6% (1)	32% (8)
ACE inhibitors	83.3% (5)	64% (16)
HMG-CoA reductase inhibitors	100% (6)	92% (23)

ACE inhibitors: angiotensin-converting enzyme inhibitors; BMI: body mass index; HMG-CoA reductase inhibitors: hydroxy-methylglutaryl-coenzyme A reductase inhibitors. Continuous variables are expressed as mean ± SD. Dichotomous variables are expressed as percentage (n).

Table 2. Number of genes up- and down-regulated in each pairwise comparison.

	EAT vs MAT		**EAT vs SAT**		**MAT vs SAT**	
	Probes	**Genes**	**Probes**	**Genes**	**Probes**	**Genes**
Up	28	22	85	73	143	116
Down	0	0	114	94	94	74
Total	**28**	**22**	**199**	**167**	**237**	**190**

Supporting Information

Figure S1. EAT intrapair correlation coefficients obtained from normalized expression data.

Figure S2. MAT intrapair correlation coefficients obtained from normalized expression data.

Figure S3. SAT intrapair correlation coefficients obtained from normalized expression data.

Figure S4. Venn diagram of the results obtained from SAM. A total of 305 unique genes were identified among the three pairwise comparisons. The false discovery rate were set at <5% for the comparisons EAT vs SAT and MAT vs SAT, and 10.1% for the comparison EAT vs MAT. A fold change threshold greater than 2 was used to claim significance.

Figure S1.

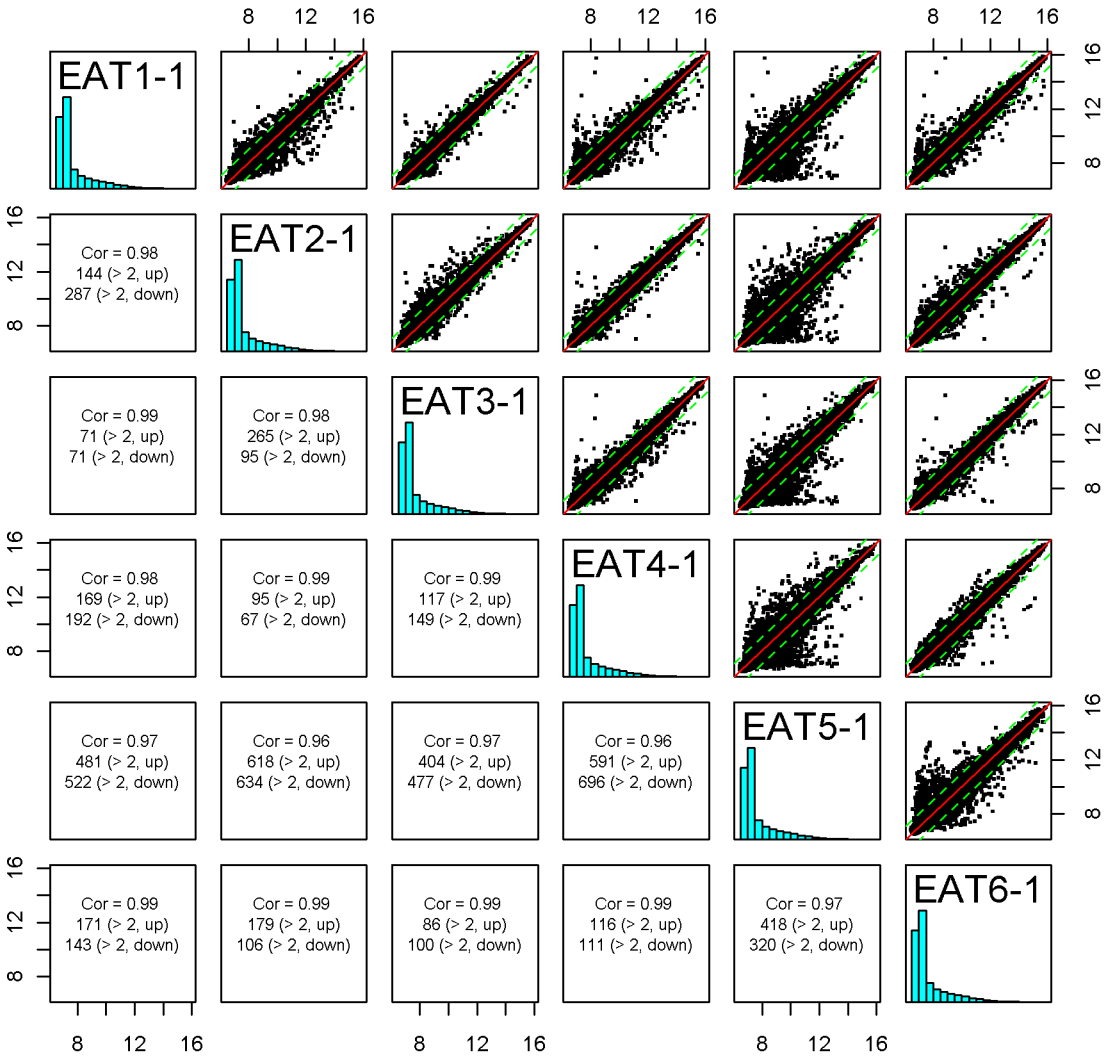
EAT1-1
EAT2-1
EAT3-1
EAT4-1
EAT5-1
EAT6-1
Cor = 0.98
144 (> 2, up)
287 (> 2, down)
Cor = 0.99
71 (> 2, up)
71 (> 2, down)
Cor = 0.98
265 (> 2, up)
95 (> 2, down)
Cor = 0.98
169 (> 2, up)
192 (> 2, down)
Cor = 0.99
95 (> 2, up)
67 (> 2, down)
Cor = 0.99
117 (> 2, up)
149 (> 2, down)
Cor = 0.97
481 (> 2, up)
522 (> 2, down)
Cor = 0.96
618 (> 2, up)
634 (> 2, down)
Cor = 0.97
404 (> 2, up)
477 (> 2, down)
Cor = 0.96
591 (> 2, up)
696 (> 2, down)
Cor = 0.99
171 (> 2, up)
143 (> 2, down)
Cor = 0.99
179 (> 2, up)
106 (> 2, down)
Cor = 0.99
86 (> 2, up)
100 (> 2, down)
Cor = 0.99
116 (> 2, up)
111 (> 2, down)
Cor = 0.97
418 (> 2, up)
320 (> 2, down)
8
12
16

Figure S2.

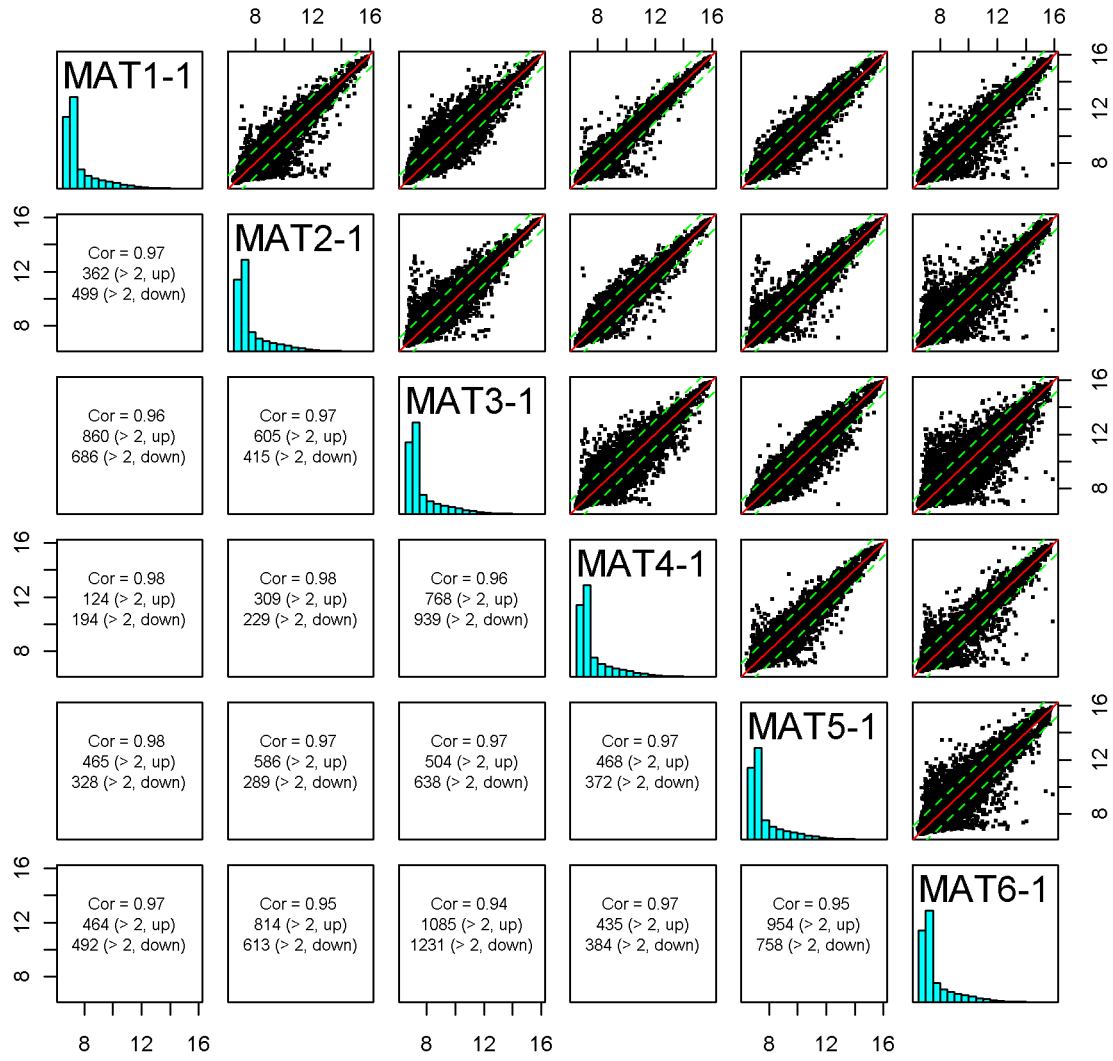
MAT1-1
MAT2-1
MAT3-1
MAT4-1
MAT5-1
MAT6-1
Cor = 0.97
362 (> 2, up)
499 (> 2, down)
Cor = 0.96
860 (> 2, up)
686 (> 2, down)
Cor = 0.97
605 (> 2, up)
415 (> 2, down)
Cor = 0.98
124 (> 2, up)
194 (> 2, down)
Cor = 0.98
309 (> 2, up)
229 (> 2, down)
Cor = 0.96
768 (> 2, up)
939 (> 2, down)
Cor = 0.98
465 (> 2, up)
328 (> 2, down)
Cor = 0.97
586 (> 2, up)
289 (> 2, down)
Cor = 0.97
504 (> 2, up)
638 (> 2, down)
Cor = 0.97
468 (> 2, up)
372 (> 2, down)
Cor = 0.97
464 (> 2, up)
492 (> 2, down)
Cor = 0.95
814 (> 2, up)
613 (> 2, down)
Cor = 0.94
1085 (> 2, up)
1231 (> 2, down)
Cor = 0.97
435 (> 2, up)
384 (> 2, down)
Cor = 0.95
954 (> 2, up)
758 (> 2, down)
8
12
16

Figure S3.

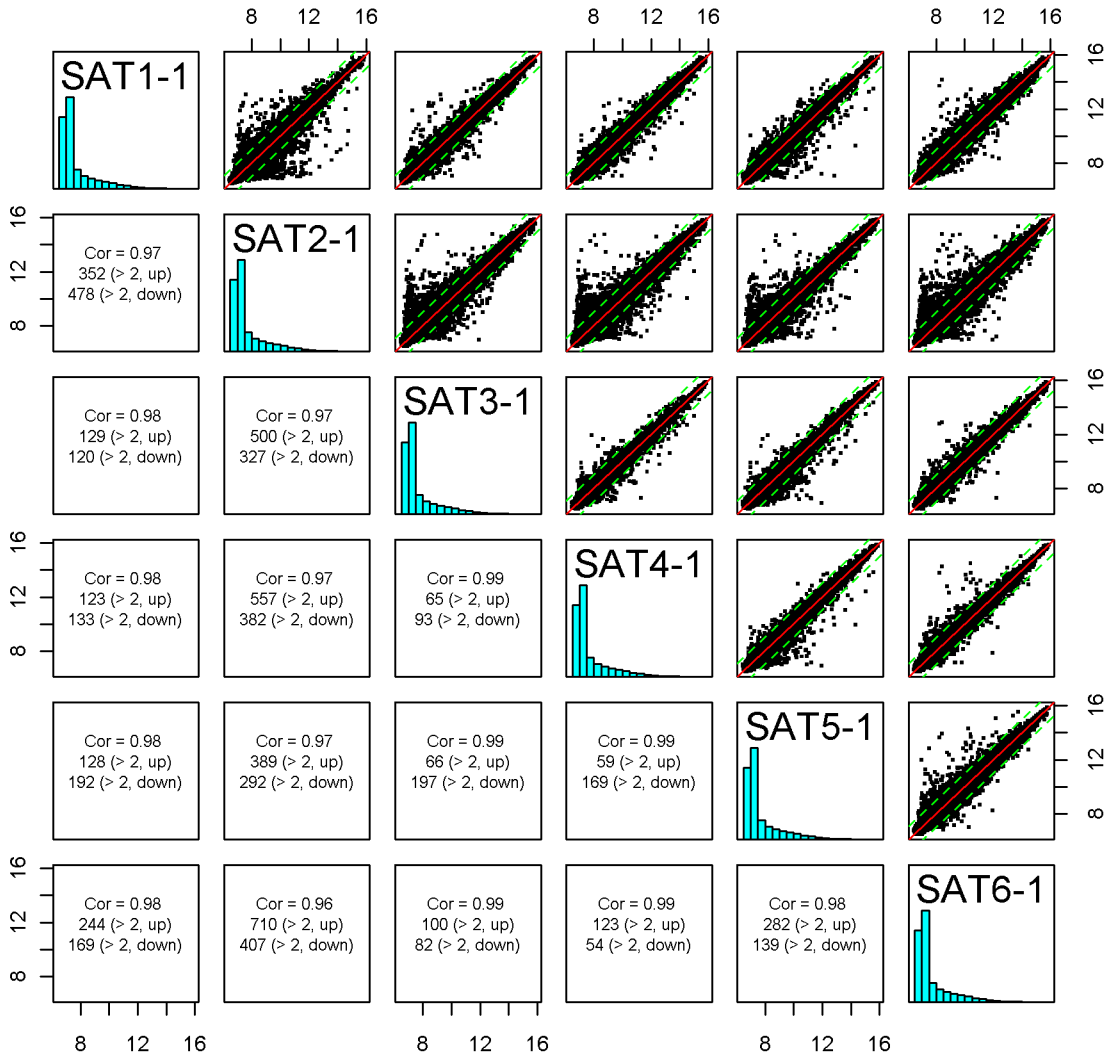
SAT1-1
SAT2-1
SAT3-1
SAT4-1
SAT5-1
SAT6-1
Cor = 0.97
352 (> 2, up)
478 (> 2, down)
Cor = 0.98
129 (> 2, up)
120 (> 2, down)
Cor = 0.97
500 (> 2, up)
327 (> 2, down)
Cor = 0.98
123 (> 2, up)
133 (> 2, down)
Cor = 0.97
557 (> 2, up)
382 (> 2, down)
Cor = 0.99
65 (> 2, up)
93 (> 2, down)
Cor = 0.98
128 (> 2, up)
192 (> 2, down)
Cor = 0.97
389 (> 2, up)
292 (> 2, down)
Cor = 0.99
66 (> 2, up)
197 (> 2, down)
Cor = 0.99
59 (> 2, up)
169 (> 2, down)
Cor = 0.98
244 (> 2, up)
169 (> 2, down)
Cor = 0.96
710 (> 2, up)
407 (> 2, down)
Cor = 0.99
100 (> 2, up)
82 (> 2, down)
Cor = 0.99
123 (> 2, up)
54 (> 2, down)
Cor = 0.98
282 (> 2, up)
139 (> 2, down)
8
12
16

Figure S4.

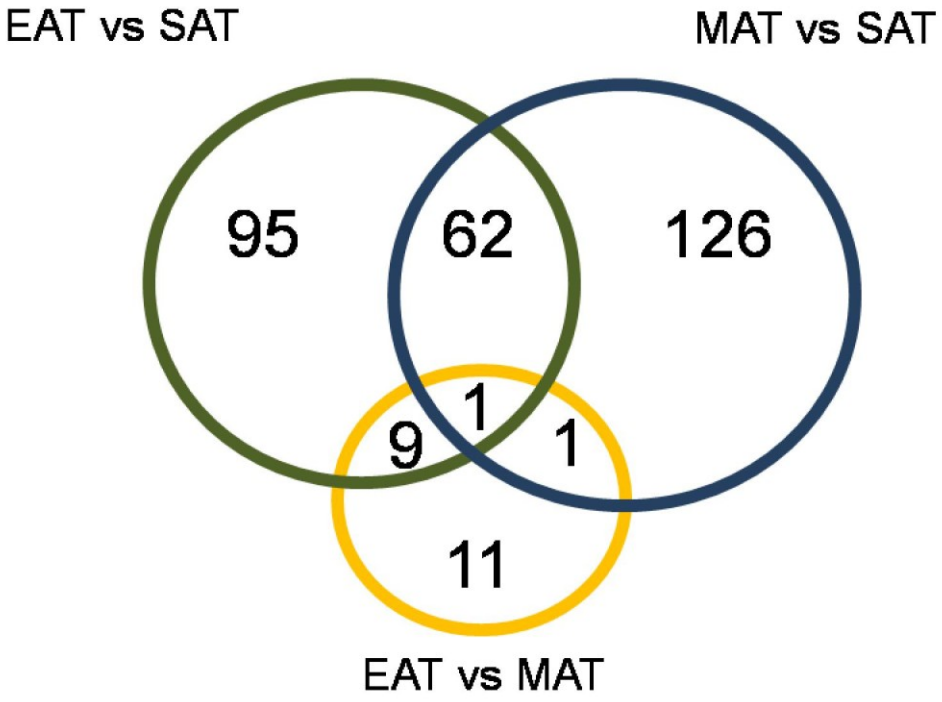

Table S1. RNA extraction yields and RNA integrity of the microarrays samples measured with the 2100 Bioanalyzer (Agilent).

Sample	Concentration (ng/ul)	rRNA Ratio (28s / 18s)	RIN
SAT-1	91.4	1.4	7.7
MAT-1	82.8	1.5	8.6
EAT-1	164.8	1.3	8.4
SAT-2	153.1	1.3	7.9
MAT-2	232.0	1.5	9.1
EAT-2	204.3	1.5	8.6
SAT-3	54.8	1.6	8.7
MAT-3	429.0	1.5	9.0
EAT-3	165.3	1.4	8.5
SAT-4	46.7	1.6	9.1
MAT-4	116.0	1.6	8.8
EAT-4	131.1	1.5	8.7
SAT-5	89.7	1.4	8.5
MAT-5	65.0	1.5	8.5
EAT-5	275.6	1.4	9.0
SAT-6	85.7	1.7	9.2
MAT-6	218.8	1.4	8.7
EAT-6	114.4	1.5	8.8

RIN: RNA integrity number

Table S2. SAM output listing all the significant up- and down-regulated probes in the comparisons EAT vs MAT.

Current settings	
Input parameters	
Data type?	Two class unpaired
Arrays centered?	FALSE
Delta	0.1613065
Minimum fold change	2
Test statistic	standard
Are data are log scale?	TRUE
Number of permutations	100
Input percentile for exchangeability factor s0	Automatic choice
Number of neighbors for KNN	10
Seed for Random number generator	1234567
Computed values	
Estimate of pi0 (proportion of null genes)	0.9426277
Exchangibility factor s0	0.0131406
s0 percentile	0
False Discovery Rate (%)	10.099582

List of Significant Genes for Delta = 0.161

Positive genes (28)

Row	Gene ID	Gene Name	Score(d)	Numerator(r)	Denominator(s+s0)	Fold Change	q-value(%)
26246	4060519	ADORA1	4.124415	1.5444	0.374453	2.916827	0
47528	7400164	NA	3.113762	1.435283	0.460948	2.704352	10.09958
48471	7610128	ANKRD38	3.077131	1.392227	0.452443	2.624836	10.09958

11940	1820379	PTGDS	3.042803	1.006281	0.330709	2.008727	10.09958
26409	4070341	MRAP	3.013427	1.223213	0.405921	2.334661	10.09958
46136	7150040	LOC131873	2.941721	1.205263	0.409714	2.305793	10.09958
36129	5690408	IRX3	2.884466	1.103235	0.382474	2.148358	10.09958
26943	4180079	CRISPLD2	2.882353	1.062594	0.368655	2.088684	10.09958
7006	1070010	MRAP	2.835675	1.06148	0.374331	2.087071	10.09958
29015	4490020	MXRA5	2.822778	1.125668	0.39878	2.182025	10.09958
776	60743	TRIM55	2.801911	1.315043	0.469338	2.488098	10.09958
39326	6180427	G0S2	2.779387	1.328587	0.478014	2.511565	10.09958
6225	940735	MGP	2.751769	1.074842	0.390601	2.106492	10.09958
34497	5360112	TCF21	2.703238	1.489729	0.55109	2.808361	10.09958
6733	1030431	ACSL1	2.673685	1.003927	0.375484	2.005451	10.09958
23879	3800500	TRIM55	2.662264	1.397065	0.524766	2.633652	10.09958
23187	3610129	HSD17B1	2.653995	1.130878	0.426104	2.18992	10.09958
45973	7100139	TCF21	2.652094	2.015348	0.759908	4.042781	10.09958
27123	4200025	OAF	2.651377	1.106097	0.417178	2.152625	10.09958
7039	1070114	HEYL	2.58745	1.083535	0.418765	2.119222	10.09958
27826	4230475	SOX9	2.532378	1.110918	0.438686	2.15983	10.09958
48382	7570484	TFF3	2.508677	1.429937	0.569996	2.694349	10.09958
998	110100	CGNL1	2.50393	1.211759	0.483943	2.316199	10.09958
21119	3290630	SERPINA5	2.461535	1.720408	0.698917	3.295295	10.09958
35966	5670594	NMB	2.46082	1.17967	0.479381	2.265249	10.09958
18515	2760541	CDH19	2.408718	1.722223	0.714996	3.299444	10.09958
39287	6180253	CDC42EP2	2.380753	1.013493	0.425703	2.018793	10.09958
9237	1430487	MGP	2.369223	1.030354	0.434891	2.042526	10.09958

Table S3. SAM output listing all the significant up- and down-regulated probes in the comparisons EAT vs SAT.

Current settings	
Input parameters	
Data type?	Two class unpaired
Arrays centered?	FALSE
Delta	0.483719511
Minimum fold change	2
Test statistic	standard
Are data are log scale?	TRUE
Number of permutations	100
Input percentile for exchangeability factor s0	Automatic choice
Number of neighbors for KNN	10
Seed for Random number generator	1234567
Computed values	
Estimate of pi0 (proportion of null genes)	0.872141628
Exchangibility factor s0	0.010953436
s0 percentile	0
False Discovery Rate (%)	4.382621245

List of Significant Genes for Delta = 0.484

Positive genes (85)

Row	Gene ID	Gene Name	Score(d)	Numerator(r)	Denominator(s+s0)	Fold Change
31170	4810575	ADAMTSL2	7.493533	1.33441	0.178075	2.521723
9039	1410403	LRRN2	7.387815	1.080657	0.146276	2.114999
32591	5050093	KBTBD11	7.298096	1.028647	0.140947	2.04011
41145	6380066	COL4A3	6.323616	1.22418	0.193589	2.336226

4345	630196	LOC649970	6.137333	2.46994	0.402445	5.540209
19227	2940291	QPRT	6.058027	1.077522	0.177867	2.110408
292	20358	MEIS2	6.055709	1.089636	0.179935	2.128203
38041	5960475	RHPN2	6.014413	1.100759	0.18302	2.144675
15446	2360672	TNFRSF19	5.954059	1.336017	0.224388	2.524533
4088	610598	CHI3L2	5.64563	1.293936	0.229192	2.45196
11940	1820379	PTGDS	5.558995	2.93478	0.527934	7.646399
5994	870575	PKNOX2	5.472791	1.102734	0.201494	2.147612
15080	2340681	RARRES1	5.162836	2.191288	0.424435	4.56713
22311	3420661	CKMT1A	5.133842	1.929992	0.375935	3.810531
25700	4010730	COL4A4	5.121312	1.108209	0.216392	2.155779
44058	6770242	MARCKSL1	5.058573	1.036236	0.204847	2.05087
46931	7320041	GALNAC4S-6ST	5.012503	1.067579	0.212983	2.095913
36481	5720441	RARB	4.998892	1.420035	0.28407	2.67592
45973	7100139	TCF21	4.97721	2.651287	0.532685	6.282273
42938	6580441	SLCO2B1	4.975698	1.178671	0.236886	2.263682
32437	4920221	C7	4.944673	1.894594	0.383159	3.718173
35632	5570021	CKMT1B	4.810667	1.296169	0.269436	2.455759
32821	5080192	SERPINE2	4.702949	1.482611	0.315251	2.794541
34497	5360112	TCF21	4.688466	1.865377	0.397865	3.643632
6464	1010132	RARRES1	4.684796	1.898928	0.405338	3.729359
7773	1230047	CBS	4.530832	1.090364	0.240654	2.129278
40105	6270487	RARB	4.481998	1.02811	0.229387	2.039351
43609	6650731	RBP1	4.452389	1.832706	0.411623	3.562046
25719	4040037	EBI2	4.413126	1.074763	0.243538	2.106376
776	60743	TRIM55	4.372968	1.702938	0.389424	3.255632
28659	4290706	EYA2	4.372587	1.08947	0.249159	2.127958

23879	3800500	TRIM55	4.352328	1.937407	0.445143	3.830166
4955	730373	TCF21	4.336766	1.247723	0.287708	2.374663
48471	7610128	ANKRD38	4.27554	1.37738	0.322153	2.597962
18515	2760541	CDH19	4.200888	2.04474	0.48674	4.125989
22216	3420288	PDPN	4.164929	1.348537	0.323784	2.546538
29126	4490520	EBI2	4.163711	1.131196	0.27168	2.190402
41445	6400463	INMT	4.16147	1.832809	0.440423	3.5623
8710	1340626	CCL21	4.095296	2.354757	0.574991	5.115082
21993	3400184	PXDNL	4.062826	1.359007	0.334498	2.565085
23187	3610129	HSD17B1	3.985896	1.407177	0.353039	2.652176
33819	5270504	FAIM2	3.984213	1.146368	0.287728	2.213559
37602	5900189	PDE1A	3.977902	1.084131	0.272538	2.120098
48382	7570484	TFF3	3.915051	2.095917	0.535348	4.274977
3851	580445	LOC649923	3.872732	2.854618	0.737107	7.23312
3365	510687	ALDH1A2	3.829754	1.260755	0.3292	2.396211
10290	1510750	ADH1C	3.697752	1.000991	0.270703	2.001374
25284	3940500	OSR1	3.664473	1.46462	0.399681	2.759907
8418	1300280	CXCR4	3.572806	1.269538	0.355334	2.410844
26246	4060519	ADORA1	3.520239	1.291588	0.366904	2.447974
18136	2710575	CD69	3.498781	1.456563	0.416306	2.744538
2662	430050	BAMBI	3.461613	1.846017	0.533282	3.595063
46989	7320288	CXCR4	3.322302	1.670903	0.502935	3.184139
29838	4590619	PNMA2	3.3045	1.013204	0.306613	2.018389
20284	3140520	TMOD1	3.303149	1.135273	0.343694	2.196602
6809	1050008	MMRN1	3.197491	1.342267	0.419788	2.535494
41716	6450102	LOC642113	3.194242	3.423259	1.071697	10.72763
7039	1070114	HEYL	3.182068	1.191249	0.374363	2.283503

998	110100	CGNL1	3.153699	1.202773	0.381385	2.301817
34644	5360689	PROX1	3.143002	1.036008	0.329624	2.050546
30632	4730747	IGLL1	3.046155	3.210053	1.053805	9.253847
28779	4390450	SGK	3.043085	1.150509	0.378073	2.219922
47275	7330739	NDRG4	3.031334	1.35883	0.448261	2.564771
2289	290669	SLC1A7	2.935194	1.301575	0.443437	2.464978
8878	1400520	CNTNAP2	2.89981	1.675834	0.577912	3.19504
36223	5700070	ALPL	2.872102	1.335378	0.464948	2.523416
24301	3840554	SPOCK2	2.845239	1.375395	0.483402	2.594389
1525	150609	LOC652493	2.838679	3.306222	1.164704	9.891721
27541	4220110	LOC647450	2.838239	3.192031	1.124652	9.138967
13116	2030414	BCHE	2.812762	1.071266	0.380859	2.101277
17760	2680605	IGJ	2.770333	2.93779	1.060446	7.662364
8280	1260482	GZMK	2.767625	1.266686	0.45768	2.406082
4069	610524	CCL3L1	2.718955	1.042083	0.383266	2.059199
5493	830201	TSKU	2.643726	1.018664	0.385314	2.026042
40219	6280168	SERPINA3	2.638639	1.840297	0.697442	3.580837
48362	7570408	CCL5	2.622816	1.356496	0.517191	2.560625
19487	2970575	CCL4L2	2.615336	1.060525	0.405502	2.085691
22983	3520102	CCL4L1	2.611167	1.472287	0.563842	2.774613
958	70681	PCK1	2.601588	1.02878	0.395443	2.040299
42897	6580270	LOC646723	2.600785	1.331292	0.511881	2.516279
42247	6520040	C6	2.588198	1.058507	0.408975	2.082775
2029	270358	FRAS1	2.341392	1.013091	0.432687	2.01823
47088	7320669	DKFZP586H2123	2.329637	1.07919	0.463244	2.11285
38177	6020255	EGR2	2.319038	1.666924	0.7188	3.175368
18566	2810010	CCL3L3	2.313698	1.286127	0.555875	2.438725

Negative genes (114)						
Row	Gene ID	Gene Name	Score(d)	Numerator(r)	Denominator(s+s0)	Fold Change
43331	6620437	HOXA5	-8.58901	-2.97957	0.346905	0.126782
18576	2810048	NNAT	-8.07225	-1.90987	0.236596	0.266117
37078	5860402	GLDN	-7.07358	-1.38816	0.196245	0.382052
34273	5340017	H19	-7.03321	-1.11598	0.158673	0.461378
26221	4060433	MAOB	-6.76279	-1.06	0.156739	0.479633
25698	4010709	NNAT	-6.36399	-3.00024	0.471441	0.124979
3846	580431	PRRX1	-6.32798	-1.12967	0.17852	0.457019
18960	2900048	HOXA3	-6.14569	-1.03685	0.168711	0.487391
23022	3520246	CXCL14	-6.12527	-3.01793	0.492702	0.123456
3009	450754	NA	-5.99494	-1.14827	0.191541	0.451165
35356	5550458	NA	-5.87832	-1.26274	0.214813	0.416752
32514	4920523	HOXC6	-5.87142	-3.53268	0.601673	0.086409
44579	6860717	HOXC4	-5.85834	-1.3911	0.237457	0.381273
26776	4150204	PRRX2	-5.78797	-1.86465	0.322159	0.274591
33967	5290333	ZNF533	-5.71025	-1.10813	0.194059	0.463896
32977	5090079	C1QTNF1	-5.50229	-1.09528	0.199059	0.468046
9845	1470500	HOXB5	-5.41455	-1.47424	0.272274	0.359923
24387	3850112	RBP7	-5.35594	-1.6815	0.313951	0.311758
5980	870524	HOXB8	-5.33993	-2.11993	0.396996	0.230058
17904	2690414	CRHBP	-5.33157	-1.40455	0.263441	0.377735
43977	6760706	MCOLN3	-5.31691	-1.45666	0.273969	0.364334
11437	1740647	LOC399888	-5.30062	-1.87856	0.354403	0.271956
36666	5810386	TPSAB1	-5.15252	-1.37611	0.267076	0.385255
36501	5720523	ADRA2A	-5.14261	-1.06837	0.207748	0.476858

30073	4640059	HOXC8	-5.1261	-2.74175	0.53486	0.149504
36045	5690095	GDF10	-5.11381	-1.92879	0.377172	0.262649
43877	6760246	LMOD1	-5.05684	-1.08901	0.215354	0.470084
39383	6180669	NPY5R	-5.03888	-1.67719	0.33285	0.312691
9673	1450646	HSD17B13	-4.97334	-1.54594	0.310846	0.342473
8576	1340100	LOC440928	-4.94179	-1.61871	0.327556	0.325626
26490	4070722	HSD17B13	-4.91282	-2.08318	0.424029	0.235994
45186	6980129	PI16	-4.89879	-1.48475	0.303086	0.357309
6285	990176	RN7SK	-4.88432	-3.28112	0.671766	0.102869
4081	610563	HOXA6	-4.85549	-1.2916	0.266008	0.408498
46129	7150019	OLFML2B	-4.85489	-1.24665	0.256783	0.421425
31754	4860546	CTHRC1	-4.69227	-2.39758	0.510963	0.189783
15947	2470328	HOXB7	-4.66452	-2.2452	0.481336	0.210924
3788	580187	PDE8B	-4.63078	-1.43051	0.308913	0.371001
5121	770291	HOXA10	-4.61864	-1.57198	0.340356	0.336346
38464	6040634	IRX2	-4.59288	-1.11725	0.243257	0.460971
32160	4890689	CTHRC1	-4.55516	-2.08503	0.45773	0.235691
279	20292	MCOLN3	-4.5513	-1.12516	0.247218	0.45845
12519	1980379	GALNTL2	-4.50302	-1.56962	0.34857	0.336898
25438	3990458	S100A4	-4.50298	-1.0316	0.229092	0.489169
18739	2810673	HOXA9	-4.46716	-1.78897	0.400472	0.289378
8700	1340593	GPC3	-4.45921	-1.08785	0.243956	0.470461
29151	4490673	TWIST1	-4.36773	-1.24327	0.28465	0.422413
37690	5900575	CD276	-4.35817	-1.03053	0.236459	0.489531
43056	6590132	IGFBP3	-4.34991	-1.02029	0.234553	0.493019
2246	290445	TNMD	-4.3433	-1.54291	0.355239	0.343193
12409	1940747	PPP1R1B	-4.33858	-1.87741	0.432725	0.272171

5065	770070	NMNAT2	-4.33513	-1.03681	0.239164	0.487405
16543	2510445	NA	-4.32677	-1.23775	0.286069	0.424033
25843	4040475	TUBA3E	-4.25353	-1.02563	0.241123	0.491197
28841	4390754	PPL	-4.2275	-1.83515	0.434098	0.280263
33949	5290270	S100A4	-4.22718	-1.04222	0.246551	0.485581
46726	7210035	SNORD13	-4.21733	-1.32904	0.315136	0.398034
13783	2120021	COL3A1	-4.13921	-1.21934	0.294583	0.429479
41568	6420240	PDZRN4	-4.13686	-1.51738	0.366796	0.349319
19561	3060095	COL12A1	-4.12403	-1.16352	0.282133	0.446421
17335	2640543	SFRP4	-4.11932	-1.19642	0.290442	0.436356
17376	2640719	RN7SK	-4.11514	-2.43096	0.590735	0.185442
15409	2360484	HOXC9	-4.10011	-1.04157	0.254033	0.4858
37590	5900152	NOX4	-4.00117	-1.19257	0.298056	0.437521
24627	3870246	NTRK2	-3.95665	-1.03806	0.262358	0.486982
18208	2750114	MAP1LC3C	-3.77697	-1.0246	0.271276	0.491547
45013	6960142	COL1A1	-3.76399	-1.557	0.413657	0.339857
23573	3780095	AOX1	-3.72887	-1.1409	0.305963	0.453477
46568	7200168	PDGFRL	-3.6668	-1.10348	0.300938	0.465392
26657	4120553	WISP2	-3.61495	-1.47391	0.407726	0.360005
25805	4040341	CD300LG	-3.60101	-1.1896	0.33035	0.438426
18204	2750092	NRCAM	-3.56105	-1.46798	0.412231	0.361489
480	50372	NA	-3.48773	-1.06581	0.305588	0.477705
9183	1430278	CTSK	-3.43344	-1.27036	0.369996	0.414557
28209	4260441	CLEC3B	-3.42612	-1.06644	0.311268	0.477496
35881	5670246	SEMA3C	-3.39214	-1.12987	0.333084	0.456958
21895	3390551	C14orf78	-3.3893	-1.55656	0.459255	0.339962
41830	6450551	TPSAB1	-3.38448	-1.3395	0.395778	0.395157

10093	1500735	CTSG	-3.36753	-1.27852	0.379661	0.412219
19144	2900747	C10orf10	-3.36086	-1.12234	0.333944	0.459349
25245	3940368	MUSTN1	-3.22596	-1.12394	0.348406	0.458838
4245	620487	CDKN2B	-3.21311	-1.08338	0.337174	0.471923
9595	1450358	HBD	-3.21189	-2.19714	0.684064	0.21807
5326	780341	CCDC3	-3.19834	-1.1666	0.36475	0.445471
28769	4390398	LCN2	-3.15481	-1.33928	0.42452	0.395218
38630	6060612	COL1A2	-3.12502	-1.2597	0.403102	0.417631
1191	130128	LOC285016	-3.02825	-1.00686	0.332487	0.49763
25459	3990544	KIAA1666	-2.95593	-1.19117	0.402975	0.437948
25061	3930424	CLIC6	-2.92309	-1.30233	0.445532	0.405471
45229	6980301	NRCAM	-2.88846	-1.072	0.371132	0.475659
39814	6250059	CYP3A5	-2.8595	-1.04499	0.365446	0.484648
16190	2480600	LOC728358	-2.82997	-2.16199	0.763964	0.223447
48745	7650497	ELA2	-2.82454	-1.13322	0.401207	0.455896
5967	870477	LOC728358	-2.81746	-2.20626	0.783067	0.216695
20804	3190156	MYH11	-2.80535	-1.32989	0.474055	0.397798
5148	770400	LOC653600	-2.78737	-1.58251	0.567743	0.333901
16665	2570154	MFAP5	-2.78409	-1.17055	0.420442	0.444252
15176	2350274	ERAF	-2.77616	-1.47342	0.530739	0.360128
29001	4480730	HBM	-2.76882	-1.23344	0.445474	0.425303
48614	7610735	CDKN2B	-2.72296	-1.07335	0.394185	0.475214
29980	4610431	ACTG2	-2.72269	-2.55777	0.939427	0.169837
19530	2970747	DEFA3	-2.70979	-2.1996	0.811726	0.217698
46176	7150170	LOC728358	-2.6753	-2.09238	0.782109	0.234494
7627	1190091	DMRT2	-2.65891	-1.87961	0.706912	0.271757
29228	4540239	DEFA1	-2.64945	-2.38458	0.900028	0.191501

6517	1010333	MSX1	-2.53315	-1.01114	0.399164	0.496153
36988	5860075	CAMP	-2.52131	-1.43921	0.570818	0.36877
2406	360402	AMPH	-2.48918	-1.2004	0.482249	0.435154
40206	6280133	MYH11	-2.47685	-1.44761	0.584454	0.366629
17273	2640286	HBA2	-2.46754	-1.13252	0.458967	0.456119
27114	4180768	ALAS2	-2.43475	-1.5651	0.642816	0.337955
37370	5890064	CALD1	-2.29369	-1.04789	0.456859	0.483674
42482	6550164	DEFA4	-2.22121	-1.04632	0.471059	0.484202
14202	2190139	CA1	-2.15203	-1.08981	0.506408	0.469825

Table S4. SAM output listing all the significant up- and down-regulated probes in the comparisons MAT vs SAT.

Current settings						
Input parameters						
Data type?						Two class unpaired
Arrays centered?						FALSE
Delta						0.387213151
Minimum fold change						2
Test statistic						standard
Are data are log scale?						TRUE
Number of permutations						100
Input percentile for exchangeability factor s0						Automatic choice
Number of neighbors for KNN						10
Seed for Random number generator						1234567
Computed values						
Estimate of pi0 (proportion of null genes)						0.869764773
Exchangibility factor s0						0.010450013
s0 percentile						0
False Discovery Rate (%)						4.587366948
List of Significant Genes for Delta = 0.387						
Positive genes (143)						
Row	**Gene ID**	**Gene Name**	**Score(d)**	**Numerator(r)**	**Denominator(s+s0)**	**Fold Change**
24301	3840554	SPOCK2	4.711833	1.956637	0.41526	3.881560529
11940	1820379	PTGDS	4.107202	1.928499	0.469541	3.806589583
3851	580445	LOC649923	4.04355	3.227911	0.798286	9.369102164
11929	1820343	WNT5A	4.000338	1.055639	0.263888	2.078639267
9857	1470551	KIAA0746	3.95842	1.760058	0.444637	3.387117336

11509	1770168	SUSD3	3.941931	1.106693	0.280749	2.15351497
6820	1050050	C9orf45	3.936704	1.079225	0.274144	2.112900689
11240	1710630	ST6GAL1	3.823891	1.135339	0.296907	2.196701797
24215	3840215	FAM102A	3.767322	1.00824	0.267628	2.011455203
18258	2750324	PRKCZ	3.766334	1.07437	0.285256	2.105802797
14598	2260241	LPAR5	3.731592	1.338803	0.358775	2.529413598
30632	4730747	IGLL1	3.690361	3.760336	1.018962	13.55107853
17760	2680605	IGJ	3.628643	3.665159	1.010063	12.6859476
41716	6450102	LOC642113	3.598871	4.004821	1.112799	16.05355684
17293	2640369	VIL2	3.550144	1.589864	0.447831	3.01020981
27541	4220110	LOC647450	3.546019	4.042527	1.140018	16.47865988
28734	4390273	RASSF7	3.513168	1.011084	0.287798	2.015424362
1525	150609	LOC652493	3.504763	4.081503	1.164559	16.92991836
20386	3170152	IL2RB	3.390089	1.22309	0.360784	2.334462303
30323	4670279	CARD11	3.358149	1.084801	0.323035	2.121082723
37024	5860204	FKBP11	3.320619	1.071414	0.322655	2.101491572
26621	4120424	COCH	3.283997	1.020121	0.310634	2.028088633
32437	4920221	C7	3.249322	1.102048	0.339162	2.146591444
43609	6650731	RBP1	3.205239	1.216951	0.379676	2.324549268
3457	520273	FLJ21438	3.087525	1.597355	0.517358	3.025879844
32821	5080192	SERPINE2	3.081739	1.042973	0.338436	2.060468903
33821	5270520	FAIM3	3.081639	1.98576	0.644384	3.96071392
45358	7000079	C13orf18	3.071836	1.115265	0.363061	2.166348251
13937	2120612	SGPP2	3.06133	1.27736	0.417257	2.423950903
28278	4260725	CD79B	3.055957	1.591886	0.520912	3.014431845
32774	5080021	BIRC3	3.030996	1.483277	0.48937	2.795831449
2983	450609	IGLL3	3.028729	2.556044	0.843933	5.880928695

18841	2850286	C13orf18	3.027723	1.072663	0.354281	2.103312705
5092	770167	CD79B	3.015356	1.691655	0.561013	3.230271558
25224	3940286	MST4	3.009329	1.024937	0.340587	2.034870817
11003	1690465	LOC650369	2.959259	1.325413	0.447887	2.506046436
760	60674	LOC652102	2.94648	2.086624	0.708175	4.247528769
3773	580136	LOC652694	2.941606	3.507802	1.192478	11.37505488
25285	3940504	CD79A	2.933157	2.357044	0.803586	5.123195224
10873	1660685	ARHGAP15	2.921269	1.107533	0.379127	2.15476837
31029	4810020	PLEK	2.910224	1.042031	0.358059	2.059124268
40563	6330091	CD7	2.907265	1.355965	0.466406	2.559682146
22636	3450338	HLA-DOB	2.906701	1.546921	0.532192	2.921929715
46756	7210136	CD19	2.900183	2.215656	0.763971	4.644927096
34735	5390246	CCR7	2.892378	1.72236	0.595482	3.29975723
44012	6770070	FCRL2	2.88707	1.343281	0.465275	2.537277099
31914	4880408	SEMA4D	2.882867	1.129235	0.391706	2.187427194
23716	3780647	KIAA0125	2.877628	1.050956	0.365216	2.071902826
40666	6330471	BLK	2.874009	1.519426	0.528678	2.866770106
23599	3780193	FCRLA	2.864892	2.432218	0.848974	5.397227065
29810	4590477	MAP4K1	2.854699	1.380136	0.483461	2.602929181
22589	3450154	TRAF3IP3	2.830682	1.39286	0.492058	2.625987509
21972	3400121	ANO9	2.815534	1.088742	0.386691	2.126884669
22955	3520020	CYFIP2	2.811387	1.345791	0.478693	2.541694882
33846	5270619	FGD3	2.809351	1.008559	0.359001	2.011900808
5883	870161	CXADR	2.803054	1.286629	0.45901	2.439573384
43714	6660379	LOC651751	2.797515	2.582015	0.922967	5.987754333
47233	7330504	BCL11A	2.796346	1.106171	0.395577	2.152735452
41835	6450594	CD79B	2.772299	1.474521	0.531877	2.77891439

200	10747	DOCK2	2.762601	1.008176	0.364937	2.011367055
41619	6420450	LIME1	2.760713	1.300352	0.471021	2.462890364
11763	1780440	CD79A	2.747535	1.48167	0.539273	2.792718547
30285	4670113	LOC90925	2.746839	1.342172	0.488624	2.535326453
37479	5890470	CCR6	2.745069	1.507164	0.549044	2.842508119
46712	7200743	SLAMF6	2.734679	1.616332	0.59105	3.065944646
35486	5560193	BCAS4	2.725514	1.512738	0.555028	2.853510325
21025	3290259	NAPSB	2.721219	1.811494	0.665692	3.510057039
8108	1240554	TNFRSF17	2.717944	1.444622	0.531513	2.721914851
9195	1430341	PTPRCAP	2.712034	1.183515	0.436394	2.271294669
43077	6590228	CD6	2.706897	1.243792	0.45949	2.368201684
18179	2710754	CD96	2.679633	1.135245	0.423657	2.196558366
41652	6420605	UBD	2.678579	1.970388	0.735609	3.918735423
24043	3830349	IL7R	2.672472	1.413019	0.528731	2.662937494
23839	3800373	CD37	2.663475	1.570026	0.589465	2.969099656
27474	4210619	CD2	2.662424	1.712303	0.643137	3.276834333
31500	4850332	TIMD4	2.661361	1.780587	0.669052	3.435660356
29516	4560743	CD96	2.660362	1.310276	0.492518	2.479889054
16672	2570176	NAPSB	2.650199	1.297927	0.489747	2.458752665
20458	3170440	BCL11A	2.646375	1.608121	0.60767	3.048546238
24862	3890400	CXCR5	2.645236	1.556458	0.5884	2.941307926
19626	3060358	NA	2.644977	1.047801	0.396147	2.067375609
22311	3420661	CKMT1A	2.637749	1.308708	0.496146	2.477196809
47011	7320372	EOMES	2.610858	1.078462	0.413068	2.11178395
12304	1940296	LOC387841	2.607621	1.037826	0.397997	2.053131713
39462	6200168	PIM2	2.606912	1.326879	0.508985	2.508594204
15080	2340681	RARRES1	2.605807	1.373206	0.526979	2.590456388

28970	4480543	TLR10	2.60161	1.685619	0.647914	3.216784487
4235	620441	TLR10	2.587157	1.602837	0.619536	3.03739928
32725	5050603	TBC1D10C	2.581379	1.485056	0.575296	2.799279568
46989	7320288	CXCR4	2.57983	1.695607	0.657255	3.239132047
26565	4120224	GPR18	2.578636	1.377717	0.534281	2.598567722
48362	7570408	CCL5	2.572943	1.599023	0.621476	3.029380296
1022	110181	KIAA1199	2.565531	2.434921	0.94909	5.40734692
9455	1440564	RUNX3	2.562907	1.534015	0.598545	2.895907046
8227	1260270	AIM2	2.559949	1.59753	0.624048	3.026247055
30251	4640768	VPREB3	2.555957	1.972285	0.771643	3.923892413
4345	630196	LOC649970	2.550752	1.583417	0.620765	2.996788247
8076	1240450	CD27	2.542668	1.280586	0.503639	2.429376993
1384	150072	IRF8	2.542586	1.389168	0.54636	2.619276635
25821	4040398	MAL	2.53629	1.737133	0.684911	3.33371956
18105	2710452	POU2AF1	2.52454	1.042456	0.412929	2.059730902
34884	5420091	LTB	2.519283	1.838724	0.72986	3.576934027
12466	1980184	P2RY10	2.515397	1.086103	0.431782	2.122998409
15307	2360035	FCRL3	2.512859	1.142267	0.454569	2.207275928
48363	7570411	NFS1	2.493395	1.170247	0.469339	2.250501959
36597	5810136	SLAMF1	2.48832	1.213597	0.487718	2.319152113
33829	5270544	GRAP	2.486745	1.183674	0.475993	2.271545623
10138	1510133	CD37	2.481498	1.420122	0.572284	2.676081543
20151	3140041	SP140	2.480768	1.213758	0.489267	2.319410358
6802	1030743	LTA	2.475523	1.156328	0.467105	2.22889457
39993	6270020	SEPT6	2.47441	1.002815	0.405274	2.003906173
22901	3460564	PRKCB1	2.470707	1.03504	0.418924	2.04916998
8710	1340626	CCL21	2.466697	2.018224	0.818189	4.050847423

11266	1710736	DOCK10	2.443624	1.078277	0.441261	2.111512593
8418	1300280	CXCR4	2.443087	1.26207	0.516588	2.398395373
13196	2030767	CD48	2.442595	1.619958	0.663212	3.07366005
8280	1260482	GZMK	2.438932	1.561013	0.64004	2.950609906
4244	620484	TNFRSF13B	2.42659	1.602487	0.660386	3.03666326
47015	7320382	SLC38A1	2.424457	1.252602	0.516653	2.382707853
34093	5310053	LTB	2.424019	2.198293	0.90688	4.589361419
36978	5860048	CRKRS	2.419261	1.30821	0.540748	2.476340399
3039	460102	CD53	2.380561	1.012926	0.425499	2.018000099
27523	4220053	SKAP1	2.378279	1.20596	0.507073	2.306907418
42941	6580450	BCL11A	2.361251	2.003553	0.848514	4.009863809
41475	6400603	PVRIG	2.361061	1.277394	0.541026	2.424007683
48229	7560632	ITK	2.354612	1.080803	0.459015	2.11521263
6700	1030296	BCL11B	2.351791	1.602722	0.68149	3.0371575
24892	3890523	IL7R	2.348183	1.626976	0.692866	3.088650093
2022	270338	TRAT1	2.347728	1.007332	0.429067	2.010189602
10607	1580411	CD3D	2.331763	2.188161	0.938415	4.557241038
43646	6660114	AMPD1	2.32743	1.256554	0.539889	2.389243625
35909	5670372	LOC606724	2.32735	1.116858	0.479884	2.168741908
5221	770682	MGC29506	2.326372	1.763792	0.758173	3.395895317
25416	3990379	ITGB7	2.324721	1.112947	0.478744	2.162869575
6230	940747	CAMK1G	2.317023	1.492552	0.644168	2.813863369
31098	4810292	CR2	2.315645	2.120473	0.915716	4.348364621
39417	6200019	KLRB1	2.313136	1.374569	0.594245	2.592905126
8878	1400520	CNTNAP2	2.309454	1.677463	0.726346	3.198650797
4286	620717	CCL5	2.307167	1.300861	0.563835	2.463758345
20895	3190521	MS4A1	2.303519	1.313115	0.570047	2.484773771

40451	6290400	CD247	2.293619	1.691674	0.737557	3.230313296
6464	1010132	RARRES1	2.291154	1.153556	0.503483	2.224616248
41038	6370414	CLECL1	2.289362	1.417712	0.619261	2.671614797

Negative genes (94)

Row	Gene ID	Gene Name	Score(d)	Numerator(r)	Denominator(s+s0)	Fold Change
36921	5820601	CCND1	-5.52905	-1.03632	0.187432	0.487568915
24627	3870246	NTRK2	-4.98494	-1.37507	0.275844	0.385534717
27332	4210075	BHMT2	-4.94275	-1.11485	0.225552	0.461740651
21165	3310022	IRX5	-4.80123	-1.31283	0.273437	0.402529489
5980	870524	HOXB8	-4.72576	-1.91186	0.404561	0.265750202
23607	3780221	LOC643911	-4.57507	-1.36891	0.299211	0.387183325
8700	1340593	GPC3	-4.54501	-1.20555	0.265247	0.433603589
8576	1340100	LOC440928	-4.52	-1.56999	0.347342	0.336811756
32160	4890689	CTHRC1	-4.47296	-2.00315	0.447836	0.249454499
11437	1740647	LOC399888	-4.44123	-1.72158	0.387636	0.303216265
31754	4860546	CTHRC1	-4.33568	-2.23413	0.51529	0.212548943
25061	3930424	CLIC6	-4.2698	-1.65425	0.38743	0.317702971
5121	770291	HOXA10	-4.20914	-1.42805	0.339273	0.371633519
36045	5690095	GDF10	-4.18518	-1.58162	0.377911	0.334105588
48402	7570598	COL6A1	-4.18102	-1.02881	0.246066	0.490115524
28841	4390754	PPL	-4.03416	-1.76847	0.438375	0.293518949
37078	5860402	GLDN	-3.95748	-1.05464	0.266494	0.481416172
32668	5050382	SPARC	-3.92501	-1.04732	0.266833	0.483864879
29151	4490673	TWIST1	-3.91534	-1.28809	0.328985	0.409493276
16543	2510445	NA	-3.87706	-1.12614	0.290462	0.45814047
45013	6960142	COL1A1	-3.78505	-1.69326	0.447353	0.3092284

19257	2940403	TUBB2A	-3.74028	-1.38039	0.369061	0.384113752
2907	450292	TUBB2A	-3.66248	-1.16942	0.319297	0.444599563
6517	1010333	MSX1	-3.66198	-1.46126	0.399036	0.363175532
24387	3850112	RBP7	-3.62936	-1.35429	0.373149	0.391126716
41568	6420240	PDZRN4	-3.61359	-1.36105	0.376648	0.389298676
13783	2120021	COL3A1	-3.5364	-1.16187	0.328546	0.446933051
18739	2810673	HOXA9	-3.53456	-1.40595	0.397772	0.377369484
23022	3520246	CXCL14	-3.52213	-1.72759	0.490497	0.301954993
37767	5910113	VCAN	-3.43755	-1.35795	0.395034	0.390136625
36666	5810386	TPSAB1	-3.42555	-1.1558	0.337405	0.448818204
21476	3360452	COL8A1	-3.37957	-1.19796	0.354473	0.435889711
48745	7650497	ELA2	-3.36789	-1.33866	0.397476	0.395388392
26657	4120553	WISP2	-3.3676	-1.47318	0.437457	0.360188165
19561	3060095	COL12A1	-3.34944	-1.1801	0.352327	0.441321444
18576	2810048	NNAT	-3.32532	-1.25347	0.376947	0.419438772
22449	3440386	ECM1	-3.28687	-1.05417	0.320722	0.481573542
16267	2490113	CD248	-3.27073	-1.12813	0.344918	0.457507286
30073	4640059	HOXC8	-3.24633	-2.00554	0.617787	0.249042226
46129	7150019	OLFML2B	-3.22627	-1.00306	0.310905	0.498939707
47528	7400164	NA	-3.18837	-1.39432	0.437316	0.38042334
42627	6550762	FBLN2	-3.14542	-1.04592	0.332523	0.484335226
18204	2750092	NRCAM	-3.13504	-1.29453	0.412921	0.407669934
26776	4150204	PRRX2	-3.13339	-1.11657	0.356344	0.461190491
3788	580187	PDE8B	-3.128	-1.23798	0.395775	0.423964672
9183	1430278	CTSK	-3.12366	-1.21465	0.388853	0.43087866
12519	1980379	GALNTL2	-3.12111	-1.42902	0.457857	0.371382896
23459	3710400	AHNAK	-3.10481	-1.00274	0.322963	0.499051041

43977	6760706	MCOLN3	-3.09497	-1.18202	0.381916	0.440735071
38525	6060113	TBX15	-3.04504	-1.09671	0.360164	0.46758035
16451	2510091	COL8A1	-3.0347	-1.69693	0.559175	0.308441712
25843	4040475	TUBA3E	-2.94561	-1.01896	0.345926	0.49347121
18702	2810482	AHNAK	-2.92263	-1.09348	0.374142	0.468630402
15947	2470328	HOXB7	-2.91	-1.71843	0.590524	0.303879998
38630	6060612	COL1A2	-2.90308	-1.29152	0.444878	0.408521759
17335	2640543	SFRP4	-2.87143	-1.07525	0.374464	0.474589725
22695	3450537	DGAT2	-2.85089	-1.10431	0.387355	0.465126005
43179	6590612	GPD1	-2.8046	-1.1087	0.395312	0.463713268
16190	2480600	LOC728358	-2.79673	-2.24406	0.802385	0.211091641
25886	4040671	COL1A2	-2.79113	-1.04521	0.374475	0.484575188
9845	1470500	HOXB5	-2.78308	-1.0714	0.384968	0.475858351
4245	620487	CDKN2B	-2.774	-1.11881	0.40332	0.460473534
11650	1770754	LIMCH1	-2.76961	-1.00847	0.364122	0.497071404
5967	870477	LOC728358	-2.75223	-2.28189	0.829104	0.20562834
35990	5670674	MME	-2.72798	-1.13056	0.41443	0.456739291
9673	1450646	HSD17B13	-2.72593	-1.00693	0.369391	0.497603186
21895	3390551	C14orf78	-2.70605	-1.52025	0.561797	0.348625645
28769	4390398	LCN2	-2.65864	-1.17994	0.443814	0.441368917
25805	4040341	CD300LG	-2.64709	-1.27188	0.480484	0.414118875
19530	2970747	DEFA3	-2.63687	-2.24198	0.850242	0.211396357
5148	770400	LOC653600	-2.63611	-1.53825	0.583529	0.3443034
29228	4540239	DEFA1	-2.62188	-2.53234	0.965849	0.172857919
46176	7150170	LOC728358	-2.58826	-2.09858	0.810808	0.233488087
41887	6480040	PODN	-2.57206	-1.02121	0.397039	0.492704363
25698	4010709	NNAT	-2.56756	-1.77292	0.690507	0.292616128

12409	1940747	PPP1R1B	-2.54728	-1.54728	0.607424	0.342154862
13293	2060364	BTNL9	-2.5462	-1.22195	0.479913	0.428702039
41830	6450551	TPSAB1	-2.54282	-1.03607	0.40745	0.487652884
10093	1500735	CTSG	-2.52644	-1.18274	0.468143	0.440515254
41435	6400427	CILP	-2.51671	-1.64566	0.653893	0.319599866
9595	1450358	HBD	-2.50247	-1.73674	0.69401	0.300047271
47241	7330544	ALDOC	-2.49348	-1.28655	0.515966	0.409928909
26490	4070722	HSD17B13	-2.46207	-1.27432	0.517579	0.413420542
9489	1440709	CILP	-2.43985	-1.69838	0.6961	0.308132421
15311	2360066	ANGPTL5	-2.40834	-1.08573	0.450821	0.471154089
7480	1170059	LIPE	-2.39793	-1.15609	0.482121	0.448726804
36129	5690408	IRX3	-2.3963	-1.12487	0.469419	0.45854427
9777	1470253	CIDECP	-2.38231	-1.1263	0.472776	0.458088501
36988	5860075	CAMP	-2.34061	-1.38242	0.590622	0.383575639
48614	7610735	CDKN2B	-2.33601	-1.10412	0.472652	0.465186576
40559	6330079	EGFL6	-2.25427	-2.0216	0.896784	0.24628562
32514	4920523	HOXC6	-2.25218	-1.71957	0.763515	0.303639002
6285	990176	RN7SK	-2.22613	-1.97529	0.887321	0.254319315
21356	3360020	CIDEC	-2.1395	-1.01397	0.47393	0.495180981

Table S5. Top 10 genes significantly up- and down-regulated in EAT vs MAT.

Gene Symbol	Full Name	Biological Process	EAT-MAT	MAT-SAT	EAT-SAT
Up-regulated genes					
TCF21	Transcription factor 21	mRNA transcription regulation	4.04	1.55	6.28
CDH19	Cadherin 19, type 2	Cell adhesion-mediated signaling	3.30	1.25	4.13
SERPINA5	Serpin peptidase inhibitor, clade A (alpha-1 antiproteinase, antitrypsin), member 5	Proteolysis	3.30	-1.89	1.74
ADORA1	Adenosine A1 receptor	G-protein mediated signaling; Macrophage and granulocyte-mediated immunity; Muscle contraction; Induction of apoptosis; Regulation of vasoconstriction, dilation	2.92	-1.19	2.45
TFF3	Trefoil factor 3 (intestinal)	Cell surface receptor mediated signal transduction; Cell motility; Defense response	2.69	1.59	4.27
TRIM55	Tripartite motif-containing 55	Proteolysis	2.63	1.45	3.83
KANK4	KN motif and ankyrin repeat domains 4	Biological process unclassified	2.62	-1.01	2.60
G0S2	G0/g1switch 2	Cell cycle	2.51	-2.21	1.14
MRAP	Melanocortin 2 receptor accessory protein	Positive regulation of cAMP biosynthetic process; Protein localization at cell surface	2.33	-1.65	1.41
CGNL1	Cingulin-like 1	Muscle contraction	2.32	-1.01	2.30
Down-regulated genes*					

ACTG2	Actin, gamma 2, smooth muscle, enteric	Exocytosis; Endocytosis; Transport; Cytokinesis	-4.95	-1.19	-5.89
HOXA5	Homeobox A5	mRNA transcription regulation; Segment specification	-4.04	-1.95	-7.89
HOXC6	Homeobox C6	mRNA transcription regulation; Segment specification	-3.51	-3.29	-3.51
CR2	Complement component (3d/Epstein Barr virus) receptor 2	Complement activation; Immune response	-3.41	4.35	1.28
CETP	Cholesteryl ester transfer protein, plasma	Cholesterol metabolic process; Phospholipid homeostasis; Triglyceride homeostasis	-3.05	1.99	-1.53
VPREB3	Pre-B lymphocyte 3	Biological process unclassified	-3.00	3.92	1.31
KIAA1199	Kiaa1199	Biological process unclassified	-2.99	5.41	1.81
CD19	CD19 molecule	B cell receptor signaling pathway; Cellular defense response	-2.99	4.64	1.55
UBD	Ubiquitin D	Protein ubiquitination	-2.95	3.92	1.33
BCL11A	B-cell CLL/lymphoma 11A (zinc finger protein)	B and T cell differentiation; Regulation of transcription	-2.85	4.01	1.41

*The top ten genes down-regulated in EAT vs MAT were not significant.

Table S6. Top 10 genes significantly up- and down-regulated in EAT vs SAT.

Gene Symbol	Full name	Biological Process	EAT-SAT	EAT-MAT	MAT-SAT
Up-regulated genes					
IGKV3D-20	Immunoglobulin kappa variable 3D-20	Immune response	10.73	-1.50	16.05
IGLL1	Immunoglobulin lambda-like polypeptide 1	B-cell- and antibody-mediated immunity	9.25	-1.46	13.55
IGJ	Immunoglobulin J polypeptide, linker protein for immunoglobulin alpha and mu polypeptides	Immune response	7.66	-1.66	12.69
PTGDS	Prostaglandin D2 synthase 21kda (brain)	Fatty acid biosynthesis; Lipid metabolism; Intracellular signaling cascade; Transport; Muscle contraction	7.65	2.01	3.81
TCF21	Transcription factor 21	mRNA transcription regulation	6.28	4.04	1.55
CCL21	Chemokine (C-C motif) ligand 21	Cytokine/chemokine mediated immunity; Inflammatory response	5.12	1.26	4.05
RARRES1	Retinoic acid receptor responder (tazarotene induced) 1	Negative regulation of cell proliferation	4.57	1.76	2.59
TFF3	Trefoil factor 3 (intestinal)	Cell surface receptor mediated signal transduction; Cell motility; Defense response	4.27	2.69	1.59
CDH19	Cadherin 19, type 2	Cell adhesion-mediated signaling	4.13	3.30	1.25
TRIM55	Tripartite motif-containing 55	Proteolysis	3.83	2.63	1.45

Down-regulated genes					
HOXB7	Homeobox B7	mRNA transcription regulation; Segment specification	-4.74	-1.44	-3.29
DEFA1	Defensin, alpha 1	Chemotaxis; Immune response	-5.22	1.11	-5.79
CTHRC1	Collagen triple helix repeat containing 1	Complement-mediated immunity	-5.27	-1.12	-4.70
ACTG2	Actin, gamma 2, smooth muscle, enteric	Exocytosis; Endocytosis; Transport; Cytokinesis	-5.89	-4.95	-1.19
HOXC8	Homeobox C8	mRNA transcription regulation	-6.69	-1.67	-4.02
HOXA5	Homeobox A5	mRNA transcription regulation; Segment specification	-7.89	-4.04	-1.95
NNAT	Neuronatin	Neurogenesis	-8.00	-2.34	-3.42
CXCL14	Chemokine (C-X-C motif) ligand 14	Cell-cell signaling; Chemotaxis; Immune response	-8.10	-2.45	-3.31
RN7SK	RNA, 7SK small nuclear	Biological process unclassified	-9.72	-2.47	-3.93
HOXC6	Homeobox C6	mRNA transcription regulation; Segment specification	-11.57	-3.51	-3.29

Table S7. Top 10 genes significantly up- and down-regulated in MAT vs SAT.

Gene Symbol	Full name	Biological Process	MAT-SAT	EAT-MAT	EAT-SAT
Up-regulated genes					
IGKV3D-20	Immunoglobulin kappa variable 3D-20	Immune response	16.05	-1.50	10.73
IGLL1	Immunoglobulin lambda-like polypeptide 1	B-cell and antibody-mediated immunity	13.55	-1.46	9.25
IGJ	Immunoglobulin J polypeptide, linker protein for immunoglobulin alpha and mu polypeptides	Immune response	12.69	-1.66	7.66
IGLL3	Immunoglobulin lambda-like polypeptide 3	Immune response	5.88	-2.72	2.16
KIAA1199	Kiaa1199	Biological process unclassified	5.41	-2.99	1.81
FCRLA	Fc receptor-like A	B-cell- and antibody-mediated immunity; Macrophage-mediated immunity; Natural killer cell mediated immunity	5.40	-2.76	1.95
CD79A	CD79a molecule, immunoglobulin-associated alpha	B cell activation, differentiation and proliferation; B cell receptor signaling pathway	5.12	-2.80	1.83
CD19	CD19 molecule	B cell receptor signaling pathway; Cellular defense response	4.64	-2.99	1.55
LTB	Lymphotoxin beta (TNF superfamily, member 3)	Cytokine/chemokine mediated immunity; T-cell, B-cell- and antibody-mediated immunity; Macrophage-mediated immunity; Natural killer cell mediated	4.59	-2.11	2.18

		immunity;			
CD3D	CD3d molecule, delta (CD3-TCR complex)	Cell surface receptor mediated signal transduction;Cell communication;T-cell mediated immunity	4.56	-2.18	2.09
Down-regulated genes					
HBD	Hemoglobin, delta	Transport; Blood circulation and gas exchange	-3.33	-1.38	-4.59
PPL	Periplakin	Keratinization	-3.41	-1.05	-3.57
NNAT	Neuronatin	Neurogenesis	-3.42	-2.34	-8.00
HOXB8	Homeobox B8	mRNA transcription regulation	-3.76	-1.16	-4.35
RN7SK	RNA, 7SK small nuclear	Biological process unclassified	-3.93	-2.47	-9.72
HOXC8	Homeobox C8	mRNA transcription regulation	-4.02	-1.67	-6.69
EGFL6	EGF-like-domain, multiple 6	Cell adhesion and differentiation; Cell cycle	-4.06	1.34	-3.02
CTHRC1	Collagen triple helix repeat containing 1	Complement-mediated immunity	-4.70	-1.12	-5.27
DEFA3	Defensin, alpha 3, neutrophil-specific	Immune response	-4.73	1.03	-4.59
DEFA1	Defensin, alpha 1	Chemotaxis; Immune response	-5.79	1.11	-5.22

Chapter III

Conclusion

The recognition of visceral adipose tissue as an endocrine organ that can interact with adjacent organs and its association with markers of cardiometabolic diseases[76], have relived the interest in studying the genetic and molecular implications of this tissue with some pathologies such as CVDs and type 2 diabetes. New therapeutic options for a broad range of disorders have emerged from the knowledge of the mechanisms that regulate the various functions of adipose tissue. Adipocyte-based therapies include alteration of the insulin/endocannabinoid/glucose-dependent insulinotropic polypeptide signaling, β3-adrenoreceptors antagonist, thiazolidinediones, and ciliary neurotrophic factor to treat obesity and insulin resistance[141]. Leptin, adiponectin, and visfatin analogs as well as 11β-hydroxy steroid dehydrogenase-1 inhibitors, PAI-1/renin angiotensin system and adiponectin blockers may also be used to treat insulin resistance, dyslipidemia, obesity, hypertension and atherosclerosis[141].

In addition, the correlation of the thickness of EAT with CAD by imaging studies have led to propose the thickness of EAT as a tool for CAD and cardiometabolic risk assessment. Iacobellis et al.[88] suggested threshold values for high-risk echocardiographic EAT thickness of 9.5 mm in men and 7.5 mm in women. The function of EAT and the molecular pathways that are responsible for the association between EAT and CAD is still unclear. The molecular interactions of the genes expressed by EAT with those expressed in the myocardium and the coronary arteries of people with and without CVD remain poorly understood. The ethical difficulties to

obtain EAT biopsies from normal individuals is a barrier. Accordingly most studies analyzing EAT gene and protein expressions have been performed in CAD patients, and sometimes compared to adipose tissue samples taken from other patients undergoing different heart surgeries. In the latter case the presence of other diseases might affect the transcription and protein profile of EAT and influence the results of such comparisons.

Gene expression microarray is a tool that permits the comparison between the expression of thousands of genes in different tissues, or the same kind of tissue under different conditions (eg. sick and normal tissues, effect of drugs or temperature). In our study, the whole-genome gene expression of EAT, mediastinal, and subcutaneous adipose tissue from the chest of 6 male CAD patients undergoing CABG was compared. The objective of this comparison was to identify genes that are up- or down-regulated in EAT compared with the other two tissues. The results of the microarrays experiment was confirmed by measuring the expression of 4 genes by qPCR. In general, our results showed that the gene expression profiles of EAT and mediastinal fat were more similar compared to the subcutaneous adipose depot. Only 22 genes were significantly differentially expressed in EAT compared to mediastinal fat. All those genes were up-regulated. Among these genes, 2 interesting genes related with CVD were identified, the adenosine A1 receptor (ADORA1) and the prostaglandin D2 synthase (PTGDS), which expression levels were confirmed by qPCR.

ADORA1 is a G protein coupled-receptor, expressed in the central nervous system, heart, adipocytes, and pre-adipocytes[142,143]. To the best of our knowledge, it is the first time that ADORA1 is found expressed in EAT, and overexpressed in this tissue compared to mediastinal fat. Exogenous ADORA1 agonists reduced cardiac infarct size in isolated heart models[143]. Thus, ADORA1 agonists have potential therapeutic uses to treat CVD. Extracellular endogenous adenosine concentration increases under ischemic conditions as a protective mediator[143]. Overexpression of ADORA1 in the

heart of transgenic mice provides additional cardioprotection to that offers by adenosine in ischemic myocardium. These mice are characterized by a decrease in cell necrosis and improvement of myocardial energetic[144]. Considering the overexpression of ADORA1 in EAT, we speculate that EAT might interfere with the beneficial action of adenosine by capturing the adenosine that the myocardium cells need to avoid ischemic injuries. The binding of adenosine to ADORA1 is well recognized to inhibit lipolysis[70]. The activation of the hormone-sensitive lipase (LIPE) increases lipolysis mediated by catecholamines in adipose tissue and results in an increase of cAMP. The fact that adenosine agonists will inhibit the synthesis of cAMP by inhibiting the membrane bound adenylate cyclase, high concentration of adenosine agonists would be expected to reduce lipolysis in EAT by preventing the activation of LIPE[145]. Indeed, in the present study the expression of LIPE in EAT and mediastinal fat, measured by qPCR, was significantly down-regulated compared to subcutaneous fat. We suggest that the up-regulation of ADORA1 may be a mechanism to reduce the greater rate of FFA release observed in EAT.

We also found a down-regulation of the alpha-2A-adrenergic receptor (ADRA2A), a G protein coupled-receptor, in EAT compared to subcutaneous fat measure by microarrays and qPCR. To the best of our knowledge, it is the first time that this overexpression is documented. Specific mutations generated in this gene causes hypertension, tachycardia and impaired baroreceptor reflexes in mice[146]. In the study by Vohl et al.[105], ADRA2A was found down-regulated in omental fat compared to the subcutaneous depot and they suggested that the lower expression of ADRA2A in omental tissue might mean lower sensitivity to antilipolytic signals. The rate of lipolysis in EAT is increased compared to other fat depots such as popliteal or perirenal fat[78], and this might be partly mediated by a low expression of ADRA2A in this adipose tissue. In summary, our results suggest EAT as a buffering mechanism of the release of FFA on the heart.

An interesting gene identified as up-regulated in EAT was PTGDS, the enzyme involved in the synthesis of prostaglandin D2 (PGD2) and a carrier protein for small lipophilic molecules[147]. PGD2 is an anticoagulant, vasodilatator, and a precursor in the synthesis of prostanoids derived from the arachidonic acid (AA)[148]. The mRNA of PTGDS was significantly up-regulated in EAT compared to mediastinal and subcutaneous fat. Our results are consistent with the study of Fain et al.[149] in which PTGDS expression was measured by qPCR in a group of CAD patients (60% male). PTGDS has anti-inflammatory properties. The PTGDS bioproduct 15d-PGJ2 binds to PPARγ which is an inhibitor of the activation of NF-κB induced by inflammatory cytokines[150]. In addition, the production of PGD2 mediated by PTGDS, lead to a reversion of the inflammatory state and plaque stabilization in human atherosclerosis[150]. Thus, PTGDS overexpression is thought to be an adaptation mechanism to prevent cardiovascular injuries. In addition, PTGDS is considered a suitable biomarker of CAD because its levels in serum increase in patients with stable CAD and with the severity of the disease[148]. The fact that the coronary arteries and their main epicardial branches are embedded in EAT suggests that part of the higher PTGDS enzyme levels observed in atherosclerotic plaques of coronary arteries, compared to the internal mammary or the carotid arteries[148], may come from EAT.

In contrast to the high expression of the anti-inflamamtory factor PTGDS in EAT, in our study, a higher expression of genes implicated in inflammatory and immune response were found in EAT and mediastinal fat compared to the subcutaneous tissue. That is supported by other studies[59,92,105] in which the expression of inflammatory markers was high in EAT and omental adipose tissue compared to abdominal subcutaneous fat. The role of inflammatory mediators in CAD has been well established[92]. Furthermore, inflammation is a suitable link between obesity and CVD risk[4]. And inflammation might be part of the link between EAT and CAD. We did not find correlations between the expression of the 4 genes confirmed by qPCR with BMI, waist circuference, LDL-cholesterol, and HDL-cholesterol. Only the expression of PTGDS in EAT has a high positive but not significant correlation with

BMI (r = 0.57, P = 0.084). This absence of correlation might be in part related to the homogeneity in the characteristics of the study participants and a low number of individuals in each category of obesity. Only 6 patients were normal weight and 8 were obese. Moreover, all patients were under treatment for dyslipidemia.

Microarray experiments have some limitations including a limited dynamic range preventing accurate measurements of low and high expressed genes caused by background and saturation of signals, respectively. In addition, microarrays cannot recognize novel transcripts and can only detect known alternative splice variants interrogated on the arrays[151,152]. Emerging technologies in genomics, the so called next-generation of sequencers, overcome these limitations. One application of these new technologies is RNA-sequencing (RNA-Seq) that allow digital gene expression levels at the genome scale[152]. RNA-Seq is becoming the state-of-the-art approach for transcriptome profiling providing unmatched accuracy, dynamic range and resolution. RNA-Seq captures the transcriptome at the quantitative gene expression level, but also at the transcriptional structure level (i.e. alternative splice variants). It also provides different species of transcripts, including mRNAs, non-coding RNAs and small RNAs. Moreover, RNA-Seq provides a first glance at genetic variants in the expressed portion of the genome. Altogether, this research tool will dramatically change our understanding of transcriptomes[152]. Next-generation of sequencers are currently available from a number of venders including Illumina, Roche/454, Life Technologies/Applied Biosystems, and Helicos Biosciences. Studies in *Arabidopsis thaliana*, yeast, mouse and human cells have been performed using RNA-Seq[153]. It would be of great interest to repeat our study using RNA-Seq to refine our molecular understanding of EAT and to compare with other adipose tissue compartments.

Other perspectives of this project include the comparison of the expression levels of ADORA1, ADRA2A and PTGDS in EAT from CAD and non-CAD subjects (from trauma patients or recent autopsies). This might help to confirm the role of these genes in the development of CAD. Additional follow-up experiments would be useful

such as measuring the enzymatic activity of PTGDS and the levels of its main product, PGD2, in EAT. More qPCR experiments would be needed to confirm the expression of other interesting genes found up-regulated in EAT compared to mediastinal fat such as the Acyl-CoA synthase (ACSL1) and neuromedin (NMB) genes, which are part of the AA pathway. It might also be important to determine the contribution of each cell type found in EAT for the expression of genes identified in this study.

The measurement of visceral fat is now clinically recognized as important because of it significant relationships with CVDs[154]. EAT correlates with CAD and CAD severity[78]. It is thus essential to understand the molecular characteristics of this tissue. In our study, we showed that some genes are differentially expressed in EAT compared to other chest fat depots. Other evidence indicates the unique pattern of gene regulation in this tissue compared to other fat depots[92]. How EAT is involved in the development or progression of CAD and whether it is damaging or beneficial for the heart function still remain to be determined. The identification of up-regulated genes in EAT such as ADORA1 and PTGDS suggests that EAT may serve as a buffer of free fatty acids and a source of anti-inflammatory factors.

Our study will allow the selection of new pathways and genes that might be involved in CAD and possibly the identification of new drugs targets against the disease. Future studies correlating the expression of the proteins encoded by the differentially regulated mRNA targets that we have identified might allow the selection of biomarkers for the disease. We have also shown differences in the expression of key genes implicated in the lipid metabolism in EAT compared with other adipose tissues. To conclude, although this study was limited to subjects with CAD, the results provide insights about the biology of EAT and its potential implication in CAD. The study also provides new targets for future experimental research in CVD.

Chapter IV

References chapters I and III

1. Mathieu P, Poirier P, Pibarot P, Lemieux I, Despres JP (2009) Visceral obesity: the link among inflammation, hypertension, and cardiovascular disease. Hypertension 53: 577-584.
2. Gastaldelli A, Basta G (2010) Ectopic fat and cardiovascular disease: what is the link? Nutr Metab Cardiovasc Dis 20: 481-490.
3. Larsson B, Svardsudd K, Welin L, Wilhelmsen L, Bjorntorp P, et al. (1984) Abdominal adipose tissue distribution, obesity, and risk of cardiovascular disease and death: 13 year follow up of participants in the study of men born in 1913. Br Med J (Clin Res Ed) 288: 1401-1404.
4. Despres JP, Lemieux I (2006) Abdominal obesity and metabolic syndrome. Nature 444: 881-887.
5. Iacobellis G, Willens HJ (2009) Echocardiographic epicardial fat: a review of research and clinical applications. J Am Soc Echocardiogr 22: 1311-1319; quiz 1417-1318.
6. Iacobellis G, Ribaudo MC, Assael F, Vecci E, Tiberti C, et al. (2003) Echocardiographic epicardial adipose tissue is related to anthropometric and clinical parameters of metabolic syndrome: a new indicator of cardiovascular risk. J Clin Endocrinol Metab 88: 5163-5168.
7. Bonow RO, Smaha LA, Smith SC, Jr., Mensah GA, Lenfant C (2002) World Heart Day 2002: the international burden of cardiovascular disease: responding to the emerging global epidemic. Circulation 106: 1602-1605.

8. Lusis AJ, Mar R, Pajukanta P (2004) Genetics of atherosclerosis. Annu Rev Genomics Hum Genet 5: 189-218.
9. Tedgui A, Mallat Z (2006) Cytokines in atherosclerosis: pathogenic and regulatory pathways. Physiol Rev 86: 515-581.
10. Libby P, Okamoto Y, Rocha VZ, Folco E (2010) Inflammation in atherosclerosis: transition from theory to practice. Circ J 74: 213-220.
11. Qiao JH, Xie PZ, Fishbein MC, Kreuzer J, Drake TA, et al. (1994) Pathology of atheromatous lesions in inbred and genetically engineered mice. Genetic determination of arterial calcification. Arterioscler Thromb 14: 1480-1497.
12. Kashiwagi M, Tanaka A, Kitabata H, Tsujioka H, Matsumoto H, et al. (2009) Relationship between coronary arterial remodeling, fibrous cap thickness and high-sensitivity C-reactive protein levels in patients with acute coronary syndrome. Circ J 73: 1291-1295.
13. Lusis AJ, Fogelman AM, Fonarow GC (2004) Genetic basis of atherosclerosis: part I: new genes and pathways. Circulation 110: 1868-1873.
14. Chen Y, Rollins J, Paigen B, Wang X (2007) Genetic and genomic insights into the molecular basis of atherosclerosis. Cell Metab 6: 164-179.
15. Conlin PR (2008) Genes and environment in blood pressure control--salt intake again shows its importance. Am J Clin Nutr 88: 255-256.
16. Leineweber K, Heusch G (2009) Beta 1- and beta 2-adrenoceptor polymorphisms and cardiovascular diseases. Br J Pharmacol 158: 61-69.
17. Heid IM, Jackson AU, Randall JC, Winkler TW, Qi L, et al. Meta-analysis identifies 13 new loci associated with waist-hip ratio and reveals sexual dimorphism in the genetic basis of fat distribution. Nat Genet 42: 949-960.
18. Thorstenson YR, Shen P, Tusher VG, Wayne TL, Davis RW, et al. (2001) Global analysis of ATM polymorphism reveals significant functional constraint. Am J Hum Genet 69: 396-412.
19. Teslovich TM, Musunuru K, Smith AV, Edmondson AC, Stylianou IM, et al. (2010) Biological, clinical and population relevance of 95 loci for blood lipids. Nature 466: 707-713.

20. Ding K, Kullo IJ (2009) Genome-wide association studies for atherosclerotic vascular disease and its risk factors. Circ Cardiovasc Genet 2: 63-72.
21. Chen SN, Ballantyne CM, Gotto AM, Jr., Marian AJ (2009) The 9p21 susceptibility locus for coronary artery disease and the severity of coronary atherosclerosis. BMC Cardiovasc Disord 9: 3.
22. Caballero B (2007) The global epidemic of obesity: an overview. Epidemiol Rev 29: 1-5.
23. Lavie CJ, Milani RV, Ventura HO (2009) Obesity and cardiovascular disease: risk factor, paradox, and impact of weight loss. J Am Coll Cardiol 53: 1925-1932.
24. Cottam DR, Mattar SG, Barinas-Mitchell E, Eid G, Kuller L, et al. (2004) The chronic inflammatory hypothesis for the morbidity associated with morbid obesity: implications and effects of weight loss. Obes Surg 14: 589-600.
25. Karastergiou K, Evans I, Ogston N, Miheisi N, Nair D, et al. (2010) Epicardial adipokines in obesity and coronary artery disease induce atherogenic changes in monocytes and endothelial cells. Arterioscler Thromb Vasc Biol 30: 1340-1346.
26. Dagenais GR, Yi Q, Mann JF, Bosch J, Pogue J, et al. (2005) Prognostic impact of body weight and abdominal obesity in women and men with cardiovascular disease. Am Heart J 149: 54-60.
27. Berg AH, Scherer PE (2005) Adipose tissue, inflammation, and cardiovascular disease. Circ Res 96: 939-949.
28. Galic S, Oakhill JS, Steinberg GR (2010) Adipose tissue as an endocrine organ. Mol Cell Endocrinol 316: 129-139.
29. Goossens GH (2008) The role of adipose tissue dysfunction in the pathogenesis of obesity-related insulin resistance. Physiol Behav 94: 206-218.
30. Van Gaal LF, Mertens IL, De Block CE (2006) Mechanisms linking obesity with cardiovascular disease. Nature 444: 875-880.
31. Kershaw EE, Flier JS (2004) Adipose tissue as an endocrine organ. J Clin Endocrinol Metab 89: 2548-2556.

32. Gustafson B (2010) Adipose tissue, inflammation and atherosclerosis. J Atheroscler Thromb 17: 332-341.

33. Ahima RS (2006) Adipose tissue as an endocrine organ. Obesity (Silver Spring) 14 Suppl 5: 242S-249S.

34. Rochford JJ (2010) Molecular mechanisms controlling human adipose tissue development: insights from monogenic lipodystrophies. Expert Rev Mol Med 12: e24.

35. Schaffler A, Scholmerich J, Buchler C (2005) Mechanisms of disease: adipocytokines and visceral adipose tissue--emerging role in intestinal and mesenteric diseases. Nat Clin Pract Gastroenterol Hepatol 2: 103-111.

36. Curat CA, Miranville A, Sengenes C, Diehl M, Tonus C, et al. (2004) From blood monocytes to adipose tissue-resident macrophages: induction of diapedesis by human mature adipocytes. Diabetes 53: 1285-1292.

37. Charriere G, Cousin B, Arnaud E, Andre M, Bacou F, et al. (2003) Preadipocyte conversion to macrophage. Evidence of plasticity. J Biol Chem 278: 9850-9855.

38. Hotamisligil GS (2006) Inflammation and metabolic disorders. Nature 444: 860-867.

39. Lago F, Gomez R, Gomez-Reino JJ, Dieguez C, Gualillo O (2009) Adipokines as novel modulators of lipid metabolism. Trends Biochem Sci 34: 500-510.

40. Fain JN, Madan AK, Hiler ML, Cheema P, Bahouth SW (2004) Comparison of the release of adipokines by adipose tissue, adipose tissue matrix, and adipocytes from visceral and subcutaneous abdominal adipose tissues of obese humans. Endocrinology 145: 2273-2282.

41. Kadowaki T, Yamauchi T (2005) Adiponectin and adiponectin receptors. Endocr Rev 26: 439-451.

42. Lord GM, Matarese G, Howard JK, Baker RJ, Bloom SR, et al. (1998) Leptin modulates the T-cell immune response and reverses starvation-induced immunosuppression. Nature 394: 897-901.

43. Chan JL, Heist K, DePaoli AM, Veldhuis JD, Mantzoros CS (2003) The role of falling leptin levels in the neuroendocrine and metabolic adaptation to short-term starvation in healthy men. J Clin Invest 111: 1409-1421.

44. Reilly MP, Lehrke M, Wolfe ML, Rohatgi A, Lazar MA, et al. (2005) Resistin is an inflammatory marker of atherosclerosis in humans. Circulation 111: 932-939.

45. Frankel DS, Vasan RS, D'Agostino RB, Sr., Benjamin EJ, Levy D, et al. (2009) Resistin, adiponectin, and risk of heart failure the Framingham offspring study. J Am Coll Cardiol 53: 754-762.

46. Saddi-Rosa P, Oliveira CS, Giuffrida FM, Reis AF (2010) Visfatin, glucose metabolism and vascular disease: a review of evidence. Diabetol Metab Syndr 2: 21.

47. Hill MJ, Kumar S, McTernan PG (2009) Adipokines and the clinical laboratory: what to measure, when and how? J Clin Pathol 62: 206-211.

48. Tilg H, Moschen AR (2006) Adipocytokines: mediators linking adipose tissue, inflammation and immunity. Nat Rev Immunol 6: 772-783.

49. Canoy D (2010) Coronary heart disease and body fat distribution. Curr Atheroscler Rep 12: 125-133.

50. Natale F, Tedesco MA, Mocerino R, de Simone V, Di Marco GM, et al. (2009) Visceral adiposity and arterial stiffness: echocardiographic epicardial fat thickness reflects, better than waist circumference, carotid arterial stiffness in a large population of hypertensives. Eur J Echocardiogr 10: 549-555.

51. Quinkler M, Bujalska IJ, Tomlinson JW, Smith DM, Stewart PM (2006) Depot-specific prostaglandin synthesis in human adipose tissue: a novel possible mechanism of adipogenesis. Gene 380: 137-143.

52. Jensen MD (2008) Role of body fat distribution and the metabolic complications of obesity. J Clin Endocrinol Metab 93: S57-63.

53. Vernochet C, Peres SB, Farmer SR (2009) Mechanisms of obesity and related pathologies: transcriptional control of adipose tissue development. FEBS J 276: 5729-5737.

54. Mathieu P, Pibarot P, Larose E, Poirier P, Marette A, et al. (2008) Visceral obesity and the heart. Int J Biochem Cell Biol 40: 821-836.

55. Thomas M, Thomas MJ (2003) The changing face of rehabilitation in leprosy. Indian J Lepr 75: 143-152.

56. Gosmanov AR, Thomason DB (2003) Regulation of Na(+)-K(+)-2Cl- cotransporter activity in rat skeletal muscle and intestinal epithelial cells. Tsitologiia 45: 812-816.

57. Kantarjian H, Talpaz M, O'Brien S, Garcia-Manero G, Verstovsek S, et al. (2004) High-dose imatinib mesylate therapy in newly diagnosed Philadelphia chromosome-positive chronic phase chronic myeloid leukemia. Blood 103: 2873-2878.

58. Auld DS, Colomar A, Belair EL, Castonguay A, Pinard A, et al. (2003) Modulation of neurotransmission by reciprocal synapse-glial interactions at the neuromuscular junction. J Neurocytol 32: 1003-1015.

59. Company JM, Booth FW, Laughlin MH, Arce-Esquivel AA, Sacks HS, et al. (2010) Epicardial fat gene expression after aerobic exercise training in pigs with coronary atherosclerosis: relationship to visceral and subcutaneous fat. J Appl Physiol.

60. Fox CS, Massaro JM, Hoffmann U, Pou KM, Maurovich-Horvat P, et al. (2007) Abdominal visceral and subcutaneous adipose tissue compartments: association with metabolic risk factors in the Framingham Heart Study. Circulation 116: 39-48.

61. Conner IP, Sharma S, Lemieux SK, Mendola JD (2004) Retinotopic organization in children measured with fMRI. J Vis 4: 509-523.

62. Montani JP, Carroll JF, Dwyer TM, Antic V, Yang Z, et al. (2004) Ectopic fat storage in heart, blood vessels and kidneys in the pathogenesis of cardiovascular diseases. Int J Obes Relat Metab Disord 28 Suppl 4: S58-65.

63. Gastaldelli A, Cusi K, Pettiti M, Hardies J, Miyazaki Y, et al. (2007) Relationship between hepatic/visceral fat and hepatic insulin resistance in nondiabetic and type 2 diabetic subjects. Gastroenterology 133: 496-506.

64. Wajchenberg BL (2000) Subcutaneous and visceral adipose tissue: their relation to the metabolic syndrome. Endocr Rev 21: 697-738.

65. Bugianesi E, Pagotto U, Manini R, Vanni E, Gastaldelli A, et al. (2005) Plasma adiponectin in nonalcoholic fatty liver is related to hepatic insulin resistance and hepatic fat content, not to liver disease severity. J Clin Endocrinol Metab 90: 3498-3504.

66. Gastaldelli A, Kozakova M, Hojlund K, Flyvbjerg A, Favuzzi A, et al. (2009) Fatty liver is associated with insulin resistance, risk of coronary heart disease, and early atherosclerosis in a large European population. Hepatology 49: 1537-1544.

67. Perseghin G, Scifo P, De Cobelli F, Pagliato E, Battezzati A, et al. (1999) Intramyocellular triglyceride content is a determinant of in vivo insulin resistance in humans: a 1H-13C nuclear magnetic resonance spectroscopy assessment in offspring of type 2 diabetic parents. Diabetes 48: 1600-1606.

68. Moro C, Bajpeyi S, Smith SR (2008) Determinants of intramyocellular triglyceride turnover: implications for insulin sensitivity. Am J Physiol Endocrinol Metab 294: E203-213.

69. Mathieu P, Lemieux I, Despres JP (2010) Obesity, inflammation, and cardiovascular risk. Clin Pharmacol Ther 87: 407-416.

70. Vikman HL, Ranta S, Kiviluoto T, Ohisalo JJ (1991) Different metabolic regulation by adenosine in omental and subcutaneous adipose tissue. Acta Physiol Scand 142: 405-410.

71. Chatterjee TK, Stoll LL, Denning GM, Harrelson A, Blomkalns AL, et al. (2009) Proinflammatory phenotype of perivascular adipocytes: influence of high-fat feeding. Circ Res 104: 541-549.

72. Alvehus M, Buren J, Sjostrom M, Goedecke J, Olsson T (2010) The human visceral fat depot has a unique inflammatory profile. Obesity (Silver Spring) 18: 879-883.

73. Zwaka TP, Hombach V, Torzewski J (2001) C-reactive protein-mediated low density lipoprotein uptake by macrophages: implications for atherosclerosis. Circulation 103: 1194-1197.

74. Ohman MK, Wright AP, Wickenheiser KJ, Luo W, Eitzman DT (2009) Visceral adipose tissue and atherosclerosis. Curr Vasc Pharmacol 7: 169-179.

75. Surmi BK, Hasty AH (2010) The role of chemokines in recruitment of immune cells to the artery wall and adipose tissue. Vascul Pharmacol 52: 27-36.

76. Verhagen SN, Visseren FL (2010) Perivascular adipose tissue as a cause of atherosclerosis. Atherosclerosis.

77. Ichiki T (2010) Perivascular adipose tissue, a Janus-faced regulator of vascular function. Circ J 74: 1300-1301.

78. Rabkin SW (2007) Epicardial fat: properties, function and relationship to obesity. Obes Rev 8: 253-261.

79. Henrichot E, Juge-Aubry CE, Pernin A, Pache JC, Velebit V, et al. (2005) Production of chemokines by perivascular adipose tissue: a role in the pathogenesis of atherosclerosis? Arterioscler Thromb Vasc Biol 25: 2594-2599.

80. Ketonen J, Shi J, Martonen E, Mervaala E (2010) Periadventitial adipose tissue promotes endothelial dysfunction via oxidative stress in diet-induced obese C57Bl/6 mice. Circ J 74: 1479-1487.

81. Sacks HS, Fain JN (2007) Human epicardial adipose tissue: a review. Am Heart J 153: 907-917.

82. Marchington JM, Mattacks CA, Pond CM (1989) Adipose tissue in the mammalian heart and pericardium: structure, foetal development and biochemical properties. Comp Biochem Physiol B 94: 225-232.

83. Abbara S, Desai JC, Cury RC, Butler J, Nieman K, et al. (2006) Mapping epicardial fat with multi-detector computed tomography to facilitate percutaneous transepicardial arrhythmia ablation. Eur J Radiol 57: 417-422.

84. Corradi D, Maestri R, Callegari S, Pastori P, Goldoni M, et al. (2004) The ventricular epicardial fat is related to the myocardial mass in normal, ischemic and hypertrophic hearts. Cardiovasc Pathol 13: 313-316.

85. Iacobellis G, Corradi D, Sharma AM (2005) Epicardial adipose tissue: anatomic, biomolecular and clinical relationships with the heart. Nat Clin Pract Cardiovasc Med 2: 536-543.

86. Shirani J, Berezowski K, Roberts WC (1995) Quantitative measurement of normal and excessive (cor adiposum) subepicardial adipose tissue, its clinical significance, and its effect on electrocardiographic QRS voltage. Am J Cardiol 76: 414-418.

87. Tansey DK, Aly Z, Sheppard MN (2005) Fat in the right ventricle of the normal heart. Histopathology 46: 98-104.

88. Iacobellis G, Willens HJ, Barbaro G, Sharma AM (2008) Threshold values of high-risk echocardiographic epicardial fat thickness. Obesity (Silver Spring) 16: 887-892.

89. Jeong JW, Jeong MH, Yun KH, Oh SK, Park EM, et al. (2007) Echocardiographic epicardial fat thickness and coronary artery disease. Circ J 71: 536-539.

90. Iacobellis G, Assael F, Ribaudo MC, Zappaterreno A, Alessi G, et al. (2003) Epicardial fat from echocardiography: a new method for visceral adipose tissue prediction. Obes Res 11: 304-310.

91. Ouwens DM, Sell H, Greulich S, Eckel J (2010) The role of epicardial and perivascular adipose tissue in the pathophysiology of cardiovascular disease. J Cell Mol Med 14: 2223-2234.

92. Mazurek T, Zhang L, Zalewski A, Mannion JD, Diehl JT, et al. (2003) Human epicardial adipose tissue is a source of inflammatory mediators. Circulation 108: 2460-2466.

93. Baker AR, Harte AL, Howell N, Pritlove DC, Ranasinghe AM, et al. (2009) Epicardial adipose tissue as a source of nuclear factor-kappaB and c-Jun N-terminal kinase mediated inflammation in patients with coronary artery disease. J Clin Endocrinol Metab 94: 261-267.

94. Azzazy HM, Pelsers MM, Christenson RH (2006) Unbound free fatty acids and heart-type fatty acid-binding protein: diagnostic assays and clinical applications. Clin Chem 52: 19-29.

95. Iozzo P (2010) Metabolic toxicity of the heart: insights from molecular imaging. Nutr Metab Cardiovasc Dis 20: 147-156.

96. Hendrickson SC, St Louis JD, Lowe JE, Abdel-aleem S (1997) Free fatty acid metabolism during myocardial ischemia and reperfusion. Mol Cell Biochem 166: 85-94.

97. Sacks HS, Fain JN, Holman B, Cheema P, Chary A, et al. (2009) Uncoupling protein-1 and related messenger ribonucleic acids in human epicardial and other adipose tissues: epicardial fat functioning as brown fat. J Clin Endocrinol Metab 94: 3611-3615.

98. Greenstein AS, Khavandi K, Withers SB, Sonoyama K, Clancy O, et al. (2009) Local inflammation and hypoxia abolish the protective anticontractile properties of perivascular fat in obese patients. Circulation 119: 1661-1670.

99. Sipahi I, Tuzcu EM, Schoenhagen P, Wolski KE, Nicholls SJ, et al. (2006) Effects of normal, pre-hypertensive, and hypertensive blood pressure levels on progression of coronary atherosclerosis. J Am Coll Cardiol 48: 833-838.

100. Sipahi I, Tuzcu EM, Schoenhagen P, Nicholls SJ, Ozduran V, et al. (2006) Compensatory enlargement of human coronary arteries during progression of atherosclerosis is unrelated to atheroma burden: serial intravascular ultrasound observations from the REVERSAL trial. Eur Heart J 27: 1664-1670.

101. Surmely JF, Nasu K, Fujita H, Terashima M, Matsubara T, et al. (2007) Association of coronary plaque composition and arterial remodelling: a virtual histology analysis by intravascular ultrasound. Heart 93: 928-932.

102. Ishii T, Asuwa N, Masuda S, Ishikawa Y (1998) The effects of a myocardial bridge on coronary atherosclerosis and ischaemia. J Pathol 185: 4-9.

103. Iacobellis G, Barbaro G (2008) The double role of epicardial adipose tissue as pro- and anti-inflammatory organ. Horm Metab Res 40: 442-445.

104. Malavazos AE, Ermetici F, Coman C, Corsi MM, Morricone L, et al. (2007) Influence of epicardial adipose tissue and adipocytokine levels on cardiac abnormalities in visceral obesity. Int J Cardiol 121: 132-134.

105. Vohl MC, Sladek R, Robitaille J, Gurd S, Marceau P, et al. (2004) A survey of genes differentially expressed in subcutaneous and visceral adipose tissue in men. Obes Res 12: 1217-1222.

106. Cheng KH, Chu CS, Lee KT, Lin TH, Hsieh CC, et al. (2008) Adipocytokines and proinflammatory mediators from abdominal and epicardial adipose tissue in patients with coronary artery disease. Int J Obes (Lond) 32: 268-274.

107. Iacobellis G, Pistilli D, Gucciardo M, Leonetti F, Miraldi F, et al. (2005) Adiponectin expression in human epicardial adipose tissue in vivo is lower in patients with coronary artery disease. Cytokine 29: 251-255.

108. Kim MK, Tanaka K, Kim MJ, Matuso T, Endo T, et al. (2009) Comparison of epicardial, abdominal and regional fat compartments in response to weight loss. Nutr Metab Cardiovasc Dis 19: 760-766.

109. Iacobellis G, Singh N, Wharton S, Sharma AM (2008) Substantial changes in epicardial fat thickness after weight loss in severely obese subjects. Obesity (Silver Spring) 16: 1693-1697.

110. Willens HJ, Byers P, Chirinos JA, Labrador E, Hare JM, et al. (2007) Effects of weight loss after bariatric surgery on epicardial fat measured using echocardiography. Am J Cardiol 99: 1242-1245.

111. Barber MC, Ward RJ, Richards SE, Salter AM, Buttery PJ, et al. (2000) Ovine adipose tissue monounsaturated fat content is correlated to depot-specific expression of the stearoyl-CoA desaturase gene. J Anim Sci 78: 62-68.

112. Bambace C, Telesca M, Zoico E, Sepe A, Olioso D, et al. (2010) Adiponectin gene expression and adipocyte diameter: a comparison between epicardial and subcutaneous adipose tissue in men. Cardiovasc Pathol.

113. Pezeshkian M, Noori M, Najjarpour-Jabbari H, Abolfathi A, Darabi M, et al. (2009) Fatty acid composition of epicardial and subcutaneous human adipose tissue. Metab Syndr Relat Disord 7: 125-131.

114. Dutour A, Achard V, Sell H, Naour N, Collart F, et al. (2010) Secretory type II phospholipase A2 is produced and secreted by epicardial adipose tissue and overexpressed in patients with coronary artery disease. J Clin Endocrinol Metab 95: 963-967.

115. Cartier A, Cote M, Lemieux I, Perusse L, Tremblay A, et al. (2009) Sex differences in inflammatory markers: what is the contribution of visceral adiposity? Am J Clin Nutr 89: 1307-1314.

116. Aydin H, Toprak A, Deyneli O, Yazici D, Tarcin O, et al. (2010) Epicardial fat tissue thickness correlates with endothelial dysfunction and other cardiovascular risk factors in patients with metabolic syndrome. Metab Syndr Relat Disord 8: 229-234.

117. Ahn SG, Lim HS, Joe DY, Kang SJ, Choi BJ, et al. (2008) Relationship of epicardial adipose tissue by echocardiography to coronary artery disease. Heart 94: e7.

118. Ahmadi N, Nabavi V, Yang E, Hajsadeghi F, Lakis M, et al. (2010) Increased epicardial, pericardial, and subcutaneous adipose tissue is associated with the presence and severity of coronary artery calcium. Acad Radiol 17: 1518-1524.

119. Iacobellis G, Lonn E, Lamy A, Singh N, Sharma AM (2010) Epicardial fat thickness and coronary artery disease correlate independently of obesity. Int J Cardiol.

120. de Vos AM, Prokop M, Roos CJ, Meijs MF, van der Schouw YT, et al. (2008) Peri-coronary epicardial adipose tissue is related to cardiovascular risk factors and coronary artery calcification in post-menopausal women. Eur Heart J 29: 777-783.

121. Djaberi R, Schuijf JD, van Werkhoven JM, Nucifora G, Jukema JW, et al. (2008) Relation of epicardial adipose tissue to coronary atherosclerosis. Am J Cardiol 102: 1602-1607.

122. Mahabadi AA, Massaro JM, Rosito GA, Levy D, Murabito JM, et al. (2009) Association of pericardial fat, intrathoracic fat, and visceral abdominal fat with cardiovascular disease burden: the Framingham Heart Study. Eur Heart J 30: 850-856.

123. Gorter PM, van Lindert AS, de Vos AM, Meijs MF, van der Graaf Y, et al. (2008) Quantification of epicardial and peri-coronary fat using cardiac computed tomography; reproducibility and relation with obesity and metabolic syndrome in patients suspected of coronary artery disease. Atherosclerosis 197: 896-903.

124. Wang TD, Lee WJ, Shih FY, Huang CH, Chang YC, et al. (2009) Relations of epicardial adipose tissue measured by multidetector computed tomography to

components of the metabolic syndrome are region-specific and independent of anthropometric indexes and intraabdominal visceral fat. J Clin Endocrinol Metab 94: 662-669.

125. Gorter PM, de Vos AM, van der Graaf Y, Stella PR, Doevendans PA, et al. (2008) Relation of epicardial and pericoronary fat to coronary atherosclerosis and coronary artery calcium in patients undergoing coronary angiography. Am J Cardiol 102: 380-385.
126. Sarin S, Wenger C, Marwaha A, Qureshi A, Go BD, et al. (2008) Clinical significance of epicardial fat measured using cardiac multislice computed tomography. Am J Cardiol 102: 767-771.
127. Yong HS, Kim EJ, Seo HS, Kang EY, Kim YK, et al. (2010) Pericardial fat is more abundant in patients with coronary atherosclerosis and even in the non-obese patients: evaluation with cardiac CT angiography. Int J Cardiovasc Imaging 26 Suppl 1: 53-62.
128. Ueno K, Anzai T, Jinzaki M, Yamada M, Jo Y, et al. (2009) Increased epicardial fat volume quantified by 64-multidetector computed tomography is associated with coronary atherosclerosis and totally occlusive lesions. Circ J 73: 1927-1933.
129. Ballman KV (2008) Genetics and genomics: gene expression microarrays. Circulation 118: 1593-1597.
130. Alberts B (2002) Molecular biology of the cell. New York: Garland Science. xxxiv, 1548 p. p.
131. Marziliano N, Grasso M, Pilotto A, Porcu E, Tagliani M, et al. (2009) Transcriptomic and proteomic analysis in the cardiovascular setting: unravelling the disease? J Cardiovasc Med (Hagerstown) 10: 433-442.
132. Brown TA (2007) Genomes 3. New York: Garland Science Pub. xxii, 713 p. p.
133. Edgar R, Domrachev M, Lash AE (2002) Gene Expression Omnibus: NCBI gene expression and hybridization array data repository. Nucleic Acids Res 30: 207-210.

134. Schmid R, Baum P, Ittrich C, Fundel-Clemens K, Huber W, et al. (2010) Comparison of normalization methods for Illumina BeadChip HumanHT-12 v3. BMC Genomics 11: 349.

135. Bolstad BM, Irizarry RA, Astrand M, Speed TP (2003) A comparison of normalization methods for high density oligonucleotide array data based on variance and bias. Bioinformatics 19: 185-193.

136. Tusher VG, Tibshirani R, Chu G (2001) Significance analysis of microarrays applied to the ionizing radiation response. Proc Natl Acad Sci U S A 98: 5116-5121.

137. Bustin SA, Benes V, Garson JA, Hellemans J, Huggett J, et al. (2009) The MIQE guidelines: minimum information for publication of quantitative real-time PCR experiments. Clin Chem 55: 611-622.

138. VanGuilder HD, Vrana KE, Freeman WM (2008) Twenty-five years of quantitative PCR for gene expression analysis. Biotechniques 44: 619-626.

139. Nolan T, Hands RE, Bustin SA (2006) Quantification of mRNA using real-time RT-PCR. Nat Protoc 1: 1559-1582.

140. Schmittgen TD, Livak KJ (2008) Analyzing real-time PCR data by the comparative C(T) method. Nat Protoc 3: 1101-1108.

141. Klein J, Perwitz N, Kraus D, Fasshauer M (2006) Adipose tissue as source and target for novel therapies. Trends Endocrinol Metab 17: 26-32.

142. Elzein E, Zablocki J (2008) A1 adenosine receptor agonists and their potential therapeutic applications. Expert Opin Investig Drugs 17: 1901-1910.

143. Urmaliya VB, Church JE, Coupar IM, Rose'Meyer RB, Pouton CW, et al. (2009) Cardioprotection induced by adenosine A1 receptor agonists in a cardiac cell ischemia model involves cooperative activation of adenosine A2A and A2B receptors by endogenous adenosine. J Cardiovasc Pharmacol 53: 424-433.

144. Regan SE, Broad M, Byford AM, Lankford AR, Cerniway RJ, et al. (2003) A1 adenosine receptor overexpression attenuates ischemia-reperfusion-induced apoptosis and caspase 3 activity. Am J Physiol Heart Circ Physiol 284: H859-866.

145. Barakat H, Davis J, Lang D, Mustafa SJ, McConnaughey MM (2006) Differences in the expression of the adenosine A1 receptor in adipose tissue of obese black and white women. J Clin Endocrinol Metab 91: 1882-1886.

146. Niederhoffer N, Hein L, Starke K (2004) Modulation of the baroreceptor reflex by alpha 2A-adrenoceptors: a study in alpha 2A knockout mice. Br J Pharmacol 141: 851-859.

147. Hirawa N, Uehara Y, Yamakado M, Toya Y, Gomi T, et al. (2002) Lipocalin-type prostaglandin d synthase in essential hypertension. Hypertension 39: 449-454.

148. Inoue T, Eguchi Y, Matsumoto T, Kijima Y, Kato Y, et al. (2008) Lipocalin-type prostaglandin D synthase is a powerful biomarker for severity of stable coronary artery disease. Atherosclerosis 201: 385-391.

149. Fain JN, Sacks HS, Bahouth SW, Tichansky DS, Madan AK, et al. (2010) Human epicardial adipokine messenger RNAs: comparisons of their expression in substernal, subcutaneous, and omental fat. Metabolism 59: 1379-1386.

150. Cipollone F, Fazia M, Iezzi A, Ciabattoni G, Pini B, et al. (2004) Balance between PGD synthase and PGE synthase is a major determinant of atherosclerotic plaque instability in humans. Arterioscler Thromb Vasc Biol 24: 1259-1265.

151. Marguerat S, Bahler J (2010) RNA-seq: from technology to biology. Cell Mol Life Sci 67: 569-579.

152. Morozova O, Hirst M, Marra MA (2009) Applications of new sequencing technologies for transcriptome analysis. Annu Rev Genomics Hum Genet 10: 135-151.

153. Wang Z, Gerstein M, Snyder M (2009) RNA-Seq: a revolutionary tool for transcriptomics. Nat Rev Genet 10: 57-63.

154. Company JM, Booth FW, Laughlin MH, Arce-Esquivel AA, Sacks HS, et al. (2010) Epicardial fat gene expression after aerobic exercise training in pigs with coronary atherosclerosis: relationship to visceral and subcutaneous fat. J Appl Physiol 109: 1904-1912.